Title

Preliminary High-Resolution Time-Lines Through the Cenomanian-Turonian (Late Cretaceous) Oceanic Anoxic Event (OAE 2)

Author

Keller, Allison Lynn

Publication Date

2015

UNIVERSITY OF CALIFORNIA
RIVERSIDE

Preliminary High-Resolution Time-Lines Through the Cenomanian-Turonian (Late Cretaceous) Oceanic Anoxic Event (OAE 2)

A Thesis submitted in partial satisfaction
of the requirements for the degree of

Master of Science

in

Geological Sciences

by

Allison Lynn Keller

August 2015

Thesis Committee:
- Dr. Peter Sadler, Chairperson
- Dr. Sandra Kirtland Turner
- Dr. Nigel Hughes

The Thesis of Allison Lynn Keller is approved:

____

____

____
Committee Chairperson

University of California, Riverside

ACKNOWLEDGMENTS

I owe the biggest thank you to my advisor, Dr. Peter Sadler, for guiding me through his CONOP program and its use for the Cenomanian-Turonian oceanic anoxic event, and for all of his suggestions during the two year program and with this thesis. I would also like to thank Dr. Jeremy Owens for creating the challenges addressed in the thesis from Ph.D. work he completed at UC Riverside. Another thank you to Drs. Sandra Kirtland Turner and Nigel Hughes for giving me insightful comments and advice during the thesis process. A last thank you to all of my family and friends including: Frances Messenger, Charles Keller, Carl and Holly Keller, Gilberto Noriega, Rachel Kolenko, Matt Knauss, Emily Dackins, Kristen and Linda Colley, and Sherry Mashburn for their support in various ways throughout my time in the program.

This research was funded by a UC Riverside Graduate Division Fellowship and Geology Departmental Teaching Assistantships. Additionally, I attended the 2014 Stratigraphic Paleobiology Field Course in south-central Montana funded by the Paleontological Society with side funding from InfoQuest where, thanks to Drs. Steve Holland and Mark Patzkowsky, I understand more about what it takes to get field data and how many various ways there are of interpreting it. The funding and experiences gained during my thesis have given me invaluable opportunities I will carry with me always.

ABSTRACT OF THE THESIS

Preliminary High-Resolution Time-Lines Through the Cenomanian-Turonian (Late Cretaceous) Oceanic Anoxic Event (OAE 2)

by

Allison Lynn Keller

Master of Science, Graduate Program in Geological Sciences
University of California, Riverside, August 2015
Dr. Peter M. Sadler, Chairperson

Rapid changes in Earth's marine environment are sufficiently rare that the scope and consequences of these events cannot be inventoried without recourse to the stratigraphic record of deep pre-historic time. Traditional stratigraphy divides geologic time into a succession of coarse biozones – uneven time bins, each recognized by distinctive index fossils and spanning several hundred thousand to even a few million years. This thesis uses the CONOP software to resolve sequences of global appearance and disappearance events at the species level across the late Cenomanian oceanic anoxic event (OAE 2) at a much finer resolution than traditional biostratigraphy. The resulting time-lines include information for the Aptian to Maastrichtian from 501 locations, 4,962 taxa, and 25,112 local last occurrences. This dataset is large enough to represent the global environment and to compensate for the inevitably patchy and incomplete record preserved at any one location. Six geographically widespread clades – ammonites,

calcareous nannofossils, dinocysts, benthic forams, planktonic forams, and radiolaria – were analyzed; they span a range of trophic levels, composition and preferred habitat.

Extinction pulses and intervals of falling diversity are not unique to OAE 2 or even uniquely severe. Several occur throughout the Albian-Santonian interval. The key is to monitor trends in diversification rate. OAE 2 is distinguished as a boundary between more positive (or equal in the ammonite case) and more negative diversification regimes. It may have been part of a general habitat deterioration or disturbance, but it would be too simplistic to describe it as a coordinated pelagic extinction event.

TABLE OF CONTENTS

LIST OF FIGURES

Chapter 1

Chapter 2

Chapter 3

Chapter 4

LIST OF TABLES

Chapter 1

Chapter 2

CHAPTER 1 - INTRODUCTION AND BACKGROUND

> *“The exact sequence of events is still not clear, but the end result is almost beyond question.” - (Wignall, 1994, for the BGS)*

1.1 MOTIVATION

Immediately prior to the Cenomanian/Turonian (C/T) stage boundary (ca. 93.9 Ma; Gradstein et al., 2012), the mid-Cretaceous ocean and its biota underwent an interval of remarkable change that was sufficiently widely preserved to assist global correlation. Laminated carbonaceous mudrocks (so called “Bonarelli” black shales) record anoxic bottom waters in several marine basins. This is the second Cretaceous oceanic anoxia event (“OAE 2” of Schlanger & Jenkyns, 1976; Jenkyns, 1980; Arthur et al., 1987). The dark shales are associated with a positive carbon isotope anomaly (Scholle & Arthur, 1980; Arthur et al., 1985; Jenkyns, 1985; Gale et al., 1993) (Figure 1.1-1), which can be recognized beyond the black shale environments and has become diagnostic for OAE 2. Changes in fossil biotas across this interval have been attributed to one of the mass extinctions that is recognizable in the classic stage and substage compilations of the fossil record of families and genera (Raup & Sepkoski, 1986; Jarvis et al., 1988; Harries & Kauffman, 1990; Jablonski, 1991; Kaiho & Hasegawa, 1994; Hallam & Wignall, 1997) (Figure 1.1-2).

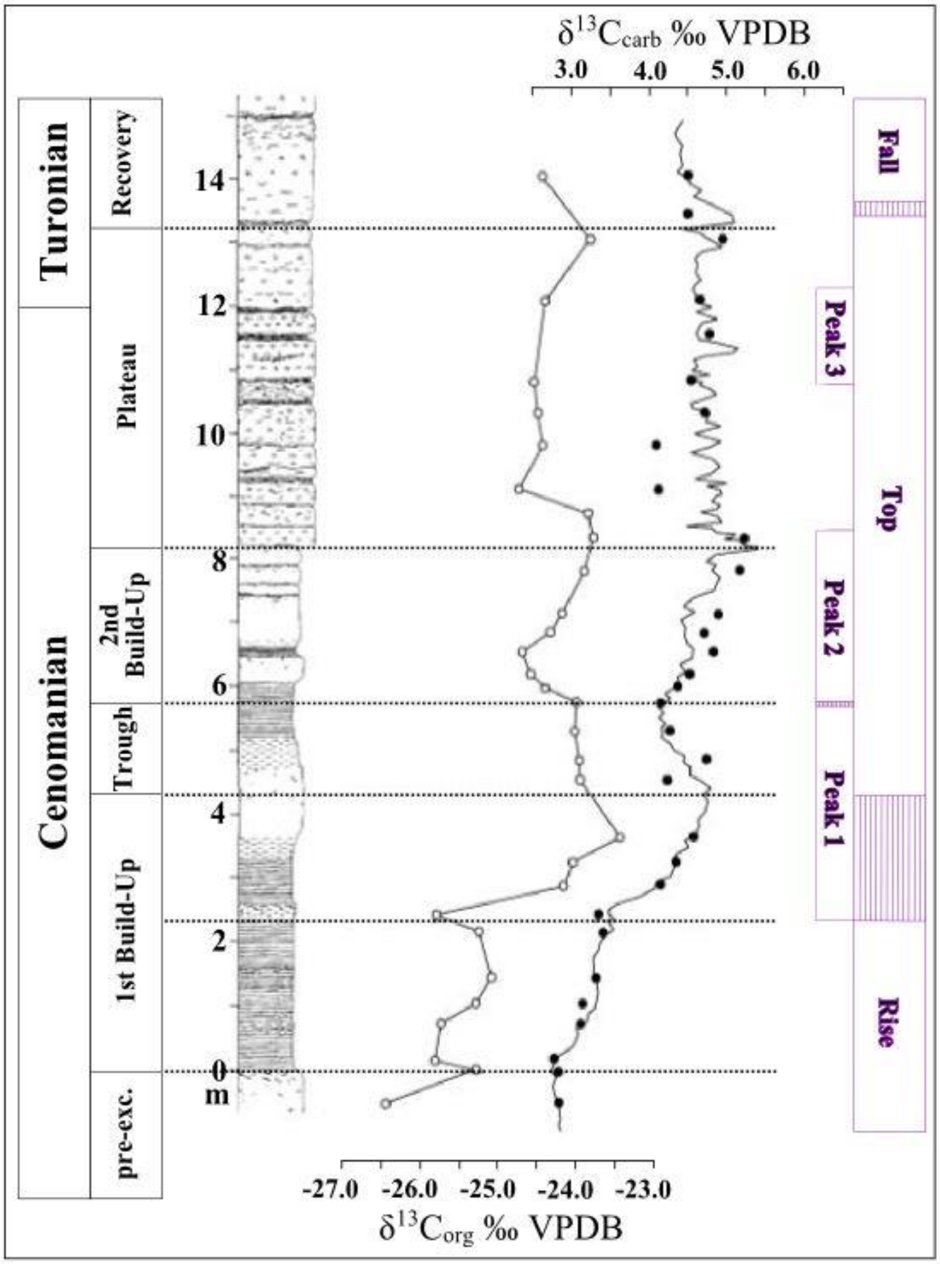

Figure 1.1-1: An example of the OAE 2 carbon isotope excursion from Eastbourne, Sussex, where it is expressed in both carbonate analysis (black dots) and organic carbon analysis (open dots) *modified after Kennedy et al. (2005) and Gale et al. (2005)* to show the subdivision on the excursion into parts - on the left - generally recognized in the literature for correlation and timing. On the right is a breakdown of how this section was entered for graphic correlation - see methods chapter. These characteristics are seen coinciding with a black shale interval.

The evolutionary response to environmental change plays out at the species level, however, and the time span of OAE 2 appears to be significantly briefer than the resolving power of published Phanerozoic mass extinction analyses such as shown in Fig. 1.1-2. The duration of OAE 2 is variously estimated at 70 Ka in the Arobes section, Spain (Melinte-Dobrinescu et al., 2013), 90 Ka in the Global Stratotype Section and Point (GSSP) locality near Pueblo, Colorado (Keller & Pardo, 2004), 250 Ka in the Dover section, England (Lamolda et al., 1994), and even upwards of half a million years or so in Bahloul, Tunisia (Caron et al., 1999), Eastbourne, England (Paul et al., 1999), and globally from nine Atlantic and Tethys Ocean basin localities (Arthur et al., 1988). Global compilations have not yet approached this fine resolving power. Although it can be achieved for parts of individual sections and cores, regional compilations are necessary to overcome the patchiness of habitats and hiatuses. Global scope is required to capture extinction. Fortunately, automated sequencing techniques now make it possible to sequence time-lines of thousands of species origination and extinction events from hundreds of localities (Sadler, 2010; Sadler et al., 2014) and approach event-to-event resolution of hundreds of thousands to tens of thousands of years for pelagic faunas, even in Paleozoic rocks (e.g. Sadler et al., 2009; Cooper et al., 2013). This thesis develops such a time-line across OAE 2 to serve as a basis for temporally and geographically highly resolved analyses of evolutionary dynamics. Specifically, the thesis will examine the hypothesis that the response of species to OAE 2 is more often migration than extinction; i.e. that the well-known concentration of species range ends in OAE 2 reflects local changes in habitat and preservation more than global disappearance.

The thesis presents a method for inferring extirpation and examines the pattern of true extinction pulses.

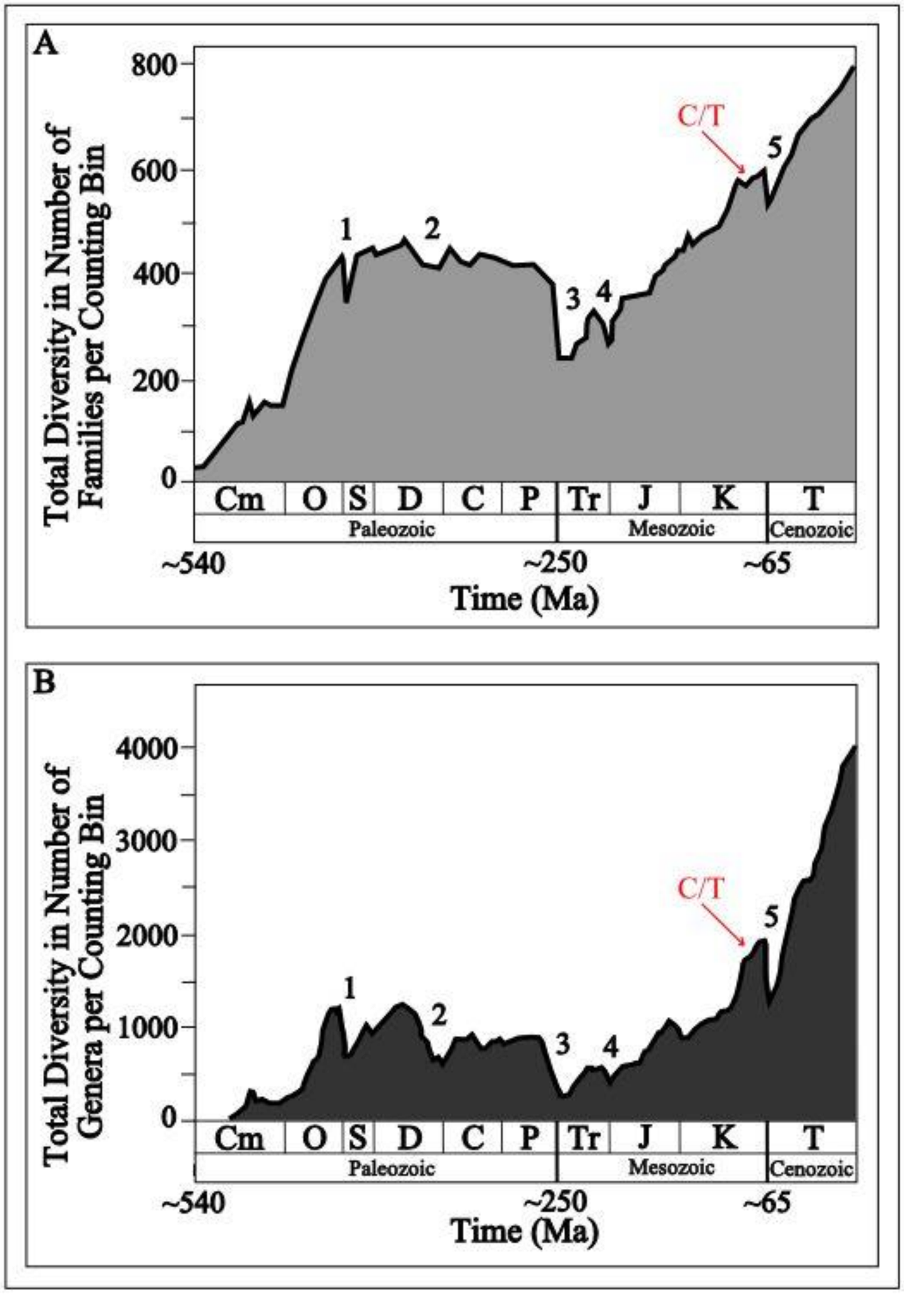

Figure 1.1-2: Phanerozoic [A] family and [B] genus richness histories, show the C/T relative loss during the so-called "big five" mass extinctions. 1) Late Ordovician, 2) Late Devonian, 3) Late Permian, 4) Late Triassic, and 5) Late Cretaceous. Abbreviations are as follows: Cm=Cambrian, O=Ordovician, S=Silurian, D=Devonian, C=Carboniferous, P=Permian, Tr=Triassic, J=Jurassic, K=Cretaceous, and T=Tertiary. The y-axis scales raw taxon totals for successive time intervals that differ between the two curves. Richness loss is a balance of origination rate and extinction rate; the extinction component cannot be separated from richness curves alone. *Modified after: http://archive.larouchepac.com/node/21941*.

First and last occurrences of species are the vast majority of events in the time-line. They are limited to pelagic fossil clades that have long been preferred for biostratigraphic zonation. These clades have not only a suitably wide geographic distribution but also the taxonomic stability that emerges from international correlation projects. The selected clades are mostly planktonic or nektonic and preserved in both deep and shallow-water sediments. The time-line may eventually provide a framework for inclusion of the more provincial, shallow-water, shelly, macro-benthos that surely contribute considerable numbers to the richness statistics on which classic recognition of Phanerozoic mass extinctions are based (Fig. 1.1-2). However, that augmentation is far beyond the scope of this 2-year foundational project.

Environmental events are also incorporated into the time-line from the outset. These include isotopic ratio excursions, black shale intervals, and dated ash falls. As in comparable published examples (Sadler, 2012; Sadler et al., 2014), the biostratigraphic and other event types have been incorporated in a manner such that neither one drives the correlation and sequencing alone. Before introducing the methods and data in greater detail, it is useful to discuss briefly the terminology of extinction, review C/T paleogeography, and lay out the challenges that the numerical methods must overcome.

1.2 BIOLOGISTS' TERMINOLOGY FOR EXTINCTION

Fossil species can disappear from a measured section or core for a variety of geological and biological reasons. To review how absence may be an artefact of the fossil record, we first need precise terms for different types of real biological disappearance. Biologists' terminology is clear and straightforward. It rests on the spatial and temporal scope of absence (Table 1.2-1). Disappearance of a taxon can have three larger contexts. It may be: 1) a local instance of global and permanent extinction; 2) a purely local, but permanent, absence that biologists term extirpation to distinguish it from full extinction; or 3) local but temporary absence, distinguished here as excursion because the species later returns, perhaps in response to restoration of the preferred habitat. By definition, therefore, extinction cannot be deduced from a single section or core, regardless of the time span or richness of the fossil-bearing beds. Given globally-distributed sections, it is also necessary that their time span be longer than the likely taxon durations. Otherwise, too many range ends will coincide with the local limits of sampling. Extirpation or excursion may be seen at a single locality. A species can have only one extinction and, technically, only one location can record the very last occurrence. A species could have as many extirpations as localities and many excursions at every locality. Thus, the hypothesis that extirpation and migration are more common responses to OAE 2 than extinction is expected to be true. It is examined here for six clades that meet the requirement that they have been recovered from widespread localities throughout the global mid-Cretaceous ocean. The time-line establishes the framework for analyzing spatial and temporal patterns of extirpation. The analytical approach will be illustrated for a sample taxon, but it is beyond the scope of the thesis to analyze and summarize the pattern of extirpation across all 25,112 local last occurrences observed for the 4,962 taxa compiled. The time-line will be analyzed in full for the timing of extinction pulses and reductions in origination rate in and around the OAE 2 interval - a test of the role of extinction.

	Global	**Local**
Temporary	(Implausible)	Excursion[2]
Permanent	Extinction[1]	Extirpation[1]

Table 1.2-1: Biological terms for the disappearance of species. ([1] Standard strict usage; [2] Adopted here).

1.3 CENOMANIAN-TURONIAN PALEOGEOGRAPHY

The mid-Cretaceous oceanic realm may be divided into four regions: Arctic, Atlantic, Pacific, and Tethys. Each region includes local records of anoxic black-shale environments. The regions differ in orientation, width, and their stage in the Wilson Cycle (Figure 1.3-1). The Atlantic and western Tethys were both narrow seas. The Atlantic Ocean extended north-south across climate belts and was in the early stages of opening. The Tethys seaway extended east-west, mostly at low latitude and was in a late stage of closing, especially on the western side. In eastern Tethys, the Indian subcontinent was still far from Asia; no Tibetan Plateau existed. There were no deep connections between the North Atlantic and Arctic Oceans, nor between the South Atlantic and Pacific Oceans.

The mid-Cretaceous climate was warm. Temperature proxies from both marine and terrestrial environments indicate an equator-to-pole temperature gradient smaller than today (Kuypers & Pancost, 2002). High Cretaceous sea-surface temperatures are associated with a higher-than-modern sea level. Sea level rose through the Cenomanian period and reached a Phanerozoic maximum in the Early Turonian (Hancock & Kauffman, 1979; Haq et al., 1987; Hallam, 1992; Gale et al., 2000). The continental lithosphere was flooded to generate epicontinental seaways and shelves of great extent, largely without good modern analogs. Volcanism figures prominently in explanations for mid-Cretaceous climate and sea level (Larson, 1991; Kerr, 1998; Snow et al., 2005; Kuroda et al., 2007; Pearce et al., 2009). Several large igneous provinces of this age have been identified (Coffin & Eldholm, 1994) and interpreted to have influenced sea-floor elevations and atmospheric CO_2 levels (Arthur et al., 1985; Bice & Norris, 2002, Leckie et al., 2002). Their impact would be enhanced by inefficient circulation likely in narrow parts of the global ocean with weak connections to cold high-latitude seas (Schlanger & Jenkyns, 1976).

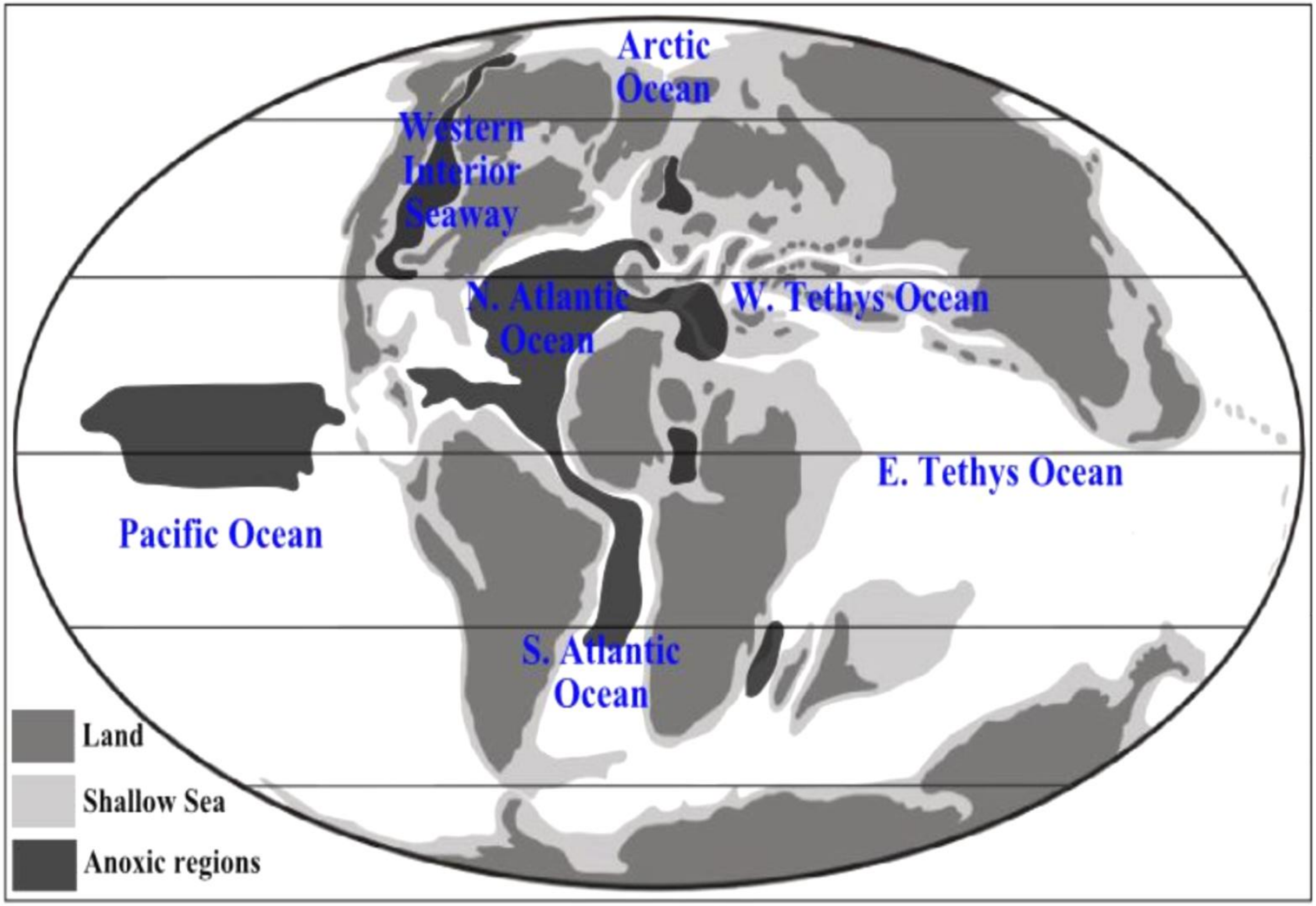

Figure 1.3-1: Narrow oceans and shallow seaways are causes for poor circulation and anoxia during the end-Cenomanian paleogeography. *Map simplified after Ron Blakey. Anoxic regions redrafted from Wignall, 1994 for the BGS.*

1.4 ANOXIA AND CARBON ISOTOPES

Anoxia has long been inferred from local late Cenomanian facies changes and OAE 2 is now defined by carbon isotope excursions which are more widely recognized than anoxic facies. The association of oxygen-deprived facies and carbon isotope anomalies can be explained by various mechanisms that are not necessarily mutually exclusive. Geochemical modelling of carbon isotope anomalies not only supports the evidence of widespread anoxia indirectly, but also makes the case that the interval of rising isotopic ratios must be sufficiently brief for precise global correlation. Of course, the OAE 2 anomaly must first be distinguished from other Cretaceous isotope excursions by biostratigraphy.

Oceanic Anoxic Event 2

In the mid-Cretaceous there were between two and seven of these global OAE-type events (Schlanger & Jenkyns, 1976; Arthur & Schlanger, 1979; Jenkyns, 1980; Arthur et al., 1987; Sliter, 1989; Arthur et al., 1990; Bralower et al., 1993, 1999; Erbacher et al., 1996; Erbacher & Thurow, 1997; Leckie et al., 2002). Anoxia is typically found in deep ocean basin environments, as well as in outer shelf-continental margins, and epicontinental seaways (Ryan and Cita, 1977; Arthur and Schlanger, 1979; Gale et al., 2000; Bowman and Bralower, 2005). Causes set forth to explain anoxic events include 1) sea-level rise with transgression in both epicontinental and marginal locations that effectively triggered high productivity (Schlanger & Jenkyns, 1976; Jenkyns, 1980; Leckie et al., 2002; Pearce et al., 2009) and 2) a warmer-than-modern climate that reduced cold oxygenated bottom waters and altered the depth of the oxygen-minimum layer (Schlanger & Jenkyns, 1976; Schlanger et al., 1987; Arthur et al., 1987; Jarvis et al., 1988; Kaiho & Hasegawa, 1994; Busson & Cornee, 1996; Hart, 1996; Caus et al., 1997).

Anoxic bottom water conditions favor high rates of burial of marine organic matter that remains unoxidized and naturally rich in ^{12}C (Arthur et al., 1987; Uličný et al., 1997). This is probably coupled with preferential extraction of the lighter carbon isotopes (^{12}C) as a result of enhanced marine plankton productivity in the warm surface waters (Jenkyns, 1980; Uličný et al., 1997; Kuypers et al., 2002; Lenniger et al., 2014). The result is such a strong association of the C/T black shales with a positive carbon isotope ratio that the excursion has become diagnostic for OAE 2.

The δ^{13}C Excursion

The OAE 2 carbon excursion peaks in the late Cenomanian. The return to background values occurs after the C/T boundary. δ^{13}C enrichment during the positive excursion was initially recorded for $\delta^{13}C_{carb}$ as ~1.5-2 per mil and $\delta^{13}C_{org}$ as ~3.5-4 per mil (Arthur et al., 1988). This pattern has since been recorded globally (Jenkyns, 1980; Herbin et al., 1986; Schlanger et al., 1987; Gale et al., 1993; Uličný et al., 1997; Gale et al., 2000) and in both carbonates ($\delta^{13}C_{carb}$; Scholle & Arthur, 1980; Schlanger et al., 1987; Jarvis et al., 1988; Gale et al., 1993; Paul et al., 1999; Tsikos et al., 2004) and organic matter ($\delta^{13}C_{org}$; Pratt & Threlkeld, 1984; Pratt, 1985; Arthur et al., 1988; Hasegawa, 1997; 2003; Hasegawa et al., 2003). Although variations in the anomaly are reported (Hilbrecht et al., 1992), the use for a global, rather than just local correlation has become common practice (Gale et al., 1993; Uličný et al., 1997; Keller & Pardo, 2004; Kennedy et al., 2005). Biostratigraphic index fossils readily distinguish the different OAE events and make the case that OAE 2 is of approximately the same age (isochronous) everywhere. Striking similarities in the details of the form of the OAE 2 excursion (but not the actual isotope ratio values) make the case for more detailed correlation, and considerations of oceanic mixing-time support this view. Gale et al. (1993) reported similar profile peaks in the isotopic anomaly from the Western Interior Seaway and the British Chalk. Uličný et al. (1997) found similarities between Bohemian, North American, and Northern African sections.

For automated correlation the excursion can be divided into several parts. The best candidate for correlation is said to be the steepest initial rise in values, but chemostratigaphers also attempt to match 2-3 individual peaks that occur after the initial build-up (e.g. Gale et al., 1993; Hasegawa, 1997; Caron et al., 2006; Melinte-Dobrinescu et al., 2013). The reported pattern of values through the anomaly typically consists of four main phases: build-up 1, build-up 2, plateau, and recovery (Paul et al., 1999; Gale et al., 2005; Caron et al., 2006; Melinte-Dobrinescu et al., 2013). For this thesis I add 1-3 local peaks, where expressed, so that the excursion is broken down into a maximum of six parts: the rise, top, fall, peak 1, peak 2, and peak 3 (Figure 1.1-1). The parts are recorded as a conservative uncertainty interval that deal with more and less distinct patterns and differences in sampling intensity. The uncertainty intervals may overlap.

One strategy in assessing uncertainty is to imagine the impact on the shape of the curve of an additional high or low ratio between adjacent samples.

1.5 REPORTED BIOTIC RESPONSES TO OAE 2

The C/T has been claimed to be the third largest post-Palaeozoic mass extinction event based on faunal turnover rates (Raup & Sepkoski, 1984; but see Gale et al., 2000). Only the end-Cretaceous and the Norian-Rhaetian events appear to have been more devastating (Raup & Sepkoski, 1984). Counts of fossil marine taxa suggest that as many as 7% of families, 26% of genera and 53% of species went extinct as a consequence of the C/T event (Raup & Sepkoski, 1986; Sepkoski, 1989; Jablonski, 1991; Harries, 1993). The counts include marine macrofossils (Raup & Sepkoski, 1986; Elder, 1989; Kauffman, 1995; Harries & Little, 1999), especially marine benthic clades (Jarvis et al., 1988; Hart & Leary, 1991; Kaiho et al., 1993; Kaiho & Hasegawa, 1994; Paul et al., 1999; Lauridsen et al., 2009), but also planktonic microbiota (Paul & Mitchell, 1994; Hart & Leary, 1991; Lamolda et al., 1994; Paul et al., 1999; Leckie et al., 2002; Gebhardt et al., 2010).

The significance and even the existence of a C/T mass extinction has, nevertheless, been cast into some doubt by closer analysis of individual clades. Gale et al. (2000) list some of the causes for doubt. Foraminiferal data from Banerjee & Boyajian (1996) reveal smaller generic extinction levels -- only a 17% loss. Reanalysis of the Raup & Sepkoski (1984) data by Patterson & Smith, (1987; 1989) find that echinoderm and fish data at the family and genus levels lack support for a significant extinction at the end of the Cenomanian. Additionally, Hora & Marshall (1998) found no evidence for an end-Cenomanian extinction event in marine faunas from the Western Interior Basin, USA.

The following paragraphs summarize the characteristics of the six clades selected for the time-line analysis. Five of them are microfossils. They include calcareous, siliceous and organic-walled shells and cysts. Conflicted findings concerning their participation in an OAE 2 extinction event probably result from the limited geographic scope of many studies. Associated faunal changes are to be expected in sections and cores at such dramatic changes in sedimentary facies and preservation potential as mark the onset of the Bonarelli black shales. The more discriminating of the single-section paleo-ecologic studies have tracked local changes in relative abundances of taxa. My time-line is limited to binary presence-absence information.

Ammonites

Ammonites are cephalopod animals with large chambered calcium carbonate shells. They are nektonic heterotrophs - the largest individual organisms and highest in the food chain of all clades to be included. Elder’s (1989) study of Western Interior Seaway ammonites during the C/T found 74% of the species going extinct. Pacific Ocean ammonite faunas are said to lose diversity in response to anoxia at the C/T boundary (Hirano et al., 2000), but the extent of extinction is found to be variable and highly dependent on location (Monnet, 2009). Monnet also notes that the richness minimum at the C/T interval may be explained by failure of origination. The time-line analysis will separate origination and extinction rates.

Calcareous Nannofossils

Calcareous nannofossils are tiny plates that coat unicellular eukaryotic phytoplankton (algae). The plates reach only a few micrometers in length. They are calcium carbonate in composition. The host organism is an autotrophic primary producer in the food chain. During OAE 2 a nannofloral turnover event is characterized by disappearance of high-fertility taxa and reduced assemblages (Melinto-Dobrinescu et al., 2013). This shift starts in the $\delta^{13}C$ second build-up phase and continues into the plateau phase (Melinto-Dobrinescu et al., 2013) where it may be due to OAE 2 (Leckie et al., 2002). Although some researchers note losses in diversity (Jarvis et al., 1988), abundance (Paul et al., 1999), and high rates of turnover (Leckie et al., 2002), others find only minor assemblage changes and select areas of enrichment and high abundance in particular nannofossil species, when compared to macrofossils and foraminifera (Bralower, 1988, Lamolda et al., 1994).

Dinoflagellates

The dinoflagellate cyst, or dinocyst, is a tiny (up to tens of micrometers) organic-walled part of the life cycle of protists that may be planktonic or benthic, and heterotrophic or autotrophic. Reported at the end of the Cenomanian is a decline in dinocyst abundance (Lamolda et al., 1994; Lamolda & Mao, 1999; Pearce et al., 2009), productivity (Pearce et al., 2009), and diversity (Jarvis et al., 1988; Lamolda & Mao, 1999). Species richness and numbers are said to remain low into the Turonian (FitzPatrick, 1995; Pearce et al., 2009).

Benthic Foraminifera

Benthic foraminifera are small (diameters typically reaching a millimeter or two), bottom dwelling heterotrophs. Most have calcium carbonate tests. The agglutinated foraminifera build tests of sand grains or other particles which they cement together. Within the C/T boundary interval, diversity, size, and abundance of benthic foraminiferal species have been found to decline (Paul et al., 1999; Gebhardt et al., 2010). The drop in abundance correlates to the onset of the $\delta^{13}C$ excursion plateau phase (Paul et al., 1999). High extinction percentages have also been found coincident with the anoxic event (Kaiho & Hasegawa, 1994).

Planktonic Foraminifera

The millimeter-sized tests of planktic foraminifera have long been used for correlation and environmental interpretation. They are multi-chambered and of calcium carbonate composition. Some local studies associate reductions in diversity (Jenkyns, 1985; Lamolda et al., 1994; Paul et al., 1999), size (Lamolda et al., 1994; Paul et al., 1999; Wagreich et al., 2008, Gebhardt et al., 2010), and abundance with the C/T boundary interval. This persists into the Turonian (Lamolda et al., 1994; Paul et al., 1999; Wagreich et al., 2008). Other studies find sections with relatively high diversity and abundance, which they recognized as possible refugia; one of these is the Penninic Ocean (Gebhardt et al., 2010).

Radiolaria

The radiolaria are tiny (a few hundreds of micrometers) siliceous tests of planktonic heterotrophs. A dramatic faunal change and diversity reduction has been reported from the mid OAE 2 (Musavu-Moussavou et al., 2007). Other authors report an extinction pulse in the lower part of the Bonarelli black shales followed by an origination pulse in the upper part (Erbacher et al., 1996; Erbacher & Thurow, 1997; Musavu-Moussavou et al., 2007). Abundances vary throughout the upper Cenomanian and into the lower Turonian, but undeniably decrease in the black shale interval before increasing again during the early Turonian (Musavu-Moussavou et al., 2007; Gebhardt et al., 2010).

1.6 STRATIGRAPHIC EVIDENCE OF ABSENCE

Stratigraphic evidence of absence is rarely unequivocal (Sadler, 2013). Failure to find fossils does not imply the species was extinct and difficulties are compounded by reliance on too few stratigraphic sections. Local first and last occurrences of fossil species may be poor approximations of local immigration and emigration events and cannot be interpreted in isolation as origination and extinction events. Contradiction in the sequence of first and last occurrence events from section to section are commonplace for many reasons: (1) patchy distribution of living taxa, (2) faunal migration, (3) diachronous extirpation, (4) incomplete preservation, (5) incomplete collecting, and (6) imperfect identification. All these factors naturally justify skepticism about hypotheses of extinction. Biases in the preserved rock record may carry forward to interpretations. Doubts may be reduced by resorting to larger datasets, standardized sample sizes, and incorporation of methods to place confidence intervals on range ends (Patzkowski & Holland, 2012).

My composite time-line applies Patzkowski and Holland’s recommendation for a large data foundation. They also improve upon the confidence interval strategy (Marshall, 2010), which was designed for single sections. Confidence intervals on the range end are infinitely long for a species that is found at only one horizon (Strauss and Sadler, 1989). To determine whether it is a truly short-lived taxon or a rarely seen long-ranging taxon, paleontologists naturally examine more sections; a truly short-lived taxon will always have a short local range and similar associated species. Composite sections incorporate this strategy. After the local ranges are mapped back into the composite, it is possible to make more insightful statements about local range-end uncertainties.

Composite time-lines remedy the fundamental shortcoming of single sections and cores. At best, a single section records only one patch in one depositional setting at any preserved moment. Not all moments are preserved, but a preserved fauna may usefully (for our purpose) telescope several habitats (different water depths) and mix true inhabitants with transported post-mortem remains. In practice preservation and collection are incomplete. Composite sections combine many places, basin-wide or globally. Those that combine nearby cores and sections can fill-in the unavoidable gaps in preservation and collection. For global interpretation composite time-lines are essential to combine disparate latitudes, habitats, and preservation styles.

Difficulties in building fully-resolved composite sections go back to the limitations of the information content of the single sections. More is better, because added sections usually bring more information and thus a better resolved time-line, but more sections increase calculation time exponentially. Optimal sequences can take many days or even a few weeks to find by hand. Historically, multiple sections were first combined into correlated fence diagrams by means of discrete biostratigraphic stages and biozones. Single researcher compilations (e.g. Sepkoski, 1989) and the first computer-assisted community databases (e.g. the Paleobiology Database) tended to rely on these same discrete time-bins, which imposed a limit on resolving power. Half a century ago, however, Shaw (1964) had already introduced the notion of building continuous time-lines (composite sections) instead of casting paleontological data into discrete time bins. Shaw’s graphic correlation allows every section to contribute information even if it is too sparse for detailed correlation into a stratigrapher’s fence diagram. This rehabilitation of all scraps of information improves the time-line but exacerbates the problem of calculation time. That dilemma is solved by heuristic search algorithms and modern computing power.

CHAPTER 2 - SCOPE AND METHODS

2.1 DATABASE SCOPE

Information content of the clades

To resolve the sequence of biotic and geochemical events during intervals of rapid global change it is crucial to combine information from as many localities as possible. Individual stratigraphic sections and drill cores are incomplete and parochial accounts of events. Global scope is essential to demonstrate extinction and requires records from many regions; using several localities in each region mitigates incompleteness. Additionally, species-level data are desirable because this is the level at which evolution operates. This thesis is based on a compilation of local records totaling 50,224 range-end observations for the 4,962 taxa in 501 sections.

The amount of information compiled for each clade can be represented by the numbers of sections and taxa included, but measures of useful information content must go deeper (Table 2.1-1). Rich sections and fossiliferous horizons are more informative than sparse sections and depauperate faunas. The total number of observed range ends captures the richness of the data compiled. To constrain their relative positions in a time-line in any useful way, however, taxa must be found with known superpositional relationship to one another in the same section. Two measures capture these constraints. One counts the number of observed pairwise coexistences of taxa. The other counts the number of instances in which the first occurrence of one taxon is seen below the last occurrence of another, whether or not they coexist. These two measures are evidence of superposition that cannot be falsified by new finds and range extensions; i.e. they are immune to the problems of evidence of absence. Both measures could be standardized by expressing them as a fraction of the number of possible pairs of taxa.

This thesis builds a separate time-line for each clade. They are calibrated to a common time scale using dated ash-fall tuffs and international estimates of the age of stage boundaries. Ultimately, a single time-line might be built from all the data, but two difficulties would have to be overcome. The first is simply the exponential increase in computation time. Faster processors and parallelized code overcome this hurdle. The second is the need for cross-clade sequence constraints. Without observed pairwise coexistences and first-before-last constraints between taxa of different clades, the sequencing algorithms will tend to cluster range ends by clade to the extent possible to avoid implying coexistences that have not been observed. Currently, the tally of cross-clade coexistences is too meagre (Table 2.1-2). Unless the level of cross-clade coexistence information reaches the level of within clade coexistence information a multi-clade time-line might artificially cluster events by clade in detail. This happens because, to the extent possible the algorithms avoid implying additional coexistence. This shortcoming is not easily remedied, because the clades tend to be best preserved and most easily extracted from different facies. There are not enough radioisotopic age determinations or magnetostratigraphic reversal horizons to compensate for the facies differences.

	Ammonites	Coccoliths	Dinocysts	Benthic Forams	Planktic Forams	Radiolaria
Sections	477	394	393	399	412	390
Taxa	1,828	444	491	1,040	373	786
Observed Range-end Events	11,330	9,754	5,110	6,500	7,912	7,620
Pairwise Coexistence Constraints	11,367	26,272	26,999	23,929	7,921	40,869
Pairwise First Before Last Constraints	85,007	58,189	62,969	69,838	25,747	100,070

Table 2.1-1: These are simple measures of the information content from the database. The top two rows summarize geographic and taxonomic scope, the middle row is the volume of raw data entered, and the bottom two rows total the derived information that constrains the time-line.

	Ammonites	Coccoliths	Dinocysts	Benthic Forams	Planktic Forams	Radiolaria
Ammonites	**XXXXX**	*0.007*	*0.005*	*0.002*	*0.005*	*0.0003*
Coccoliths	**5,690**	**XXXXX**	*0.09*	*0.03*	*0.1*	*0.02*
Dinocysts	**4,496**	**20,353**	**XXXXX**	*0.03*	*0.7*	*0*
Benthic Forams	**3,223**	**14,370**	**14,987**	**XXXXX**	*0.02*	*0.003*
Planktic Forams	**3,184**	**15,973**	**125,818**	**8,548**	**XXXXX**	*0.01*
Radiolaria	**453**	**6,016**	**0**	**2,763**	**2,838**	**XXXXX**

Table 2.1-2: The tally of observed, cross-clade, coexistence constraints. Bold font values are the raw counts of observed pairwise coexistences involving species from two different clades. The italic font values express the raw counts as a fraction of all possible cross-clade pairs.

Information content of other events

Other events incorporated into the database include: stage boundary ages, carbon isotopic ratio changes (carbonate and organic), marker beds (black shales, red beds), and heavy metal isotopes (Fe, Mn, Mo). The stage ages aid in correlation between individual clade experiments. $\delta^{13}C$ excursions observed in both carbonate and organic material fall into their appropriate places on the single clade ordinal scale and later assist in determination of diachronism or synchronism. The marker beds and heavy metal isotopes in the database were not analyzed for this thesis, but are among the geochemical indicators of the environment.

2.2 SEQUENCING METHODS

All information must be correlated with better resolving power than traditional biozones. Neither geochemical signals nor taxon range ends may drive the correlation exclusively. Instead, we use the principles of graphic correlation, introduced by Shaw (1964), to find sequences of events that best fit all the field data. To overcome the huge volume of information we use an automated CONstrained OPtimization (CONOP) method.

Literal correlation of first and last occurrences of taxa leaves unreasonable crossed lines or “tangles” in the fence diagram (Figure 2.2-1a). This is direct evidence that many events are diachronous, but does not identify which are diachronous or by how much. In effect, traditional biostratigraphic zonation resolves the tangles by removing events -- the fewest necessary such that no crossed lines occur. The result is simple but low in resolution. The few remaining events are found in the same order everywhere (Figure 2.2-1b). This strategy must succeed if enough taxa are removed, leaving only those that do not coexist. If ranges do not overlap, it is not possible to find the range-end events in contradictory order, even if preservation is incomplete. Unfortunately, the strategy cannot possibly resolve all species range ends; many taxa do coexist (Tables 2.1-1 and 2.1-2 are minimum estimates).

Following Shaw's (1964) graphic correlation method, CONOP approaches the problem differently. It finds the least amount of adjustment necessary to place all trustworthy events in the same order everywhere. Adjustments of local range ends are limited to those that stretch the observed range ends. Shaw (1964) solved for sequencing and spacing of events. Spacing was determined by rock thicknesses between events in the best local section. Thus, in traditional graphic correlation the spacing problem was solved using a weak assumption that greater rock thickness indicated more elapsed time, even when the thicknesses were not measured in the same sections. The sequencing task is much better constrained by stratigraphic superposition and requires fewer and simpler assumptions. Edwards' (1978) "no-space graphs" were an early variant of graphic correlation that isolates and solves the sequencing problem only. CONOP follows this strategy; it applies additional assumptions to solve the spacing task after the optimal sequence has been found. To mimic Edward's logic, I set the CONOP run-time variables to measure range adjustments by the numbers of event horizons, not rock thickness.

It is computationally simple to integrate the adjustments of taxon ranges (which stretch to fit), carbon isotope excursion segments (which shrink to fit), and ash bed horizons (which may not move) because all adjustments are measured in the same units. CONOP finds the composite time-line that requires the least sum of adjustments by brute-force trial-and-error (Sadler, 2010). With the smallest sum of all adjustments made, all the local range charts can be put into agreement with the best high-resolution global sequence of events where all observed coexistences are honored (Figure 2.2-1c).

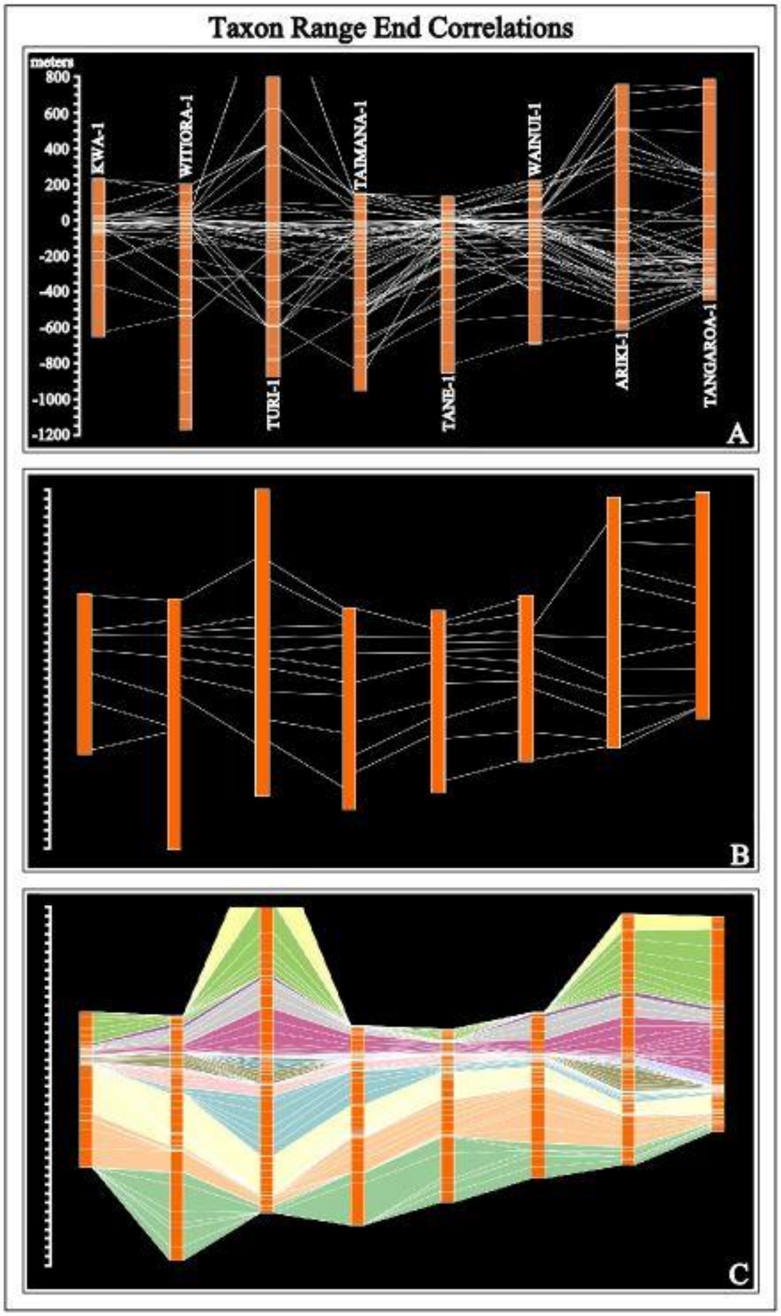

Figure 2.2-1: Paleocene to lower Miocene correlation in Taranaki Basin, New Zealand, illustrates resolving power of different biostratigraphic strategies. Literal correlation of raw range ends [A] is not reasonable. Traditional biostratigraphy [B] removes the fewest possible crossed lines to resolve the unreasonable "tangles," which lowers resolution. Graphic correlation and CONOP algorithms [C] adjust the lines by the least amount possible resulting in a higher resolution outcome. *Modified from Cooper et al., 2001*.

In the final time-line the composite range will be drawn through all times at which the taxon is known *anywhere* (Fig. 2.2-2). The best estimate for the position of an event that has been represented by uncertainty intervals will be the time interval in which it may be seen *everywhere.* When uncertainty intervals for an isotope excursion (the six segments - each with their own maximum and minimum stratigraphic value) are mapped back into the composite time-line, some appear surprisingly long. This is a result not so much of the local indistinctness as it is of a lack of accompanying fossils that indicate age. Local taxon ranges are less prone to this effect because they are much more abundant in the data set. Nevertheless, it remains difficult to determine the age of range ends that coincide with the top and bottom of a section; the limits of a section artificially truncate ranges and, unlike levels within the section, cannot be bracketed by fossils above and below.

In addition to acceptable approximations of real taxon range ends there will be many range ends in the compiled data that are mere coincidences with the ends of a measured section or core. Within the sampled interval, these will be mitigated by two factors: 1) extension of local ranges beyond a section limit is cost-free in the optimization process; and 2) section limits are likely to be randomly distributed within the sampled interval. The bigger potential problem occurs at the limits of the sampled interval which, for this reason, must be extended beyond the interval to be interpreted. Thus the artificial range truncations are limited to "buffer zones" that are ignored during interpretation. The Aptian through Maastrichtian stages were exhaustively compiled to broaden this dataset and buffer the Cenomanian-Turonian interval from interference by artificial range ends.

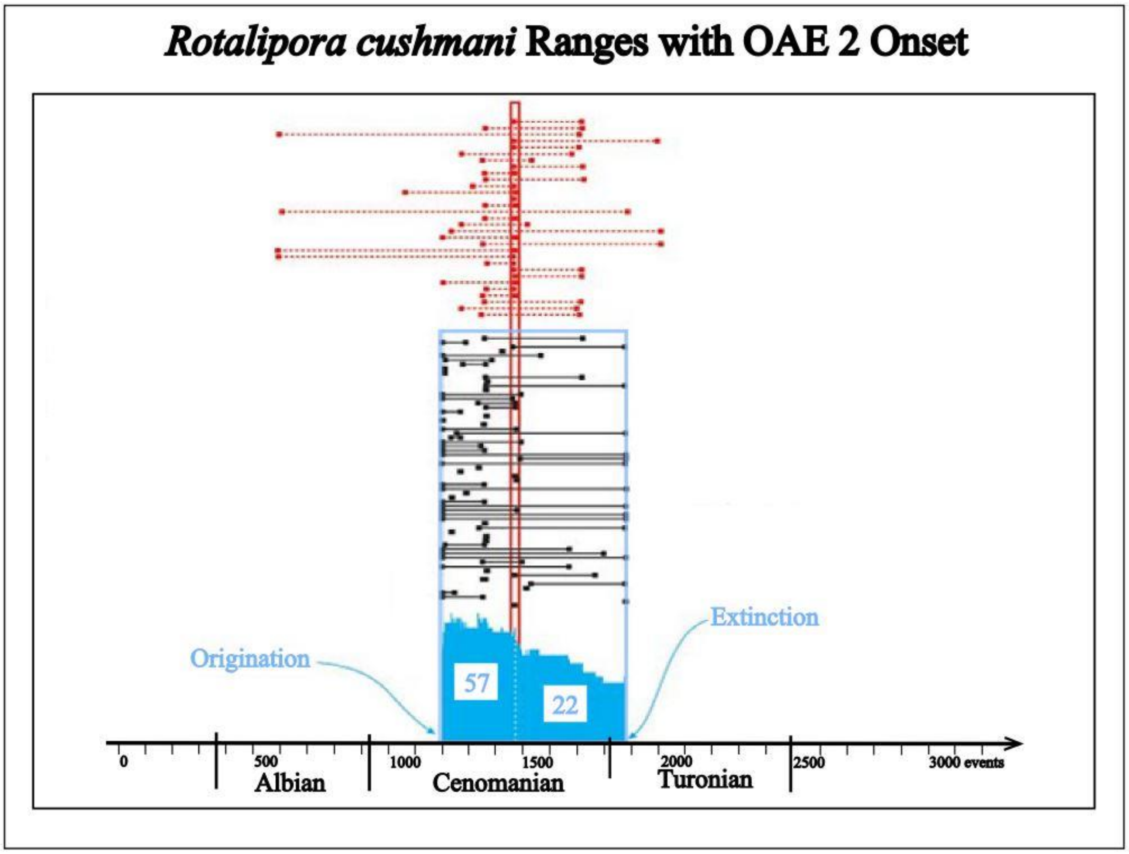

Figure 2.2-2: Local ranges for the planktonic foraminiferan species *Rotalipora cushmani* (black) through the onset (red) of the $\delta^{13}C_{carb}$ excursion in OAE 2 on a best-fit ordinal composite time-line of 3,275 events from 489 localities. The onset is where the biggest impact is expected on the species being a time of rapid environmental change. Events are those found in two or more localities. Counts reveal a drop in observances through the composite range (blue box) but no global extinction during the onset of OAE 2.

2.3 ANALYTICAL METHODS

A standard set of macroevolutionary analyses was undertaken for the output of each single-clade CONOP run: incremental composite range support, taxon richness, rarefied richness, per-lineage -- million year (ammonites; benthic forams), one and a half million year (nannofossils; dinoflagellates), and two million year (planktic forams; radiolaria) -- origination and extinction rate, turnover rate, diversification rate, and a map summary of the geographic scope. This is a preliminary sample of all the analyses and quality-control measures that a highly resolved time-line makes possible.

Incremental composite range support (Fig. 2.2-2) examines the distribution of local ranges within the composite range. It is a standard CONOP output. Gaps in support and outliers are indicative of data quality problems that are corrected.

Taxon richness can be calculated for every event level in the time-line. It is the count of all taxa whose ranges span that level. Richness curves may include spurious peaks and troughs as a result of severely uneven sampling. To guard against this possibility, rarefied richness plots were generated following the standard ecologists' rarefaction formulation of Hsieh & Li (1998). Rarefaction estimates the expected richness for sampling that has been reduced to a uniform level. It takes into account uneven abundance of taxa in the samples. The stratigraphic data already use a temporal "range-through" convention that assumes each taxon is present from local first to last occurrence. For a global temporal range it is possible to know that a species must have been present even if it was not sampled, because it is known from older and younger samples to exist. Because gaps in a spatial range may be commonplace, there is no acceptable range-through logic for the spatial snapshot data of ecology - one of the main motivations for their use of rarefaction. Not surprisingly, therefore, rarefied richness curves for composite paleobiological time-lines are typically subdued replicas of the raw richness curves, showing the same peaks and troughs. Rarefaction does serve to eliminate any artificial peaks that may be associated with biostratigraphers' tendency to measure many short sections near stage boundaries, resulting in excessive sampling (Raup, 1972; Peters & Foote, 2001; Smith & McGowan, 2007). The ammonite example (Figure 2.3-1) is typical. In practice many rarefaction levels are examined as a guide to the relative reliability of different peaks and troughs, prior to interpretation.

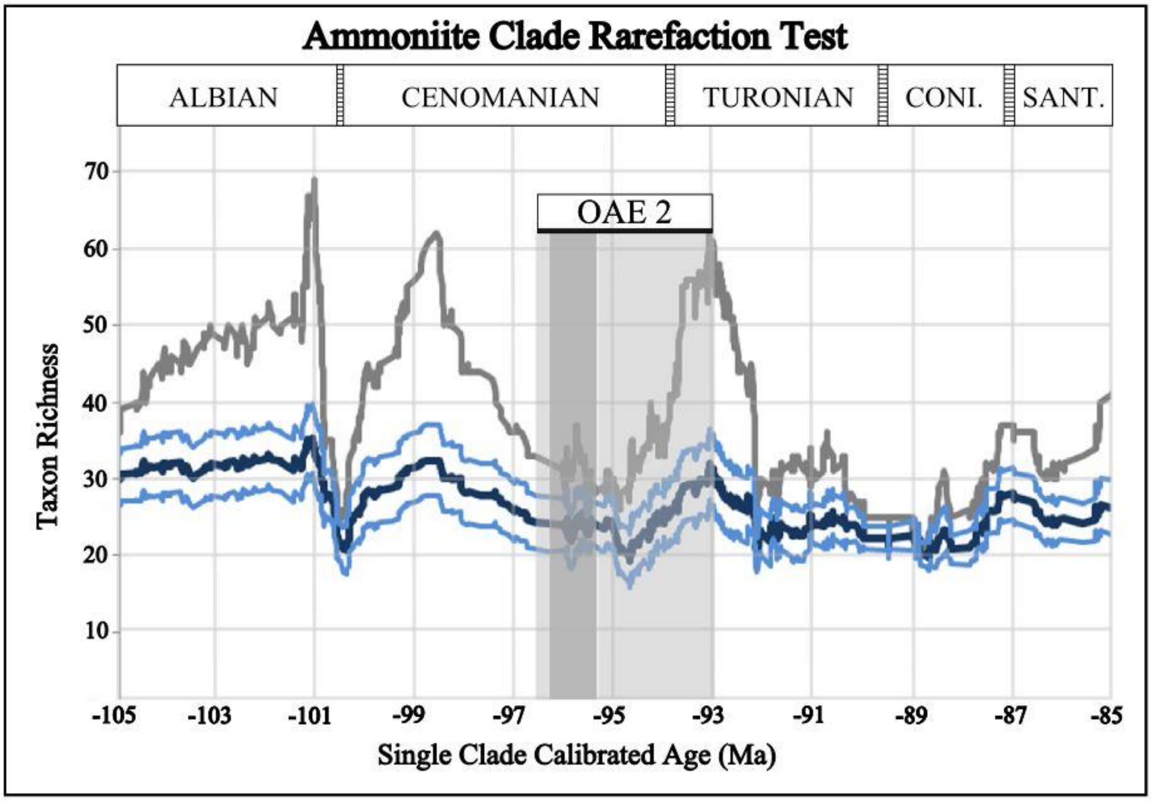

Figure 2.3-1: Raw taxon richness (dark grey curve) rarefied (dark blue) with 95% confidence intervals (light blue) through OAE 2. Prominent peaks in the raw form are still present themselves when rarefied.

Richness history is the pattern that emerges from the balance of two processes: origination and extinction rate. These cannot be inferred unambiguously from the richness trajectory but must be extracted independently from the time-line. Although the time-line data are not binned, rate is an inherently binned concept. Originations and extinctions are counted within the bin, corrected for bin duration and divided by the sum of the lengths of all ranges within the bin. The result is a per-lineage, per-million-year rate. The logic of the per-lineage standardization is that a given origination or extinction count is more notable if sustained by a less diverse stock. By similar logic, mass extinctions are usually measured by percentage extinction rather than extinction count. Ideally, per-lineage rates are less than 1.0, but counts may exceed richness if there is anagenetic evolution within the bin; that is, if species originations and extinctions occur at artificial divisions of a continuum of morphologic change through time. Without a cladistic phylogeny, however, I cannot separate anagenesis from cladogenesis.

From these origination and extinction rates, turnover and diversification rates are derived. Turnover is the sum of both, while diversification is the differences in originations and extinctions. They are used as a different viewpoint for comparing origination and extinction trajectories from clade to clade. Turnover graphs amplify change, but do not distinguish the type of change. Diversification graphs will be relatively flat (close to zero) if origination and extinction curves remain close, regardless of the amplitude of their fluctuations. Points on the richness graphs are counts of taxa extant at a given moment in time. The gradient of lines connecting adjacent points are enrichment rate or diversification. Points on the diversification graphs are analogous to the slopes of the richness graph. Thus, the linear segments of the diversification graph represent quickening (positive slope changes) and slackening (negative slope changes) of diversification (enrichment rate).

The time bin sizes vary between clades, because the finest reasonable resolution is sought for each clade. Bin duration is evidently too short if the content of any bin falls to zero or values from successive bins vary too noisily. Spurious values near the limits of the data set are confined to the buffer zones and not presented. Bin duration does not vary between analyses of the same clade. Sliding bins of fixed size are offset along the time axis by one quarter bin width. Thus the bins scan efficiently for maxima and minima, but consequentially widen the peaks and troughs. For ease of comparison between clades some figures rescale the rate values as fractions of the maximum reached in the study interval (105 - 85 Ma).

Among the possible further analyses are those that examine the longevity and paleogeography of individual species. Although this is beyond the scope of this thesis, one example is presented because the same CONOP output served in the quality control process. A standard preliminary screen shot of the planktic foraminiferan species *Rotalipora cushmani* reveals how extirpation can readily be mistaken for extinction if too few sections are examined (Figure 2.2-2). Although the onset of OAE 2 dramatically reduces the number of local ranges observed for this species, the extinction of the species is not seen until much later in the Turonian. This figure additionally shows that local taxon ranges must be diachronous while the uncertainty intervals on the isotope excursion permit the view that some part of it is isochronous. On an evolutionary level this works because species do not appear nor disappear everywhere at once, therefore, time is needed for global coverage. Examining these local range occurrences (for extirpation) during OAE 2 for each species would be a straightforward but very time consuming task, ultimately needing the development of innovative graphics to summarize the local behavior of so many species and regions. It is reserved for a later project.

CHAPTER 3 - RESULTS FROM SINGLE-CLADE TIME-LINES

3.1 QUALITY CONTROL

The incorporation of local carbon isotope data and stage boundary placements as uncertainty intervals enables some automated quality control prior to optimization. Taxon ranges can be stretched to force agreement between any sequences of events. Because uncertainty intervals adjust by shrinking, however, irresolvable conflicts may exist between locally observed placements of excursions and stage boundaries. These are automatically detected prior to optimization.

Two forms of carbon isotope data were included - carbonate carbon and organic carbon. The segments of the carbonate carbon curves generated no sequencing conflicts; they are plausible time-stratigraphic controls. The organic carbon data generated some conflicts in sequencing between all pairs of parts of the local curves, except the fall, and between parts of the curve and the C/T stage boundary. Evidently, the disposition of peaks in the local organic carbon isotope curve cannot provide precise correlation. This suggests the influence of changing organic carbon composition in the $\delta^{13}C$ record where peaks in organic carbon isotopes may sometimes simply reflect changing proportions in the mixture of organic compounds: i.e. marine and terrestrial. For this reason clades were analyzed with the carbonate carbon excursion and not the organic carbon excursion.

Age boundaries were entered into the database with their maximum and minimum uncertainty limits from the most recent geologic time scale, (Gradstein et al., 2012) as follows: Albian/Cenomanian (A/C) -- 101.3 to 99.7 Ma; Cenomanian/Turonian (C/T) -- 94.3 to 93.5 Ma; Turonian/Coniacian (T/C) -- 90.4 to 89.2 Ma; and Coniacian/Santonian

(C/S) -- 87.3 to 85.3 Ma. The placement of these uncertainty intervals in the time-lines guided the later sixth-order (or lower) polynomial age calibration of the time-lines. The resulting calibrated ages differ slightly from clade to clade and in comparison with the published uncertainties. The differences reflect the unequal power of each clade to resolve the position of the stage boundaries and the placement of the limits of OAE 2, as indicated by carbon isotopes.

3.2 MACROEVOLUTIONARY PATTERNS AND OAE 2 PLACEMENT

For each clade, five preliminary macroevolutionary time series have been determined from the order of events in the time-lines: taxon richness, origination rate, extinction rate, turnover and diversification (Figs. 3.2-1 to 3.2-5). The compromised buffer zones at the ends of the time-lines are excluded. A global map reveals the geographic scope of data sources for each clade.

Stage boundaries and OAE 2 are placed independently for each clade, according to their placement in each time-line. A later section, which compares trends across clades, uses a consensus placement. The graphs in this section allow assessment of the relative time-stratigraphic constraint provided by the six clades and the reliability of the other events for correlation. The first five segments of the OAE 2 excursion were in the late Cenomanian, the fall portion persisted into the Turonian. The return to pre-excursion values did not occur until the early Turonian. The span of OAE 2 in these diagrams is a combination of the true length of segments of the excursion and the resolving power of each clade. The position of the rising carbon isotope ratios during the Cenomanian varies from clade to clade with notably longer uncertainty intervals in the time-lines for dinoflagellates, benthic forams, and radiolaria.

The general form of several curves helps estimate the extent to which species have been recognized primarily at branching points in an evolutionary tree (cladogenesis) or at relatively arbitrary thresholds in a continuum of morphologic change along a lineage (anagenesis). The anagenetic mode of evolution (or taxonomic practice) produces an extinction for every origination and allows the number of turnover events in a time interval to exceed species richness. This must be suspected where origination and extinction rate curves closely shadow one another and per-lineage rates of change are high. The ammonite clade has these characteristics.

Ammonites (Figure 3.2-1)

All stage boundaries fall within the expected ranges but with narrower uncertainty. The C/T boundary places at the center of its published estimate, from 93.71 to 93.69 Ma.

Raw Taxon Richness has two conspicuous peaks, one near the A/C boundary and the other at the C/T. Richness rises irregularly through OAE 2 with fluctuations of increasing amplitude in the second half. A long decline of richness starts in the Turonian.

Origination and Extinction Rates clearly distinguish the two richness peaks. Both originations and extinctions peak dramatically at the end of the Albian. The high per-lineage rates indicate that species changes have been recognized along lineages, not at branching points. The peak may be an artefact of taxonomic practice; i.e. finer splitting species in studies near the stage boundary. During OAE 2, origination rate and extinction rate are more independent, with origination exceeding extinction until close to the end of the excursion.

Turnover and Diversification Rates differ considerably. Turnover exaggerates the end-Albian pulse in species differentiation. Diversification rates are close to zero because origination and extinction curves are so similar. The differences between them may include a considerable random element superimposed on a gentle ~8 million year fluctuation.

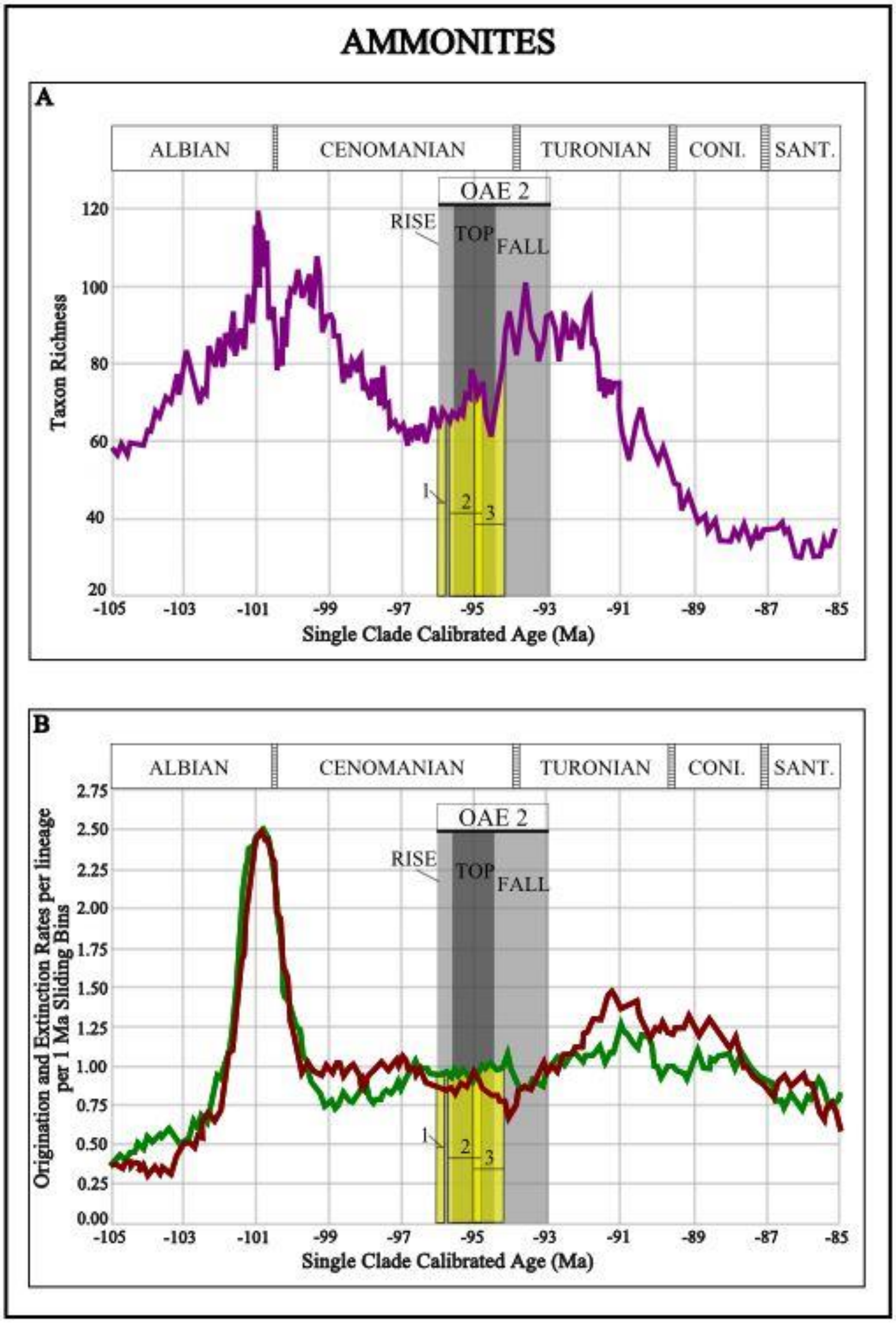
AMMONITES
A
ALBIAN
CENOMANIAN
TURONIAN
CONI.
SANT.
OAE 2
RISE
TOP
FALL
1
2
3
Taxon Richness
120
100
80
60
40
20
-105
-103
-101
-99
-97
-95
-93
-91
-89
-87
-85
Single Clade Calibrated Age (Ma)
B
ALBIAN
CENOMANIAN
TURONIAN
CONI.
SANT.
OAE 2
RISE
TOP
FALL
1
2
3
Origination and Extinction Rates per lineage per 1 Ma Sliding Bins
2.75
2.50
2.25
2.00
1.75
1.50
1.25
1.00
0.75
0.50
0.25
0.00
-105
-103
-101
-99
-97
-95
-93
-91
-89
-87
-85
Single Clade Calibrated Age (Ma)

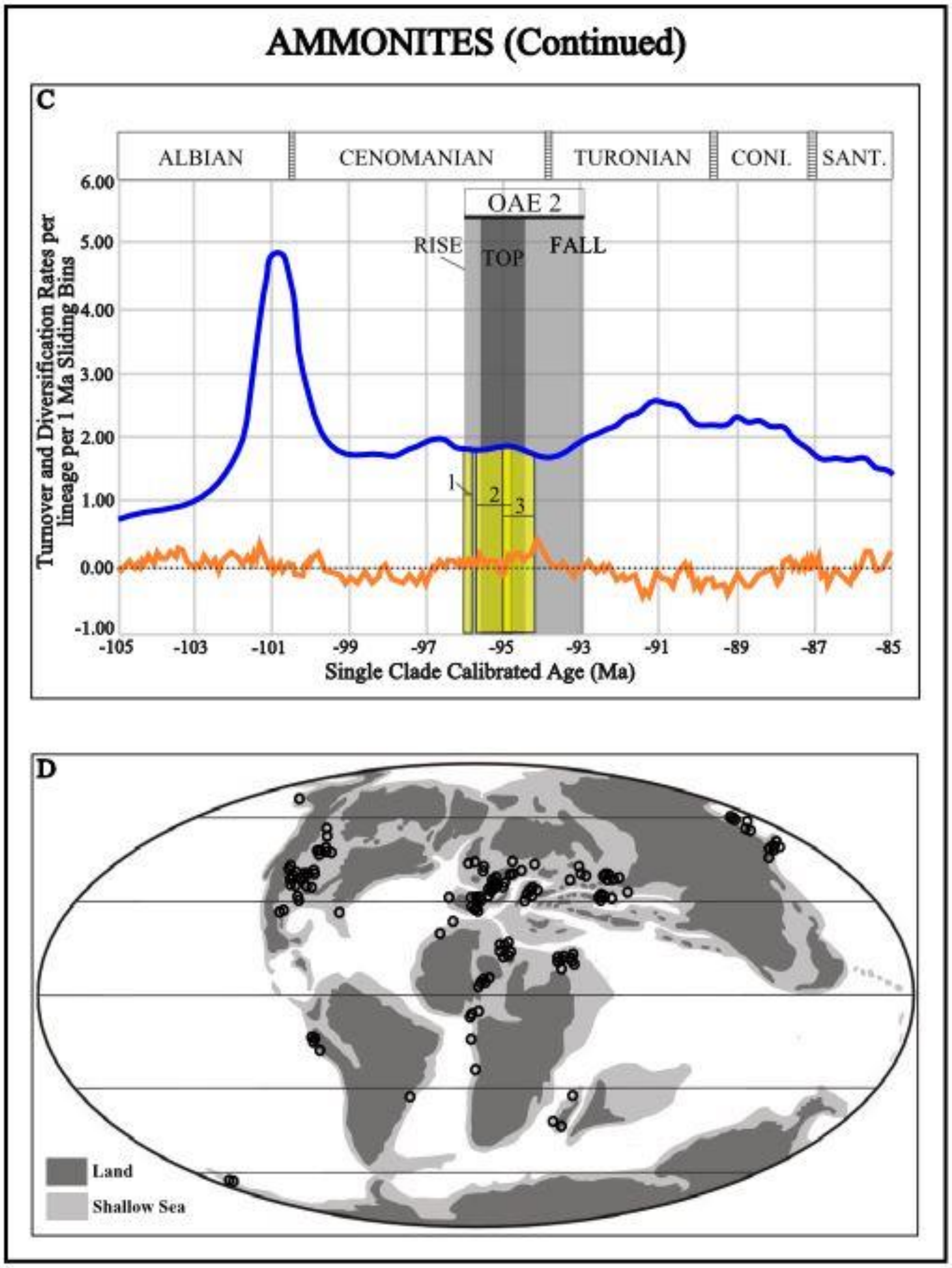

Figure 3.2-1: Ammonite range results with the carbonate carbon excursion - OAE 2 clade calibrated length shown as a black horizontal bar near the top of figures [A]-[C]. The excursion is labeled with a rise, top, and fall interval (shades of grey), and the three main peaks (yellow blocks). Single clade calibrated age in millions of years is on the x-axis for [A]-[C]. OAE 2 spans most of the late Cenomanian with exception of the fall in the early Turonian. Figure descriptions: [A] Taxon Richness (purple); [B] Originations (green) and extinctions (red) per lineage through one million year sliding bins; [C] Turnover (blue) and diversification (orange) per lineage through one million year sliding bins with dotted line indicating where zero is on the y-axis; [D] Global distribution of data localities used (black open circles). *Map simplified after Ron Blakey.*

Calcareous Nannofossils (Figure 3.2-2)

All stage boundaries, except the C/T, place within published expectations but with narrower uncertainty. The C/T falls approximately 0.1 Ma later than expected at 93.46 to 93.41 Ma.

Raw Taxon Richness peaks near the close of the Albian, Cenomanian and Turonian stages. OAE 2 marks the end of the most sustained rise in richness. Richness and carbon isotope ratios both decline during the early Turonian. After the anoxic interval, as indicated by the isotope excursion, richness increases abruptly.

Origination and Extinction Rates are both rising prior to OAE 2. Extinction accelerates at the onset of OAE 2; origination rate peaks later.

Turnover and Diversification Rates have fluctuations of comparable amplitude suggesting that species are less commonly recognized by dividing a continuum of change than may have been the case for ammonite species.

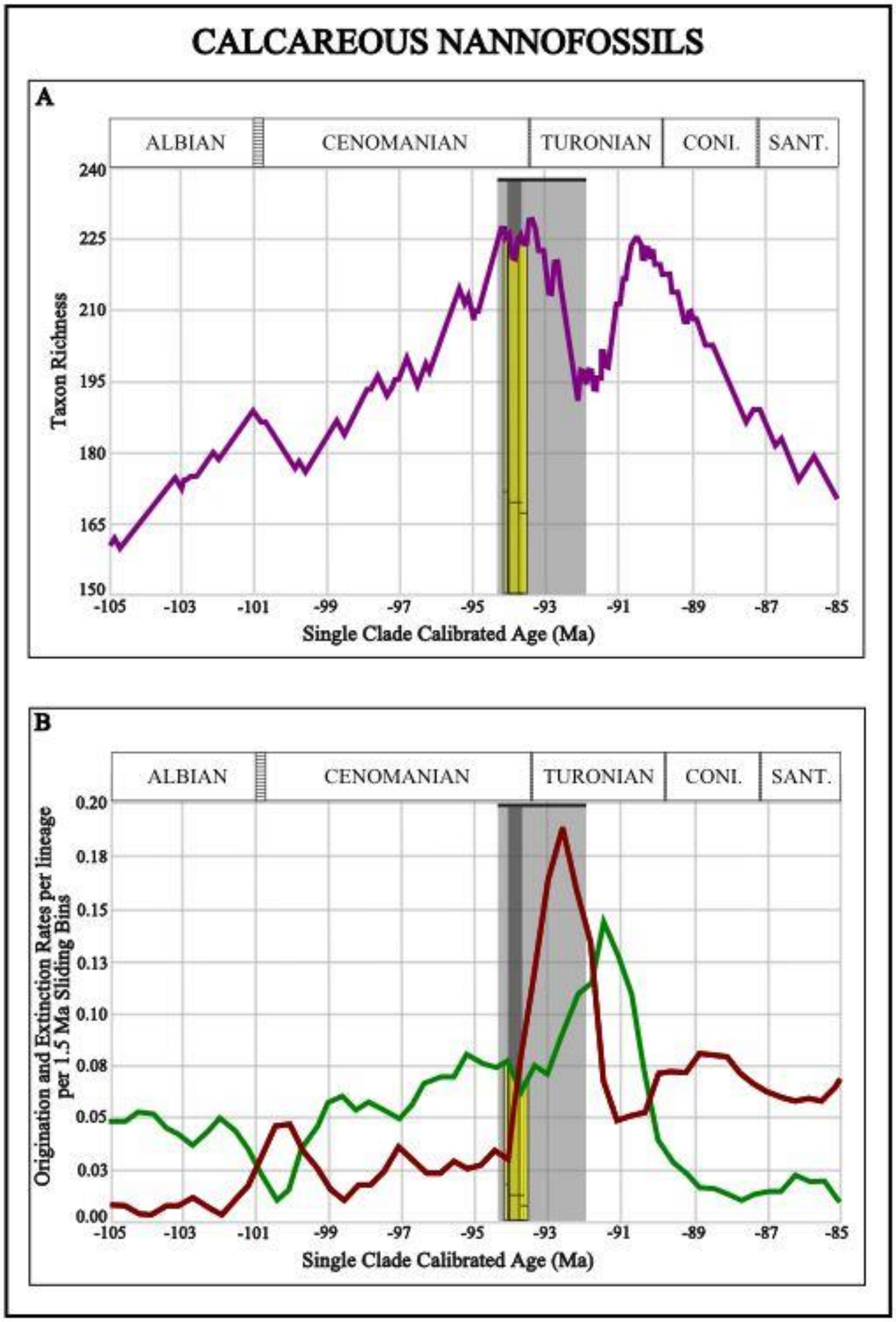
CALCAREOUS NANNOFOSSILS
A
ALBIAN
CENOMANIAN
TURONIAN
CONI.
SANT.
Taxon Richness
240
225
210
195
180
165
150
-105
-103
-101
-99
-97
-95
-93
-91
-89
-87
-85
Single Clade Calibrated Age (Ma)
B
ALBIAN
CENOMANIAN
TURONIAN
CONI.
SANT.
Origination and Extinction Rates per lineage per 1.5 Ma Sliding Bins
0.20
0.18
0.15
0.13
0.10
0.08
0.05
0.03
0.00
-105
-103
-101
-99
-97
-95
-93
-91
-89
-87
-85
Single Clade Calibrated Age (Ma)

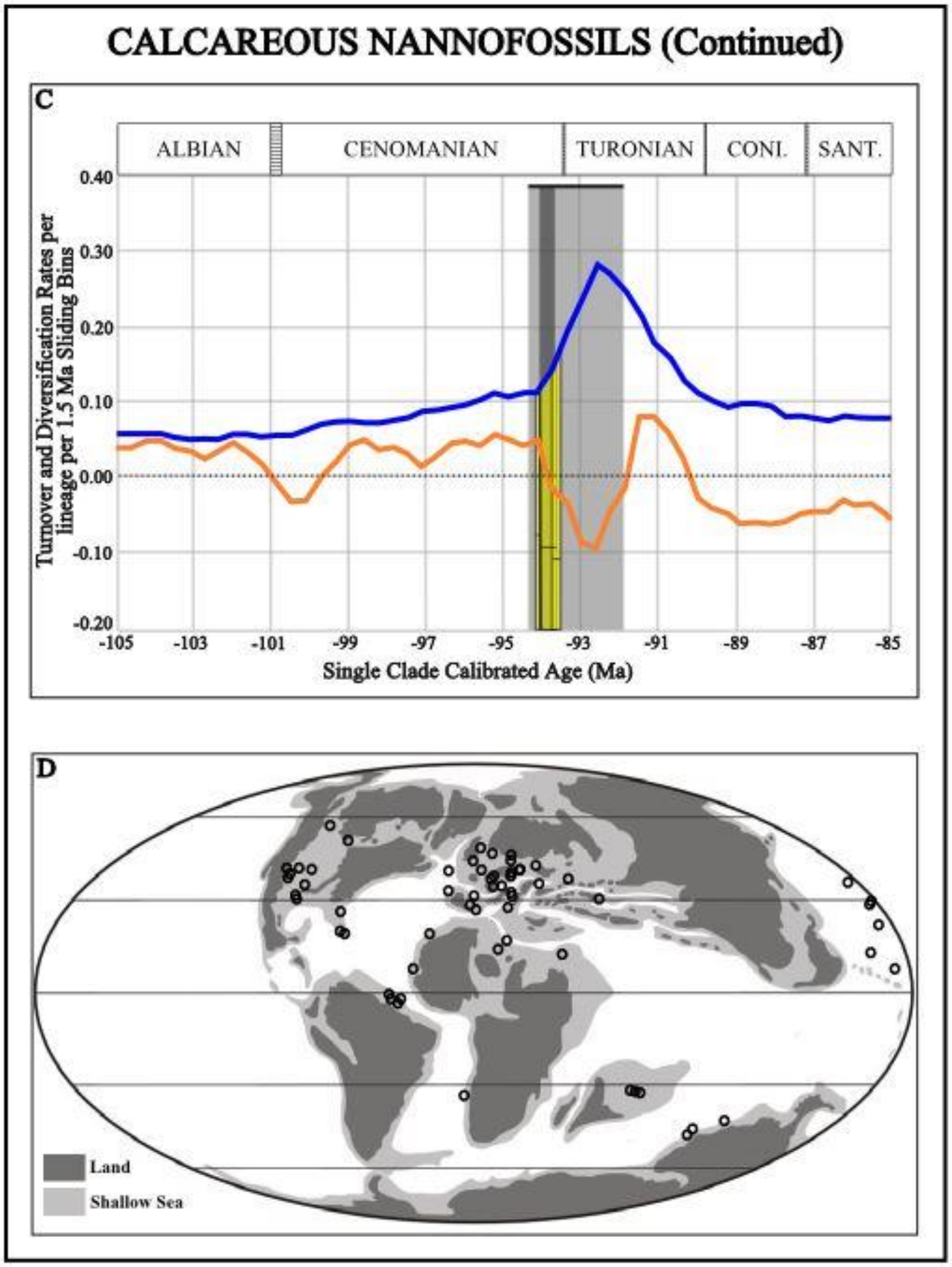

Figure 3.2-2: Calcareous nannofossil range results with the carbonate carbon excursion. For detailed figure descriptions see Figure 3.1-1. [A] Taxon Richness (purple); [B] Originations (green) and extinctions (red) per lineage through one and a half million year sliding bins; [C] Turnover (blue) and diversification (orange) per lineage through one and a half million year sliding bins; [D] Global distribution of data localities used (black open circles). *Map simplified after Ron Blakey.*

Dinoflagellates (Figure 3.2-3)

The T/C and C/S stage boundaries fall very close to expected ages: ~0.2 Ma younger and ~0.1 Ma older, respectively. All others are placed within expectation but with narrower spans. The C/T uncertainty shrinks to 94.29 to 94.25 Ma. Placement of OAE 2 is looser by dinoflagellate control than by other clades. The possible span starts in the mid Cenomanian and the younger limit of peak 3 can hardly be separated from the C/T stage boundary.

Raw Taxon Richness, which had steadily increased prior to OAE 2 declines sharply when carbon isotope ratios reach their peak. The subsequent decrease in richness continues after the Turonian where it likely reflects a lack of data.

Origination and Extinction Rates both rise near the onset of OAE 2. Extinction rate exceeds origination immediately after the rise in OAE 2 carbon isotope ratios and stays ahead for the remainder of the study interval.

Turnover and Diversification Rates have fluctuations of comparable magnitude and their separation reflects prominent extinction pulses at the onset of OAE 2 and in the Coniacian. The older peak is accompanied by a pulse of originations while the younger peak is not.

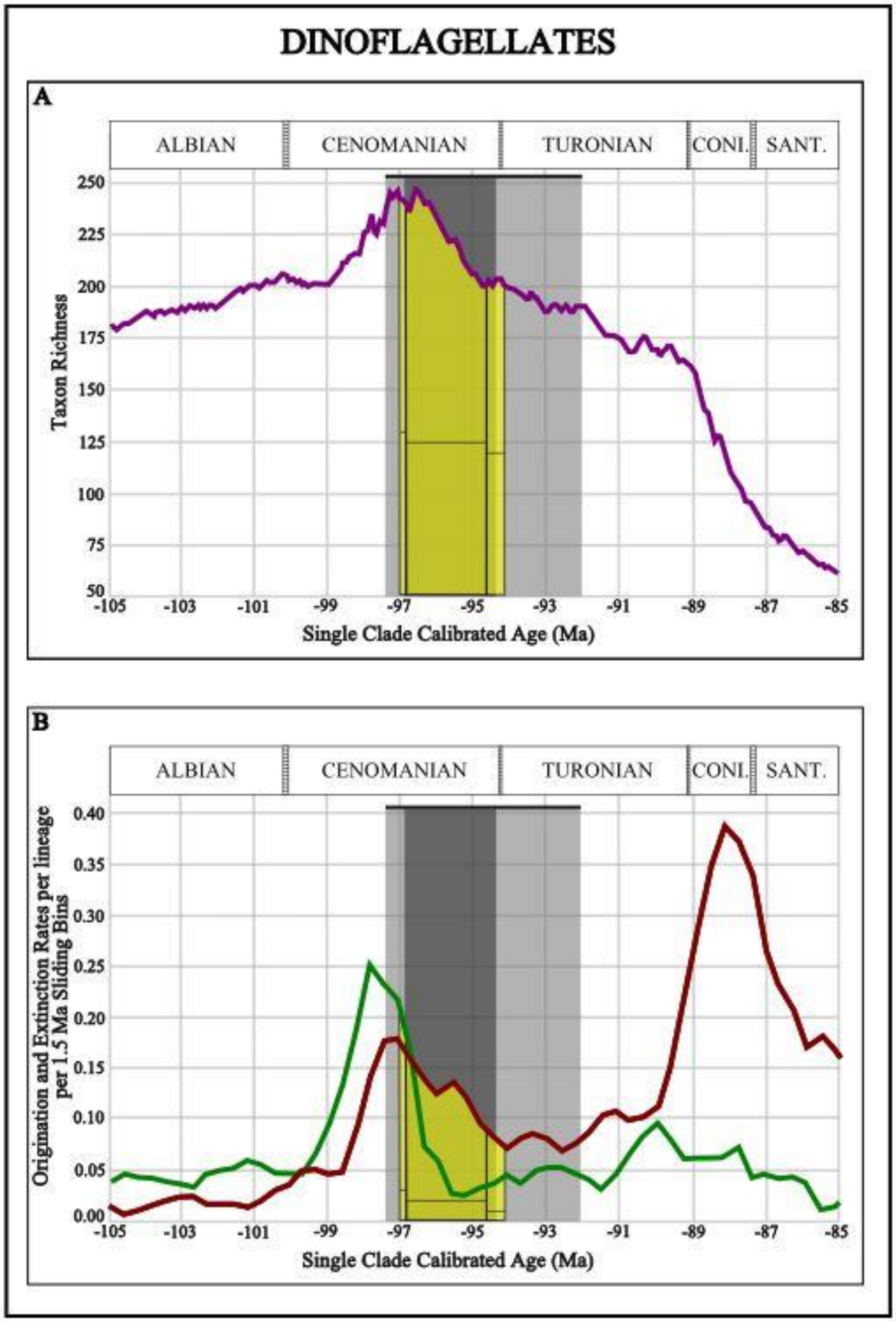
DINOFLAGELLATES
A
ALBIAN
CENOMANIAN
TURONIAN
CONI.
SANT.
Taxon Richness
250
225
200
175
150
125
100
75
50
-105
-103
-101
-99
-97
-95
-93
-91
-89
-87
-85
Single Clade Calibrated Age (Ma)
B
ALBIAN
CENOMANIAN
TURONIAN
CONI.
SANT.
Origination and Extinction Rates per lineage per 1.5 Ma Sliding Bins
0.40
0.35
0.30
0.25
0.20
0.15
0.10
0.05
0.00
-105
-103
-101
-99
-97
-95
-93
-91
-89
-87
-85
Single Clade Calibrated Age (Ma)

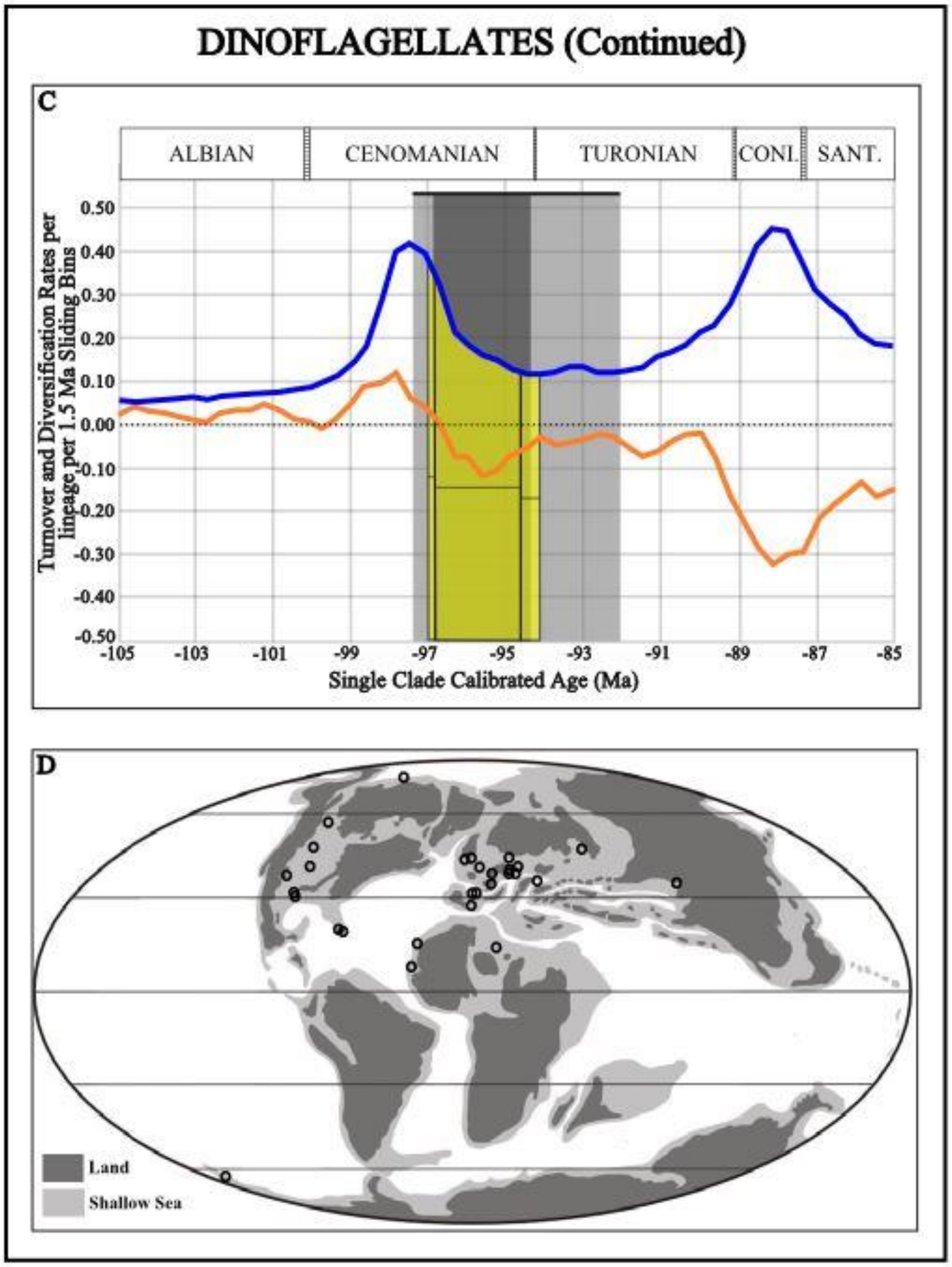

Figure 3.2-3: Dinoflagellate range results with the carbonate carbon excursion. For detailed figure descriptions see Figure 3.1-1. [A] Taxon Richness (purple); [B] Originations (green) and extinctions (red) per lineage through one and a half million year sliding bins; [C] Turnover (blue) and diversification (orange) per lineage through one and a half million year sliding bins; [D] Global distribution of data localities used (black open circles). *Map simplified after Ron Blakey.*

Benthic Foraminifera (Figure 3.2-4)

All stage boundaries place within the published expectation for their ages but with narrower uncertainty. The C/T boundary places toward the younger end of the published uncertainty at 93.64 to 93.62 Ma. Unlike the five other clades, the benthic foraminifera cannot constrain the rising segment of the OAE 2 carbon isotope excursion to a narrow interval.

Raw Taxon Richness peaks twice within OAE 2. It rose consistently prior to OAE 2 and fell thereafter. Thus, OAE 2 coincides with the dominant feature of this curve.

Origination and Extinction Rates both rise irregularly prior to OAE 2 and fall irregularly after OAE 2. Origination dominates during the rise and extinction during the fall.

Turnover and Diversification Rates appear quite different. Turnover peaks in OAE 2. Diversification fluctuates without long term trend throughout the study interval.

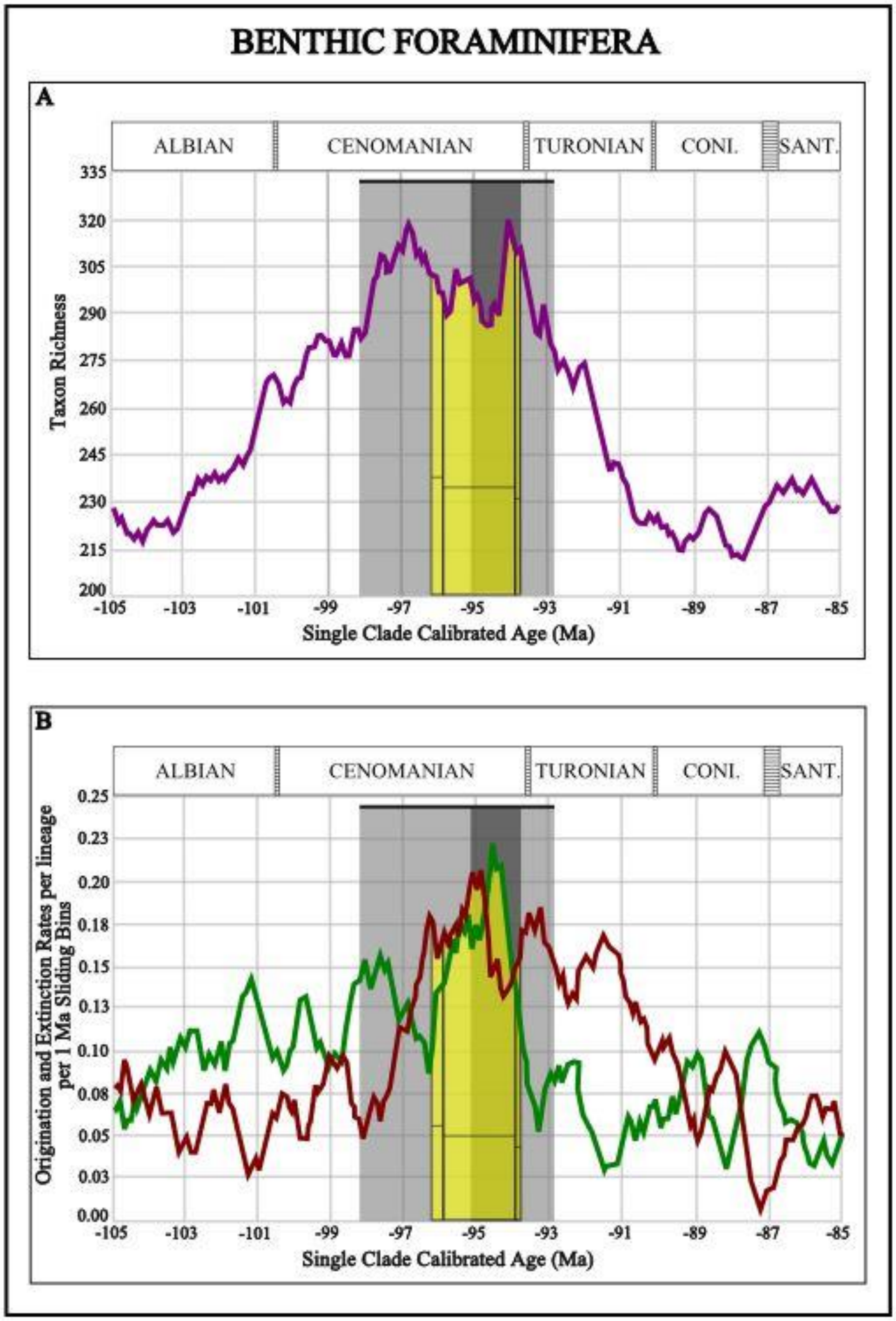
BENTHIC FORAMINIFERA
A
ALBIAN
CENOMANIAN
TURONIAN
CONI.
SANT.
Taxon Richness
335
320
305
290
275
260
245
230
215
200
-105
-103
-101
-99
-97
-95
-93
-91
-89
-87
-85
Single Clade Calibrated Age (Ma)
B
ALBIAN
CENOMANIAN
TURONIAN
CONI.
SANT.
Origination and Extinction Rates per lineage per 1 Ma Sliding Bins
0.25
0.23
0.20
0.18
0.15
0.13
0.10
0.08
0.05
0.03
0.00
-105
-103
-101
-99
-97
-95
-93
-91
-89
-87
-85
Single Clade Calibrated Age (Ma)

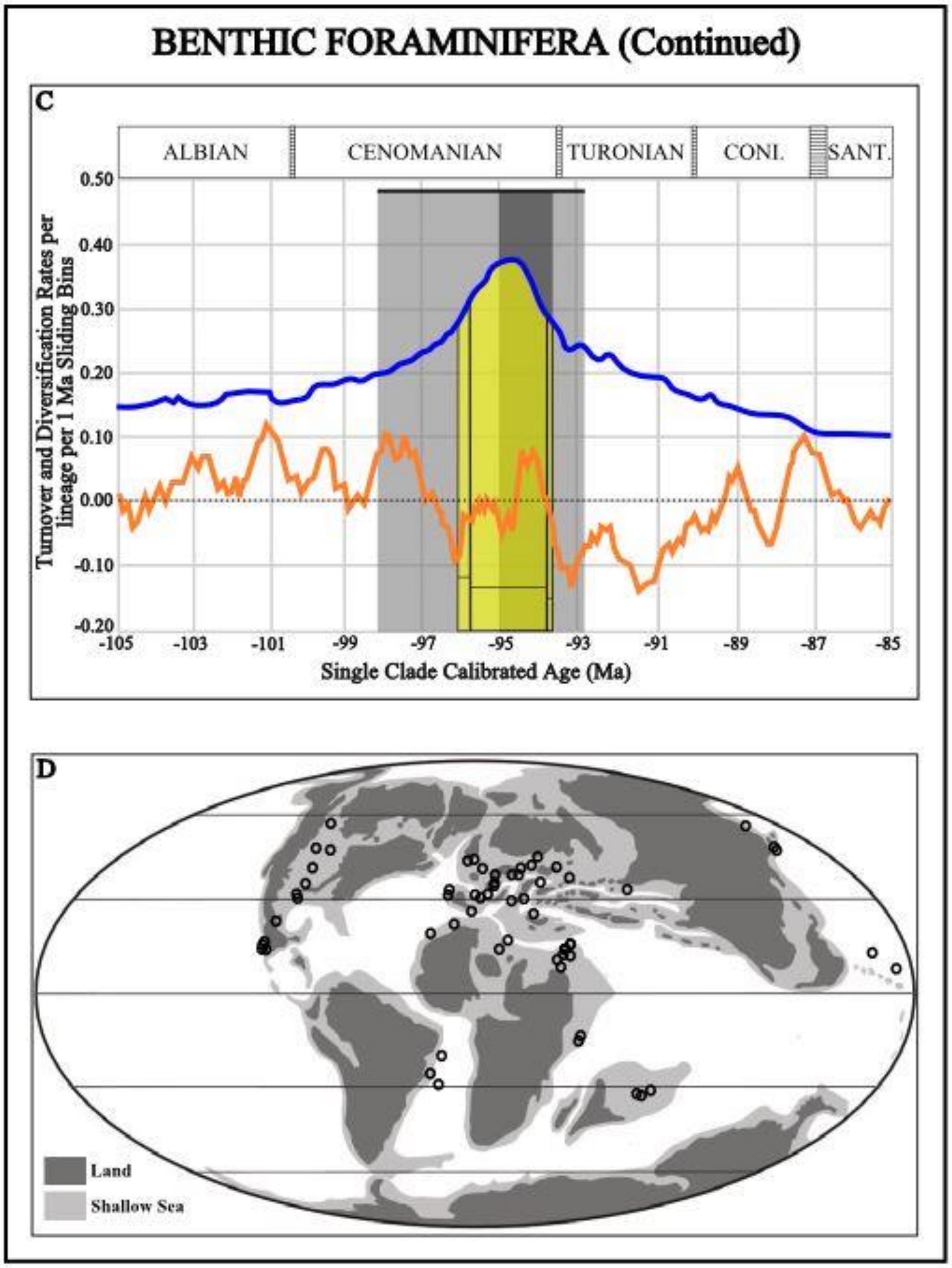

Figure 3.2-4: Benthic foraminiferal range results with the carbonate carbon excursion. For detailed figure descriptions see Figure 3.1-1. [A] Taxon Richness (purple); [B] Originations (green) and extinctions (red) per lineage through one million year sliding bins; [C] Turnover (blue) and diversification (orange) per lineage through one million year sliding bins; [D] Global distribution of data localities used (black open circles). *Map simplified after Ron Blakey.*

Planktonic Foraminifera (Figure 3.2-5)

The A/C, C/T, and C/S boundaries place outside the expected uncertainties by ~0.3 Ma (older), ~0.6 Ma (younger), and ~1.0 Ma (older), respectively. Others are within the expected uncertainty but with narrower spans. The C/T places at 92.89 to 92.87 Ma. The age calibration regression for planktic foraminifera has an R-squared coefficient of 0.9956625498, which is lower than all other clades except for dinoflagellates. Planktic foraminifera are respected index fossils but have the lowest taxon count in the database for this study.

Raw Taxon Richness peaks late in OAE 2 after a long interval of rising richness with a subsidiary peak at the onset of OAE 2.

Origination and Extinction Rates are markedly out of phase and fluctuate considerably on a time scale of several million years.

Turnover and Diversification Rates are both smoothly dynamic and reflect the independence of the origination and extinction curves. This outcome is less likely for anagenetic evolution than cladogenesis.

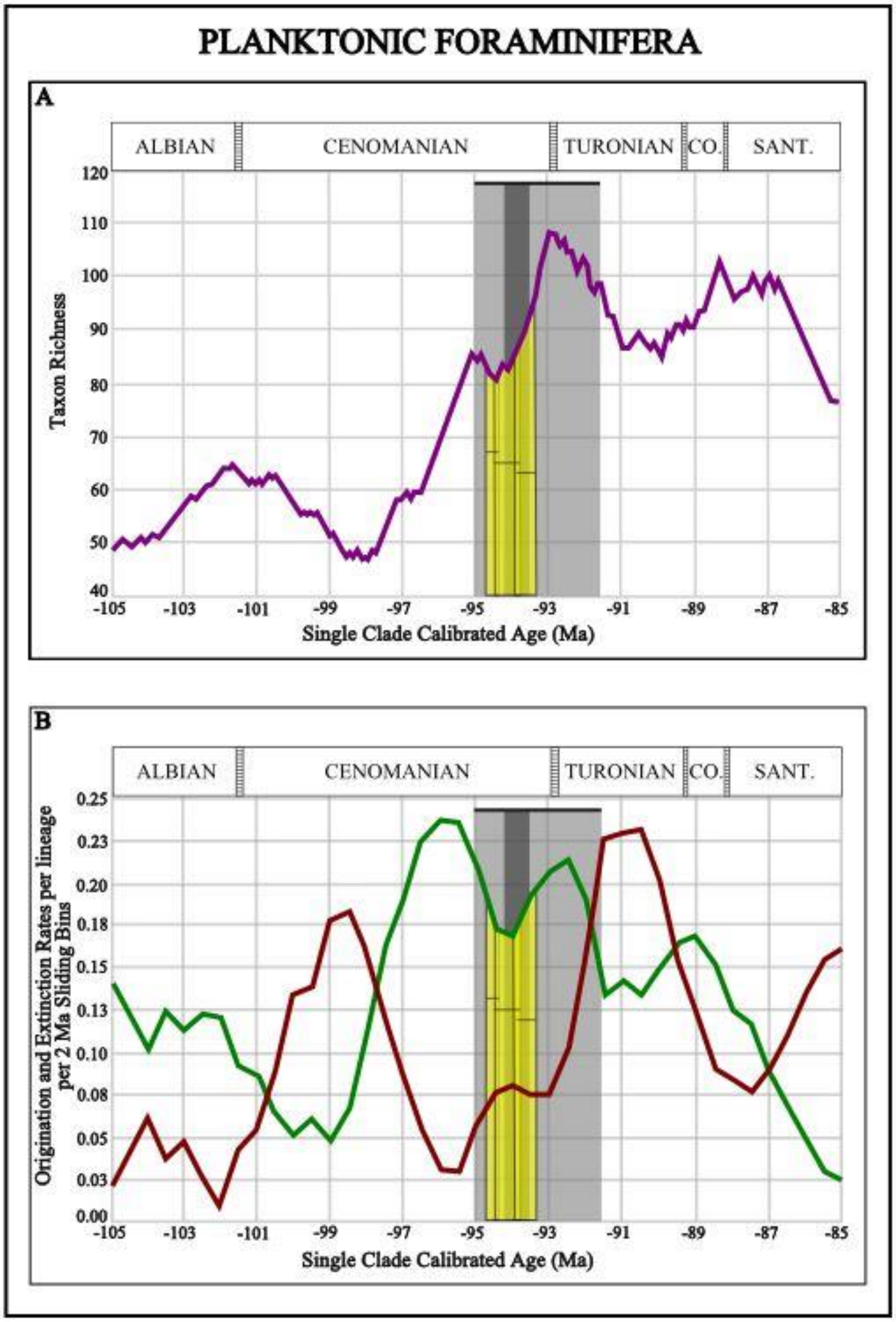
PLANKTONIC FORAMINIFERA
A
ALBIAN
CENOMANIAN
TURONIAN
CO.
SANT.
Taxon Richness
120
110
100
90
80
70
60
50
40
-105
-103
-101
-99
-97
-95
-93
-91
-89
-87
-85
Single Clade Calibrated Age (Ma)
B
ALBIAN
CENOMANIAN
TURONIAN
CO.
SANT.
Origination and Extinction Rates per lineage per 2 Ma Sliding Bins
0.25
0.23
0.20
0.18
0.15
0.13
0.10
0.08
0.05
0.03
0.00
-105
-103
-101
-99
-97
-95
-93
-91
-89
-87
-85
Single Clade Calibrated Age (Ma)

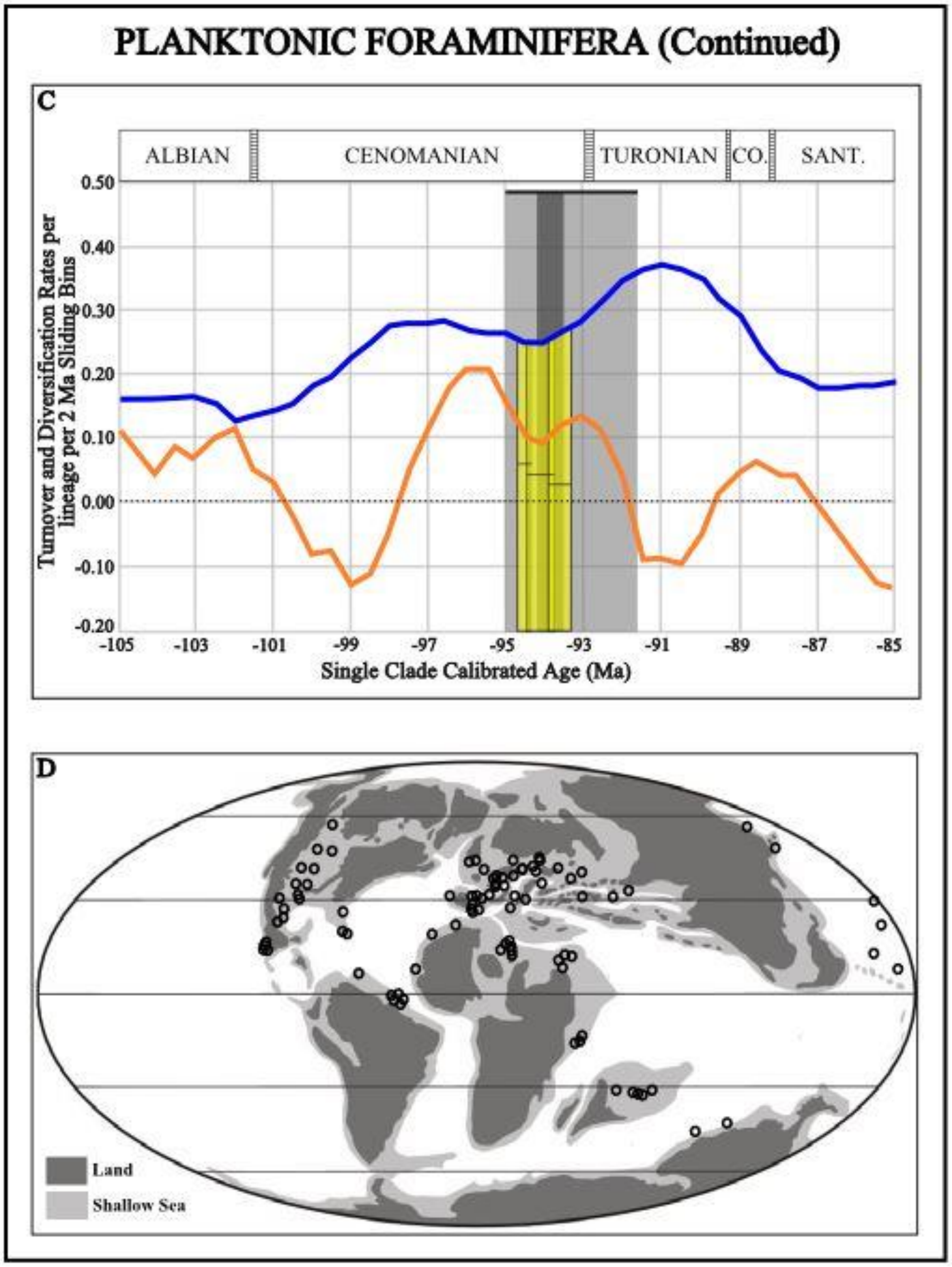

Figure 3.2-5: Planktonic foraminiferal range results with the carbonate carbon excursion. For detailed figure descriptions see Figure 3.1-1. [A] Taxon Richness (purple); [B] Originations (green) and extinctions (red) per lineage through two million year sliding bins; [C] Turnover (blue) and diversification (orange) per lineage through two million year sliding bins; [D] Global distribution of data localities used (black open circles). *Map simplified after Ron Blakey.*

Radiolaria (Figure 3.2-6)

All stage boundaries, except the C/S which radiolarian constraints place older than expected, land within the published uncertainty limits and with narrower limits. The C/T places approximately at the center of its published uncertainty at 93.71 to 93.70 Ma. The OAE 2 interval is loosely constrained; the rise, in particular, has a wide uncertainty which starts in the mid Cenomanian. Like the benthic foraminifera, the radiolarian clade is not the best suited for correlation in this time interval.

Raw Taxon Richness of the radiolaria resembles the pattern for benthic foraminifera; i.e. one general peak centered on the late Cenomanian dominates the study interval.

Origination and Extinction Rates come nearly into phase in OAE 2 but are out of phase elsewhere.

Turnover and Diversification Rates have broadly independent and smooth trajectories.

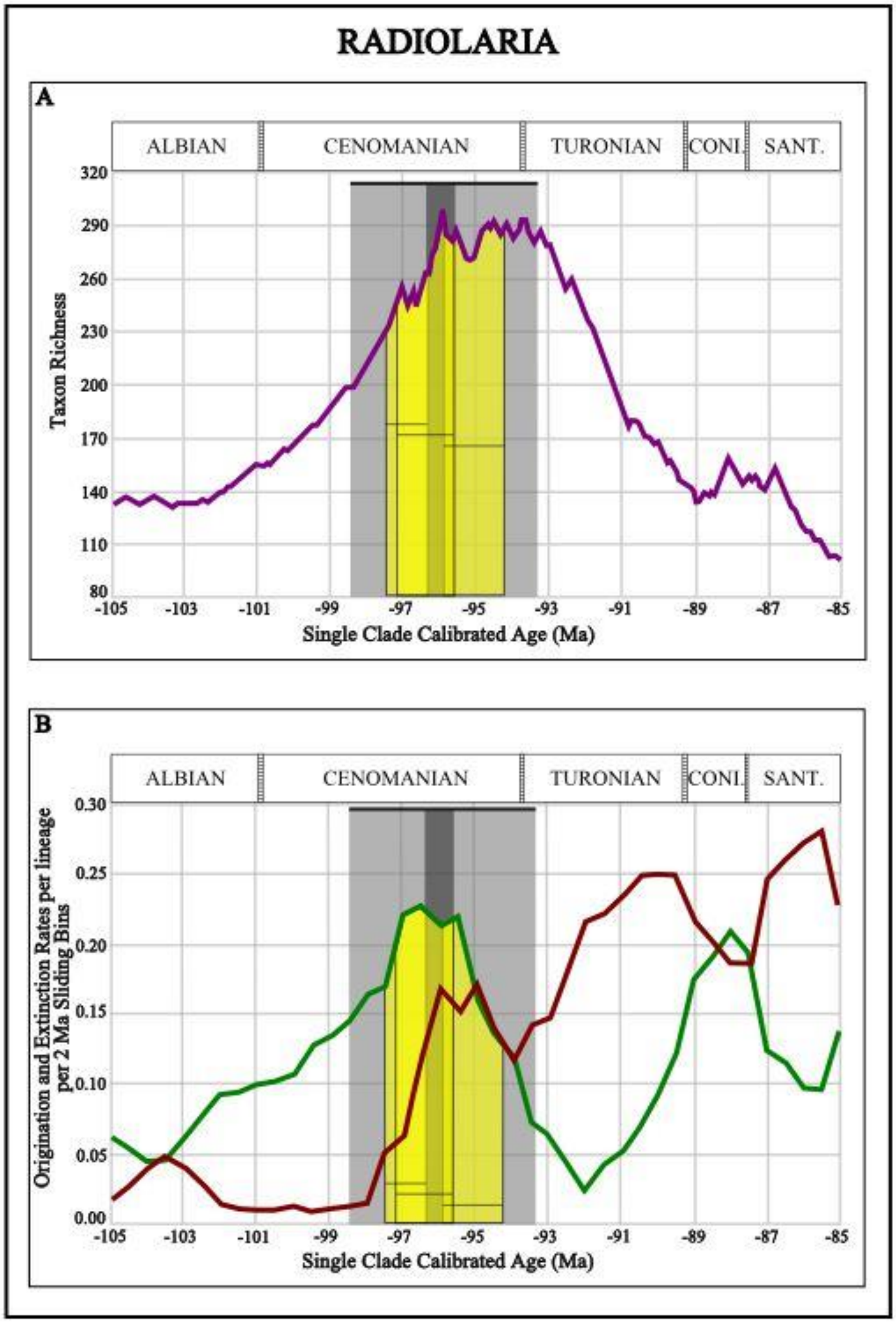
RADIOLARIA
A
ALBIAN
CENOMANIAN
TURONIAN
CONI.
SANT.
Taxon Richness
320
290
260
230
200
170
140
110
80
-105
-103
-101
-99
-97
-95
-93
-91
-89
-87
-85
Single Clade Calibrated Age (Ma)
B
ALBIAN
CENOMANIAN
TURONIAN
CONI.
SANT.
Origination and Extinction Rates per lineage per 2 Ma Sliding Bins
0.30
0.25
0.20
0.15
0.10
0.05
0.00
-105
-103
-101
-99
-97
-95
-93
-91
-89
-87
-85
Single Clade Calibrated Age (Ma)

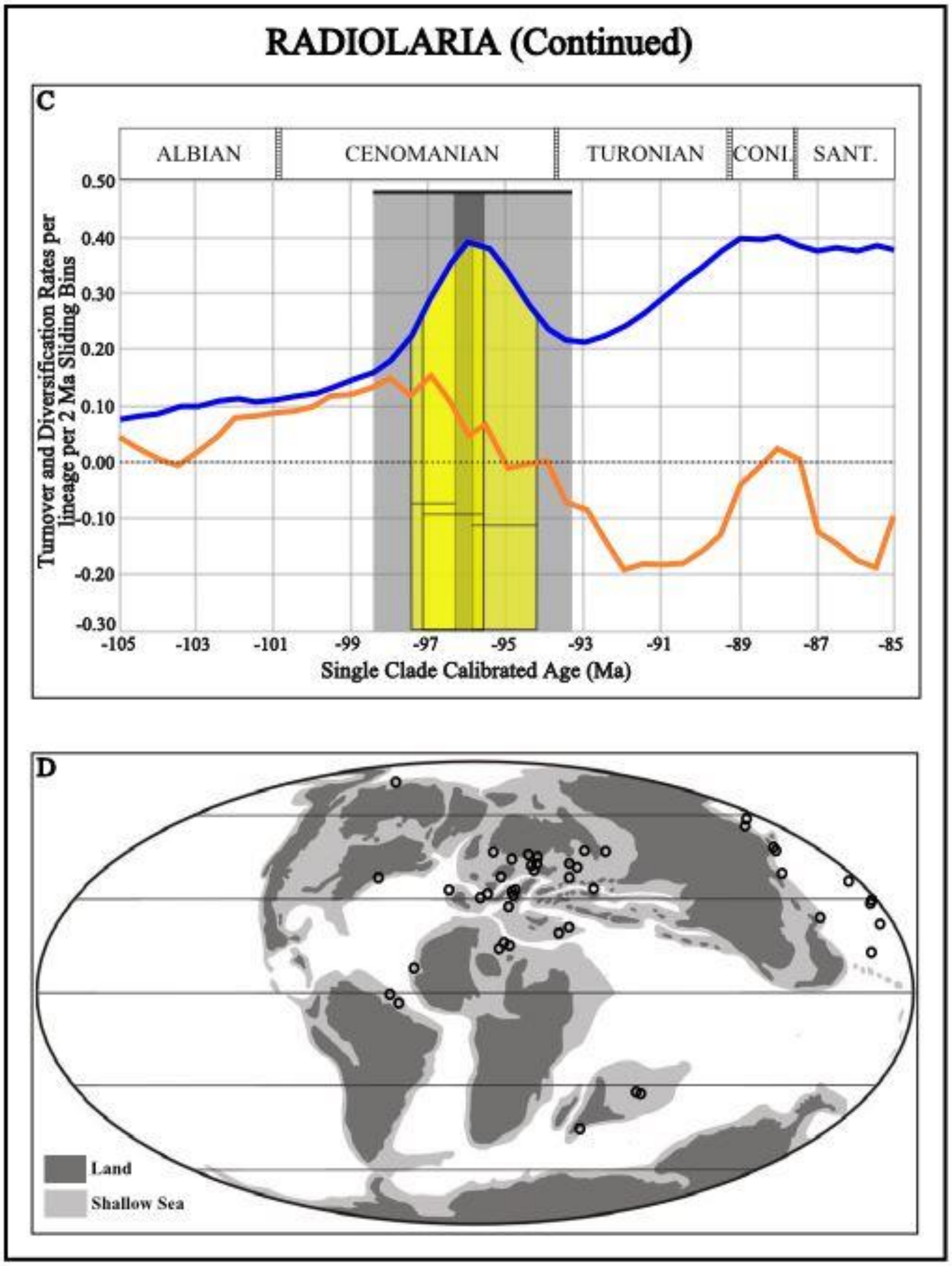

Figure 3.2-6: Radiolaria range results with the carbonate carbon excursion. For detailed figure descriptions see Figure 3.1-1. [A] Taxon Richness (purple); [B] Originations (green) and extinctions (red) per lineage through two million year sliding bins; [C] Turnover (blue) and diversification (orange) per lineage through two million year sliding bins; [D] Global distribution of data localities used (black open circles). *Map simplified after Ron Blakey.*

CHAPTER 4 - MULTI-CLADE RESPONSE TO OAE 2

4.1 A SHARED TIME SCALE

In order to reveal more general pelagic responses to OAE 2, the macroevolutionary patterns for all six clades need to be summarized on a single time scale and with the same sliding bin size. The bins must all be matched to the most coarsely binned clades, which were the planktonic forams and radiolaria at two million year sliding bins. The macroevolutionary charts are fitted together using the carbonate carbon isotopic maximum and minimum stratigraphic range segments of OAE 2, because this is the environmental perturbation of interest. Figure 4.2-1a rescales origination and extinction rate peaks for figure 4.2-1b to the time scale of the ammonite clade with seven calibration points met in each – two boundaries at the edges, three boundaries within the buffered zone, and the beginning and end of the OAE 2 interval. The ammonite clade had the best controlled age calibration.

4.2 TIMING AND EXTENT OF EXTINCTION RATE INCREASES

In terms of the timing of their closest extinction rate increase relative to OAE 2, within one and a half million years before and after the event (Figure 4.2-1a), the clades fall into two groups. These are found in figure 4.2-1b and were termed phase-1: extinction-rates that increased before the onset of OAE 2 - calcareous nannofossils, dinoflagellates, benthic forams, and planktonic forams, and phase-2: those that did not increase until after OAE 2 was initiated - ammonites, radiolaria, and the second pulse from dinoflagellates.

The extent and timing of OAE 2, as seen by responses of extinction-rates, vary between clades. Of the clades that started to show extinction rate increases before the onset of OAE 2, origination peaks are found within one million years of the extinction-rate range beginning point. However, all other origination peaks and troughs appear random throughout the ranges, suggesting that each clade had a differing response to OAE 2.

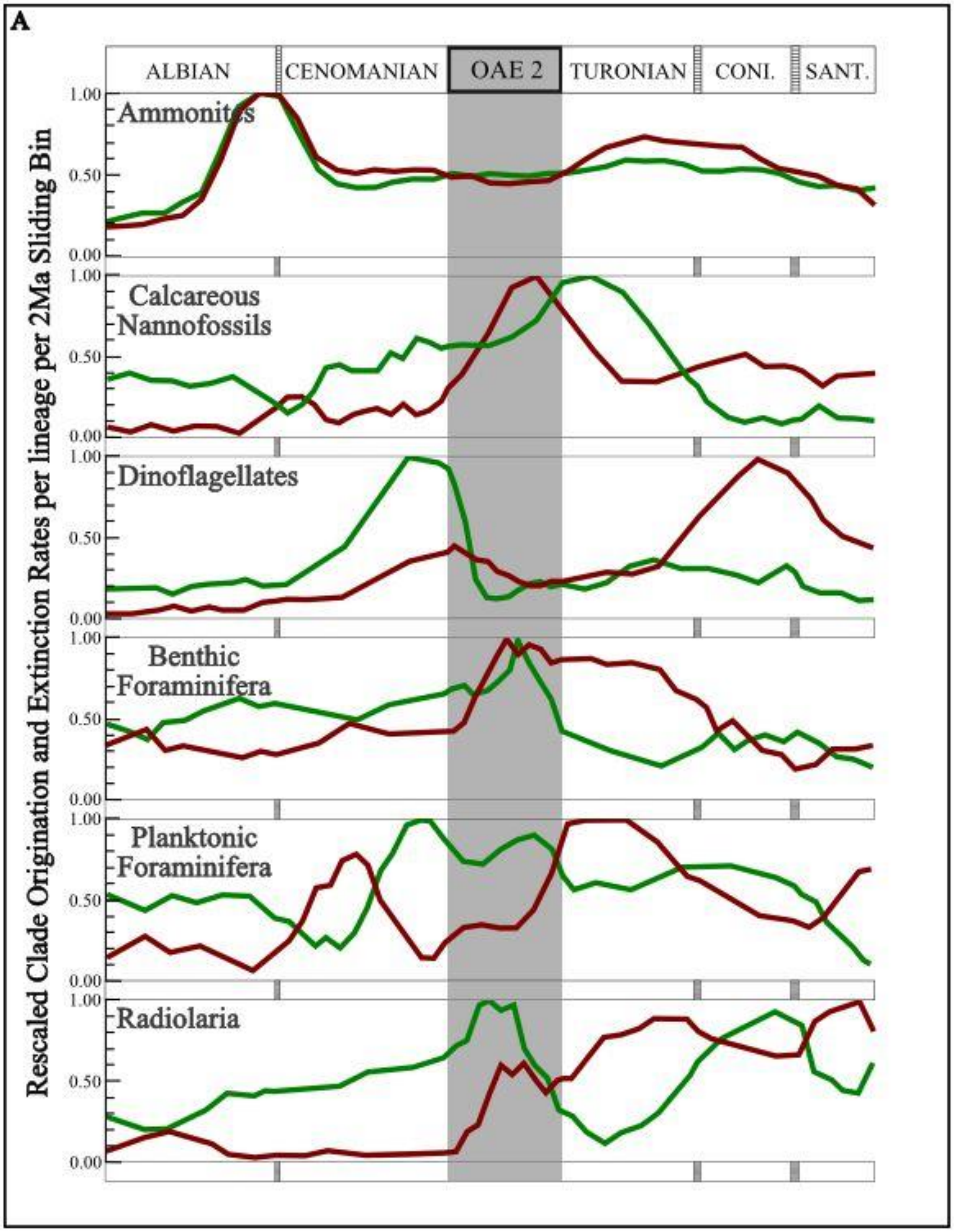
A
ALBIAN
CENOMANIAN
OAE 2
TURONIAN
CONI.
SANT.
Rescaled Clade Origination and Extinction Rates per lineage per 2Ma Sliding Bin
Ammonites
Calcareous Nannofossils
Dinoflagellates
Benthic Foraminifera
Planktonic Foraminifera
Radiolaria
1.00
0.50
0.00

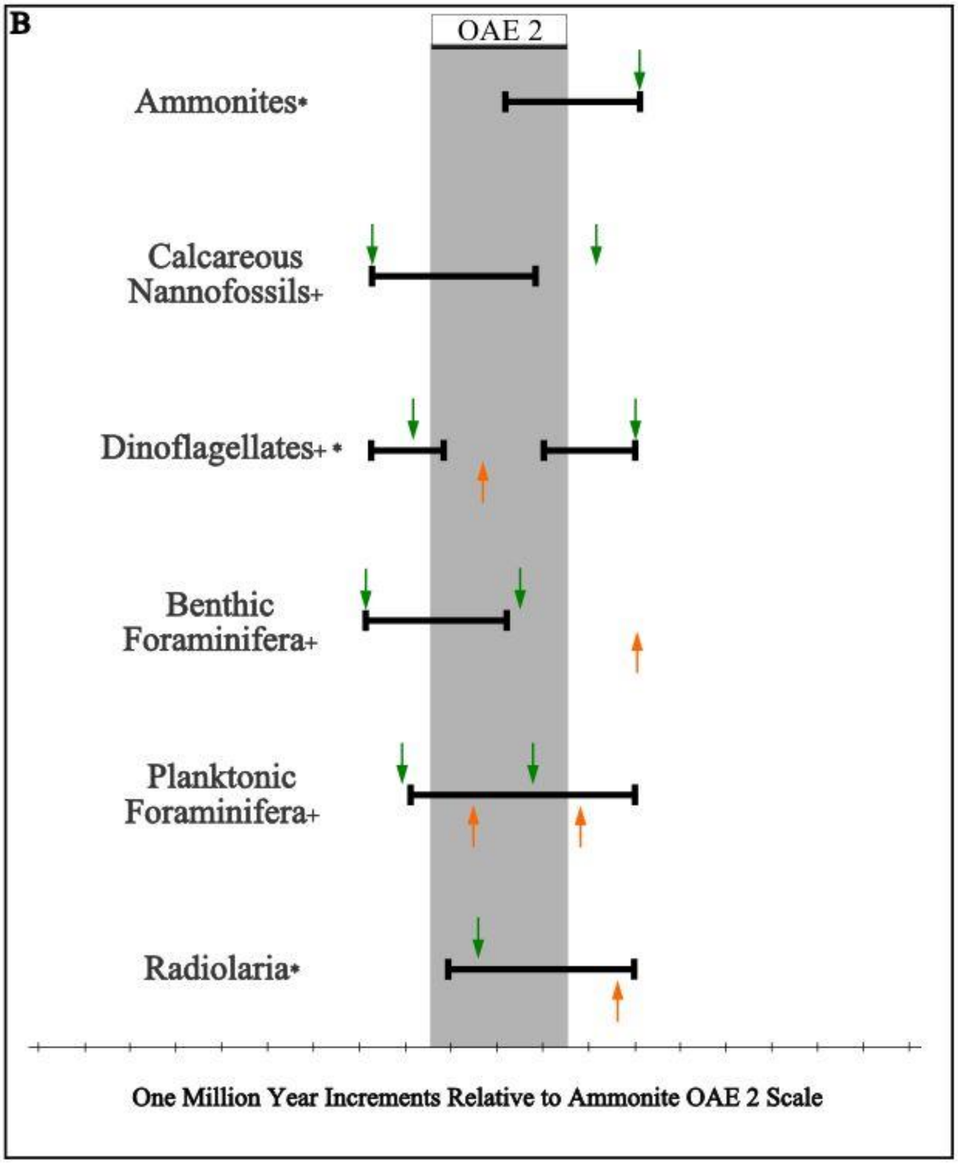

Figure 4.2-1: [A] Origination and extinction rate peaks for each clade. These have been rescaled to the ammonite stage boundaries in two million year sliding bins, and between zero and one for amplitude on the y-axis. There is no clear extinction coordination between clades. [B] Clades that started before OAE 2 (+) were termed phase-1, and those that started inside (*) were phase-2. Rescaled to a two million year sliding bin, extinction rate increases (black bar) were from lowest point in the interval to highest point and found greater than or equal to 0.1 amplitude difference and span greater than 1 million years. Origination peaking points (green arrows) distinguished again as being significant when a greater than or equivalent to amplitude difference of 0.1 was reached from lowest point to highest in a span over 1 million years; origination trough (orange arrow) were done the same but from highest point to lowest. Additionally, the significant peaks and troughs are at least a million years apart where they occur in the same clade. The zone of interest included one and a half million years outside the OAE 2 interval.

4.3 IMPACT OF OAE 2 ON DIVERSIFICATION

The fluctuating origination and extinction rates failed to show a common pattern during OAE 2, but it remains to examine the difference between these two rates – diversification rate. Figure 4.3-1 uses the same two million year sliding time bin as figure 4.2-1. The six time scales are reconciled at the stage boundaries and the OAE 2 interval according to the ammonite clade ranges.

There are two aspects of this figure to be considered: 1) intervals of positive diversification vs negative rate (green vs red) and 2) whether these intervals have any special alignment with the position of OAE 2.

1 - All clades have overall positive (or equal in the case of the ammonites) diversification rates going into OAE 2. The anoxic interval is a boundary between two different diversification dynamics. Prior to OAE 2 intervals of positive diversification dominate. After OAE 2 intervals of negative diversification are more extensive than the positive.

2 - Moving the OAE 2 band to other positions along the x-axis, cannot align it with any more fundamental change.

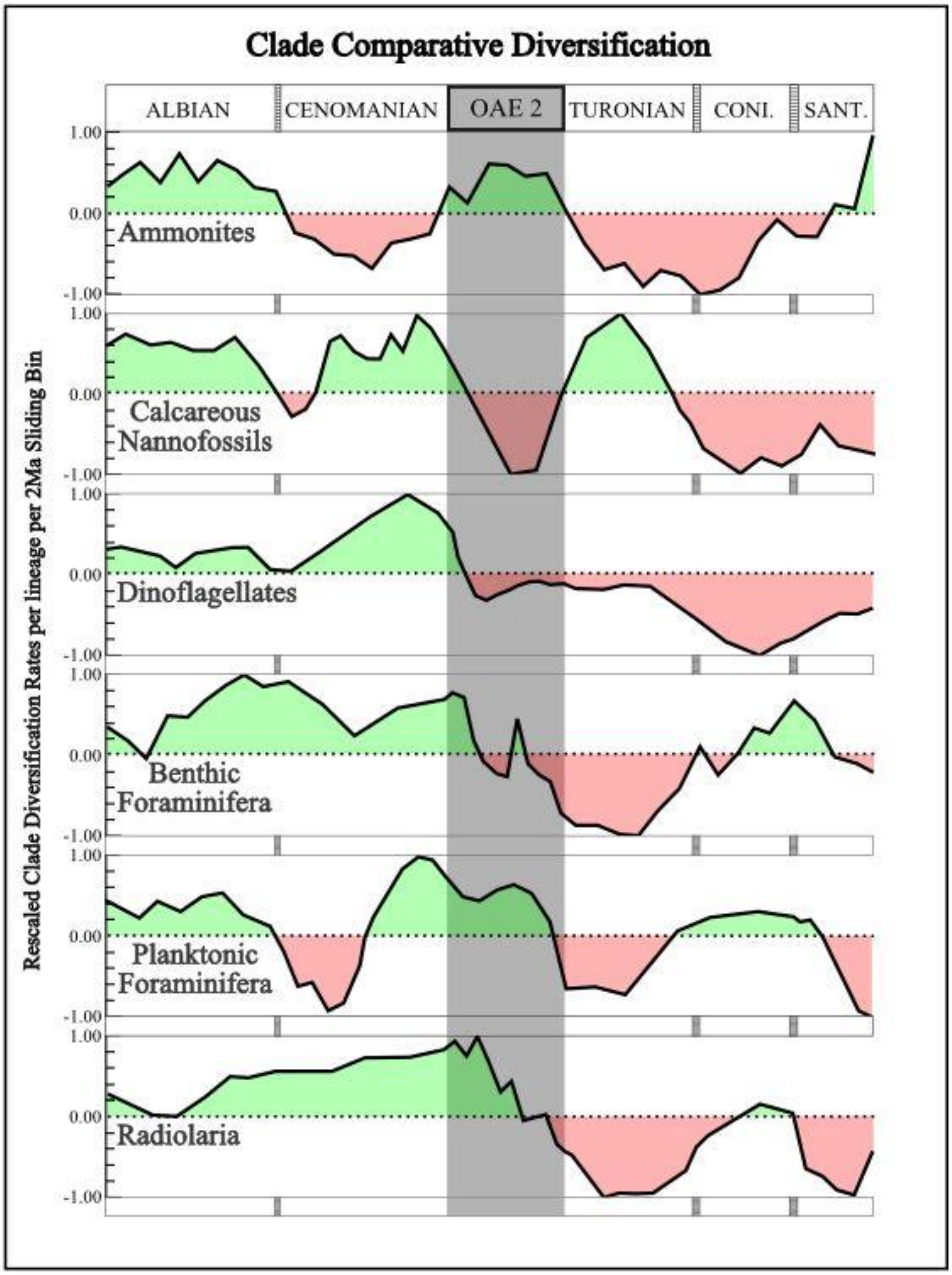

Figure 4.3-1: Diversification rates through time. All clades scaled to ammonite OAE 2 and stage boundaries. Dotted line at zero; regions of less extinctions than originations (green) are positive values; and dominating extinction rates (red) are negative values.

CHAPTER 5 - HIGH RESOLUTION TIME-LINES

The CONOP time-lines reveal that for pelagic organisms a more nuanced interpretation of OAE 2 is required than a simple mass-extinction model. Now that the computer-optimized time-lines are available, more questions can be answered than fully pursued during this project. The time-lines may be examined at the level of local ranges rather than global composite ranges and in terms of biogeographic and ecological variables such as water depth, temperature, latitude, and ecology. The local range ends have all been mapped into the time-line, but there are on the order of 50,000 local range-end events compared with the ~10,000 global range-end events analyzed here for extinction; the local range-ends will be the foundation for the later extirpation exercise. The methods developed for this database could be applied to other Phanerozoic time intervals.

CHAPTER 6 - SUMMARY

1) Traditionally binned data give lower resolution results than those achieved for this dataset. Letting range-ends fall continuously across a time-line without constraining bins leads to finer resolution than coarse traditional biozones.
2) Extinction and origination rates fluctuate for each clade through OAE 2 and extinction pulses are not coordinated across clades or with the onset of the positive carbon isotope excursion in carbonates.
3) OAE 2 is the boundary between positive and negative diversification regimes for these six clades.
4) The data and tools are available for the analysis of local ranges and exploration of a coordinated extirpation event.

REFERENCES

Arthur, M.A., and Schlanger, S.O. (1979). Cretaceous ‘oceanic anoxic events’ as casual factors in development of reef-reservoired giant oil fields. *AAPG bulletin*, v. 63(6), p. 870-885.

Arthur, M.A., Dean, W.E., and Schlanger, S.O. (1985). Variations in the global carbon cycle during the Cretaceous related to climate, volcanism, and changes in atmospheric CO_2. In: Sundquist, E.T., Broecker, W.S. (eds.), *The Carbon Cycle and Atmospheric* CO_2*: Natural Variations Archean to Present*, v. 32, p. 504-529.

Arthur, M.A., Schlanger, S.T., and Jenkyns, H.C. (1987). The Cenomanian-Turonian Oceanic Anoxic Event, II. Palaeoceanographic controls on organic-matter production and preservation. *Geological Society, London, Special Publications*, v. 26(1), p. 401-420.

Arthur, M.A., Dean, W.E., and Pratt, L.M. (1988). Global ocean–atmosphere geochemical and climatic effects of the Cenomanian/Turonian marine productivity event. *EOS. Transactions of the American Geophysical Union*, v. 69, 300 pp.

Arthur, M.A., Brumsack, H.J., Jenkyns, H.C., and Schlanger, S.O. (1990). Stratigraphy, geochemistry, and paleoceanography of organic carbon-rich Cretaceous sequences. *In:* Ginsburg, R.N., Beaudoin, B. (eds.), *Cretaceous Resources, Events and Rhythms: Background and Plans for Research*, v. 304, p. 75-119.

Banerjee, A., and Boyajian, G. (1996). Changing biologic selectivity of extinction in the Foraminifera over the past 150 m.y. *Geology*, v. 24(7), p. 607–610.

Bice, K.L., and Norris, R.D. (2002). Possible atmospheric CO_2 extremes of the Middle Cretaceous (late Albian–Turonian). *Paleoceanography*, v. 17(4), 22 pp.

Blakey, R. (2011). Global Paleogeography. Retrieved October 1, 2014, from http://jan.ucc.nau.edu/~rcb7/index.html

Bowman, A. R., and Bralower, T. J. (2005). Paleoceanographic significance of high-resolution carbon isotope records across the Cenomanian–Turonian boundary in the Western Interior and New Jersey coastal plain, USA. *Marine Geology*, v. 217, p. 305–321.

Bralower, T.J. (1988). Calcareous nannofossils biostratigraphy and assemblages of the Cenomanian-Turonian boundary interval: implications for the origin and timing of oceanic anoxia. *Paleoceanography*, v. 3, p. 275-316.

Bralower, T.J., Sliter, W.V., Arthur, M.A., Leckie, R.M., Allard, D.J., and Schlanger, S.O. (1993). Dysoxic/anoxic episodes in the Aptian–Albian (Early Cretaceous). *Am. Geophys. Union Monogr.*, v. 73, p. 5–37.

Bralower, T.J., CoBabe, E., Clement, B., Sliter, W.V., Osburn, C.L., and Longoria, J. (1999). The record of global change in mid-Cretaceous (Barremian-Albian) sections from the Sierra Madre, northeastern Mexico. *The Journal of Foraminiferal Research,* v. 29(4), p. 418-437.

Busson, G., and Cornée, A. (1996). *L'événement océanique anoxique du Cénomanien supérieur–terminal: une revue et une interprétation mettant en jeu une stratification des eaux marines par le CO_2 mantellique.* Société géologique du Nord, v. 23.

Caron, M., Robazynski, F., Amedro, F., Baudin, F., Deconinck, J.F., Hochhuli, P., von Salis-Perch Nielsen, K., and Tribovillard, N. (1999). Estimation de la duree de l'evenement anoxique global au passage Cenomanien/Turonien; approche cyclostratigraphique dans la formation Bahloul en Tunisie centrale. *Bulletin de la Société géologique de France,* v. 170(2), p. 145-160.

Caron, M., Dall'Agnolo, S., Accarie, H., Barrera, E., Kauffman, E.G., Amédro, F., and Robaszynski, F. (2006). High-resolution stratigraphy of the Cenomanian-Turonian boundary interval at Pueblo (USA) and wadi Bahloul (Tunisia): stable isotope and bio-events correlation. *Geobios*, v. 39, p. 171–200.

Caus, E., Teixell, A., and Bernaus, J.M. (1997). Depositional model of a Cenomanian–Turonian extensional basin (Sopeira Basin, NE Spain): interplay between tectonics, eustasy and biological productivity. *Palaeogeography, Palaeoclimatology, Palaeoecology,* v. 129, p. 23–36.

Coffin, M.F., and Eldholm, O. (1994). Large igneous provinces: crustal structure, dimensions, and external consequences. *Reviews of geophysics-Richmond Virginia then Washington-,* v. 32, 36 pp.

Cooper, R.A., Crampton, J.S., Raine, J.I., Gradstein, F.M., Morgans, H.E.G., Sadler, P.M., Strong, C.P., Waghorn, D., and Wilson, G.J. (2001). Quantitative biostratigraphy of the Taranaki Basin, New Zealand – A deterministic and probabilistic approach. *American Association of Petroleum Geologists Bulletin,* v. 85, p. 1469-1498.

Cooper, R.A., Sadler, P.M., Munnecke, A., and Crampton, J.S. (2013). Graptoloid evolutionary rates track Ordovician–Silurian global climate change. *Geological Magazine*, v. 151, 349-364.

Deniston, B. (2012, March 10). Mass extinctions as shadows of anti-entropic growth - macro-ecological revolutions. Retrieved August 27, 2015, from http://archive.larouchepac.com/node/21941.

Edwards, L.E. (1978). Range Charts and No-Space Graphs. *Computers & Geosciences,* v. 4, p. 247-255.

Elder, W.P. (1989). Paleontological society molluscan extinction patterns across the Cenomanian-Turonian stage boundary in the Western Interior of the United States. *Paleobiology,* v. 15, p. 299–320.

Erbacher, J.V.J.T., and Thurow, J. (1997). Influence of oceanic anoxic events on the evolution of mid-Cretaceous radiolaria in the North Atlantic and western Tethys. *Marine Micropaleontology,* v. 30, p. 139-158.

Erbacher, J., Thurow, J., and Littke, R. (1996). Evolution patterns of radiolaria and organic matter variations: A new approach to identify sea–level changes in mid-Cretaceous pelagic environments. *Geology*, v. 24, p. 499–502.

FitzPatrick, M.E.J. (1995). Dinoflagellate cyst biostratigraphy of the Turonian (Upper Cretaceous) of southern England. *Cretaceous Research*, v. 16, p. 757-791.

Gale, A.S., Jenkyns, H.C., Kennedy, W.J., and Corfield, R.M. (1993). Chemostratigraphy versus biostratigraphy: data from around the Cenomanian–Turonian boundary. *Journal of the Geological Society, London,* v. 150, p. 29–32.

Gale, A.S., Smith, A.B., Monks, N.E. A., Young, J.A., Howard, A., Wray, D.S., and Huggett, J.M. (2000). Marine biodiversity through the Late Cenomanian–Early Turonian: palaeoceanographic controls and sequence stratigraphic biases. *Journal of the Geological Society, London,* v. 157, p. 745–757.

Gale, A.S., Kennedy, W.J., Voigt, S., and Walaszczyk, I. (2005). Stratigraphy of the Upper Cenomanian-Lower Turonian Chalk succession at Eastbourne, Sussex, UK: Ammonites, inoceramid bivalves and stable carbon isotopes. *Cretaceous Research*, v. 26, p. 460–487.

Gebhardt, H., Friedrich, O., Schenk, B., Fox, L., Hart, M., and Wagreich, M. (2010). Paleoceanographic changes at the northern Tethyan margin during the Cenomanian-Turonian Oceanic Anoxic Event (OAE-2). *Marine Micropaleontology,* v. 77, p. 25-45.

Gradstein, F.M., Ogg, J.G., Schmitz, M.D., and Ogg, G.M. (2012). *The geologic time scale 2012,* v. 2.

Hallam, A. (1992). *Phanerozoic sea-level changes*. Columbia University Press, New York. 266 pp.

Hallam, A., and Wignall, P. B. (1997). *Mass extinctions and their aftermath*. Oxford University Press. 328 pp.

Hancock, J.M., and Kauffman, E.G. (1979). The great transgressions of the Late Cretaceous. *Journal of the Geological Society*, v. 136, p. 175–186.

Haq, B.U., Hardenbol, J., and Vail, P.R. (1987). Chronology of fluctuating sea levels since the Triassic. *Science (New York, N.Y.)*, v. 235(4), p. 1156–1167.

Harries, P.J. (1993). Dynamics of survival following the Cenomanian–Turonian (Upper Cretaceous) mass extinction event. *Cretaceous Research,* v. 14, p. 563–583.

Harries, P.J., and Kauffman, E.G. (1990). Patterns of survival and recovery following the Cenomanian-Turonian (Late Cretaceous) mass extinction in the Western Interior Basin, United States. In: *Extinction events in earth history,* Springer Berlin Heidelberg, p. 277-298.

Harries, P.J., and Little, C.T.S. (1999). The early Toarcian (Early Jurassic) and the Cenomanian-Turonian (Late Cretaceous) mass extinctions: similarities and contrasts. *Palaeogeography, Palaeoclimatology, Palaeoecology,* v. 154, p. 39–66.

Hart, M.B. (1996). Recovery of the food chain after the Late Cenomanian extinction event. *Geological Society, London, Special Publications*, v. 102(1), p. 265–277.

Hart, M.B., and Leary, P.N. (1991). Stepwise mass extinctions: the case for the Late Cenomanian event. *Terra Nova,* v. 3(2), p. 42–147.

Hasegawa, T. (1997). Cenomanian-Turonian carbon isotope events recorded in terrestrial organic matter from northern Japan. *Palaeogeography, Palaeoclimatology, Palaeoecology*, v. 130, p. 251–273.

Hasegawa, T. (2003) A global carbon–isotope event in the Middle Turonian (Cretaceous) sequence in Japan and Russian Far East. *Proc. Japan Acad.,* v. 79(B), p. 141–144.

Hasegawa, T., Pratt, L.M., Maeda, H., Shigeta, Y., Okamoto, T., Kase, T., and Uemura, K. (2003). Upper Cretaceous stable carbon isotope stratigraphy of terrestrial organic matter from Sakhalin, Russian Far East: A proxy for the isotopic composition of paleoatmospheric CO_2. *Palaeogeography, Palaeoclimatology, Palaeoecology*, v. *189*, p. 97–115.

Herbin, J. P., Montadert, L., Müller, C., Gomez, R., Thurow, J., and Wiedmann, J. (1986). Organic-rich sedimentation at the Cenomanian-Turonian boundary in oceanic and coastal basins in the North Atlantic and Tethys. *Geological Society, London, Special Publications*, v. 21(1), p. 389-422.

Hilbrecht, H., Hubberten, H.-W., and Oberhänsli, H. (1992). Biogeography of planktonic foraminifera and regional carbon isotope variations: productivity and water masses in late Cretaceous Europe. *Palaeogeography, Palaeoclimatology, Palaeoecology,* v. 92, p. 407–421.

Hirano, H., Toshimitsu, S., Matsumoto, T., and Takahashi, K. (2000). Changes in Cretaceous ammonoid diversity and marine environments of the Japanese Islands. *Developments in Palaeontology and Stratigraphy,* v. 17, p. 145-154.

Hora, J.M., and Marshall, C.R. (1998). The Cenomanian macrofossil extinctions in the western interior seaway, USA, after correcting for the incompleteness of the fossil record. *Paleobios,* v. 18 [Supplement to number 3], 4 pp.

Hsieh, H.L., and Li, L.A. (1998). Rarefaction diversity: a case study of polychaete communities using an amended fortran program. *Zoological Studies,* v. 31(1), p. 13-21.

Jablonski, D. (1991). Extinctions: a paleontological perspective. *Science,* v. 253(5021), p. 754–757.

Jarvis, I., Carson, G.A., Cooper, K., Hart, M.B., Leary, P., Tocher, B.A., Horne, D., and Rosenfeld, A. (1988). Microfossil assemblages and the Cenomanian–Turonian (Late Cretaceous) Oceanic Anoxic Event. *Cretaceous Research,* v. 9, p. 3–103.

Jenkyns, H.C. (1980). Cretaceous anoxic events: from continents to oceans. *Journal of the Geological Society*, v. 137, p. 171–188.

Jenkyns, H.C. (1985). The early Turonian and Cenomanian-Turonian anoxic events in Europe: comparisons and contrasts. *Geologische Rundschau,* v. 74(3), p. 505-518.

Kaiho, K., Fujiwara, O., and Motoyama, I. (1993). Mid-Cretaceous faunal turnover of intermediate-water benthic foraminifera in the northwestern Pacific Ocean margin. *Marine Micropaleontology,* v. 23, p. 13–49.

Kaiho, K., and Hasegawa, T. (1994). End–Cenomanian benthic foraminiferal extinctions and oceanic dysoxic events in the northwestern Pacific Ocean. *Palaeogeography, Palaeoclimatology, Palaeoecology*, v. 111(1), p. 29–43.

Kauffman, E.G. (1995). Global change leading to biodiversity crisis in a greenhouse world: the Cenomanian–Turonian (Cretaceous) mass extinction. *Effects of Past Global Change on Life*. National Academies Press. 272 pp.

Keller, G., and Pardo, A. (2004). Age and paleoenvironment of the Cenomanian-Turonian global stratotype section and point at Pueblo, Colorado. *Marine Micropaleontology*, v. 51, p. 95–128.

Kennedy, W.J., Walaszczyk, I., and Cobban, W.A. (2005). The global boundary stratotype section and point for the base of the Turonian stage of the Cretaceous: Pueblo, Colorado, U.S.A. *Episodes*, v. 28, p. 93–104.

Kerr, A.C. (1998). Oceanic plateau formation: a cause of mass extinction and black shale deposition around the Cenomanian–Turonian boundary? *Journal of the Geological Society*, v. 155(4), p. 619–626.

Kuroda, J., Ogawa, N.O., Tanimizu, M., Coffin, M.F., Tokuyama, H., Kitazato, H., and Ohkouchi, N. (2007). Contemporaneous massive subaerial volcanism and late cretaceous Oceanic Anoxic Event 2. *Earth and Planetary Science Letters*, v. 256, p. 211-223.

Kuypers, M.M.M., Pancost, R.D., Nijenhuis, I.A., and Damste, J.S.S. (2002). Enhanced productivity led to increased organic carbon burial in the euxinic North Atlantic basin during the late Cenomanian oceanic anoxic event. *Paleoceanography*, v. 17(4), p. 1–13.

Lamolda, M.A., Gorostidi, A., and Paul, C.R.C. (1994). Quantitative estimates of calcareous nannofossil changes across the Plenus Marls (latest Cenomanian), Dover, England: implications for the generation of the Cenomanian-Turonian boundary event. *Cretaceous Research*, v. 15, p. 143-164.

Lamolda, M.A., and Mao, S. (1999). The Cenomanian–Turonian boundary event and dinocyst record at Ganuza (northern Spain). *Palaeogeography, Palaeoclimatology, Palaeoecology*, v. 150, p. 65-82.

Larson, R.L. (1991). Geological consequences of superplumes. *Geology*, v. 19, p. 963–966.

Lauridsen, B.W., Gale, A.S., and Surlyk, F. (2009). Benthic macrofauna variations and community structure in Cenomanian cyclic chalk-marl from Southerham Grey Pit, SE England. *Journal of the Geological Society*, v. 166, p. 115–127.

Leckie, R.M., Bralower, T.J., and Cashman, R. (2002). Oceanic anoxic events and plankton evolution: Biotic response to tectonic forcing during the mid–Cretaceous. *Paleoceanography*, v. 17(3), 29 pp.

Lenniger, M., Nøhr-Hansen, H., Hills, L.V., Bjerrum, C.J. (2014). Arctic black shale formation during Cretaceous Oceanic Anoxic Event 2. *Geology*, v. 42(9), p. 799–802.

Marshall, C. R. (2010). Using confidence intervals to quantify the uncertainty in the end-points of stratigraphic ranges. *In:* Alroy, J. , and Hunt, G., (eds.) Quantitative Methods in Paleobiology, Paleontological Society papers, v. 16, p. 291-316.

Melinte-Dobrinescu, M.C., Bernardez, E., Kaiho, K., and Lamolda, M.A. (2013). Cretaceous Oceanic Anoxic Event 2 in the Arobes section, northern Spain: nannofossil fluctuations and isotope events. *Geological Society, London, Special Publications*, v. 382, 22 pp.

Monnet, C. (2009). The Cenomanian-Turonian boundary mass extinction (Late Cretaceous): New insights from ammonoid biodiversity patterns of Europe, Tunisia and the Western Interior (North America). *Palaeogeography, Palaeoclimatology, Palaeoecology*, v. 282, p. 88–104.

Musavu-Moussavou, B., Danelian, T., Baudin, F., Coccioni, R., and Fröhlich, F. (2007). The Radiolarian biotic response during OAE2. A high-resolution study across the Bonarelli level at Bottaccione (Gubbio, Italy). *Revue de Micropaleontologie*, v. 50, p. 253–287.

Patterson, C., and Smith, A.B. (1987). Is the periodicity of extinctions a taxonomic artefact? *Nature*, v. 330(6145), p. 248–251.

Patterson, C., and Smith, A.B. (1989). Periodicity in extinction: the role of systematics. *Ecology*, v. 70(4), p. 802-811.

Patzkowsky, M.E., and Holland, S.M. (2012). *Stratigraphic paleobiology: understanding the distribution of fossil taxa in time and space*. University of Chicago Press. 259 pp.

Paul, C.R.C., and Mitchell, S.F. (1994). Is famine a common factor in marine mass extinctions? *Geology*, v. 22(8), p. 679–682.

Paul, C.R.C., Lamolda, M.A., Mitchell, S.F., Vaziri, M.R., Gorostidi, A., and Marshall, J.D. (1999). The Cenomanian–Turonian boundary at Eastbourne (Sussex, UK): a proposed European reference section. *Palaeogeography, Palaeoclimatology, Palaeoecology*, v. 150(1), p. 83–121.

Pearce, M.A., Jarvis, I., and Tocher, B.A. (2009). The Cenomanian–Turonian boundary event, OAE2 and palaeoenvironmental change in epicontinental seas: New insights from the dinocyst and geochemical records. *Palaeogeography, Palaeoclimatology, Palaeoecology*, v. 280, p. 207-234.

Peters, S.E., and Foote, M. (2001). Biodiversity in the Phanerozoic: a reinterpretation. *Journal Information*, v. 27, p. 593-601.

Pratt, L.M., and Threlkeld, C.N. (1984). Stratigraphic significance of $^{13}C/^{12}C$ ratios in mid-Cretaceous rocks of the Western Interior, USA. *In:* Stoff, D.F., and Glass, D.J. (eds), *The Mesozoic of Middle North America*, Canadian Society of Petroleum Geologists, Memoirs, v. 9, p. 305–312.

Pratt, L.M. (1985). Isotopic studies of organic matter and carbonate in rocks of the Greenhorn marine cycle. *In:* Pratt, L.M., Kauffman, E.G., Zelt, F.B. (eds.), *Fine–Grained Deposits and Biofacies of the Cretaceous Western Interior Seaway: Evidence of cyclic Sedimentary Processes.* SEPM, Second Annual Meeting Golden, CO, Field Trip Guidebook, v. 4, p. 38-48.

Raup, D. M. (1972). Taxonomic diversity during the Phanerozoic. *Science*, v. 177(4054), p. 1065-1071.

Raup, D.M., and Sepkoski, J.J. (1984). Periodicity of extinctions in the geologic past. *Proceedings of the National Academy of Sciences of the United States of America*, v. 81, p. 801–805.

Raup, D.M., and Sepkoski, J.J. (1986). Periodic extinction of families and genera. *Science*, v. 231, p. 833–836.

Ryan, W.B.F., and Cita, M.B. (1977). Influence of abyssal circulation on sedimentary accumulations in space and time. *Developments in Sedimentology*, v. 23, p. 197–215.

Sadler, P.M., Cooper, R.A., and Melchin, M. (2009). High-resolution, early Paleozoic (Ordovician-Silurian) time scales. *GSA Bulletin*, v. 121(5/6), p. 887-906.

Sadler, P.M. (2010). Brute-force biochronology: sequencing paleobiologic first- and last-appearance events by trial and error, *In:* Alroy, J. , and Hunt, G., (eds.) Quantitative Methods in Paleobiology, Paleontological Society papers, v. 16, p.271-289.

Sadler, P.M. (2012). Integrating carbon isotope excursions into automated stratigraphic correlation: an example from the Silurian of Baltica. *Bulletin of Geosciences*, v. 87(4), p. 681-694.

Sadler, P.M. (2013). Stratigraphic Completeness, in Macleod, N., Archibald, D., and Levin, P., Grzimek's Animal Life Encyclopedia: Extinction, Gale (Cengage). Farmington Mills, MI, v. 2, p.51-62.

Sadler, P.M., Cooper, R.A., and Crampton, J.S. (2014). High-resolution geobiologic time-lines: progress and potential, fifty years after the advent of graphic correlation. *The Sedimentary Record,* v. 12(3), p. 4-10.

Schlanger, S.O., and Jenkyns, H.C. (1976). Cretaceous oceanic anoxic events: causes and consequences. *Geologie En Mijnbouw*, v. 55(3–4), p. 176–184.

Schlanger, S.O., Arthur, M.A., Jenkyns, H.C., and Scholle, P.A. (1987). The Cenomanian–Turonian Oceanic Anoxic Event, I. Stratigraphy and distribution of organic carbon-rich beds and the marine $\delta^{13}C$ excursion. *Geological Society, London, Special Publications*, v. 26(1), p. 371–399.

Scholle, P.A., and Arthur, M.A. (1980). Carbon isotope fluctuations in Cretaceous pelagic limestones: potential stratigraphic and petroleum exploration tool. *AAPG Bulletin*, v. 64(1), p. 67–87.

Sepkoski, J.J. (1989). Periodicity in extinction and the problem of catastrophism in the history of life. *Journal of the Geological Society*, v. 146, p. 7–19.

Shaw, A. B. (1964). *Time in stratigraphy*. New York: McGraw-Hill.

Sliter, W.V. (1989). Biostratigraphic zonation for Cretaceous planktonic foraminifera examined in thin section. *Journal of Foraminiferal Research*, v. 19, 19 pp.

Smith, A.B., and McGowan, A.J. (2007). The shape of the phanerozoic marine palaeodiversity curve: How much can be predicted from the sedimentary rock record of Western Europe? *Palaeontology*, v. 50, p. 765–774.

Snow, L.J., Duncan, R.A., and Bralower, T.J. (2005). Trace element abundances in the Rock Canyon Anticline, Pueblo, Colorado, marine sedimentary section and their relationship to Caribbean plateau construction and oxygen anoxic event 2. *Paleoceanography*, v. 20, 14 pp.

Strauss, D., and Sadler, P.M. (1989). Classical confidence intervals and Bayesian probability estimates for ends of local taxon ranges. *Mathematical Geology*, v. 21(4), p. 411–427.

Takashima, R., Nishi, H., Hayashi, K., Okada, H., Kawahata, H., Yamanaka, T., Fernando, A.G., and Mampuku, M. (2009). Litho-, bio- and chemostratigraphy across the Cenomanian/Turonian boundary (OAE 2) in the Vocontian Basin of southeastern France. *Palaeogeography, Palaeoclimatology, Palaeoecology,* v. 273, p. 61-74.

Tsikos, H., Jenkyns, H.C., Walsworth–Bell, B., Petrizzo, M.R., Forster, A., Kolonic, S., Erba, E., Premoli Silva, I., Baas, M., Wagner, T., and Sinninghe Damsté, J. S. (2004). Carbon-isotope stratigraphy recorded by the Cenomanian–Turonian Oceanic Anoxic Event: correlation and implications based on three key localities. *Journal of the Geological Society*, v. 162, p. 576–576.

Uličný, D., Hladíková, J., Attrep Jr, M.J., Čech, S., Hradecká, L., & Svobodová, M. (1997). Sea-level changes and geochemical anomalies across the Cenomanian–Turonian boundary: Pecınov quarry, Bohemia. *Palaeogeography, Palaeoclimatology, Palaeoecology*, v. 132(1), p. 265–285.

Wagreich, M., Bojar, A.V., Sachsenhofer, R.F., Neuhuber, S., and Egger, H. (2008). Calcareous nannoplankton, planktonic foraminiferal, and carbonate carbon isotope stratigraphy of the Cenomanian–Turonian boundary section in the Ultrahelvetic Zone (Eastern Alps, Upper Austria). *Cretaceous Research*, v. 29, p. 965-975.

Wignall, P.B. (1994). Black Shales. *In:* Woods, M. (ed.), Greenhouse Earth — the story of ancient climate change. British Geological Survey, Natural Environment Research Council. Retrieved October 1, 2014, from http://www.bgs.ac.uk/discoveringGeology/climateChange/greenHouseEarth.

APPENDIX

References with an asterisk for missing information denote those that were found second hand through Robert Scott's online database (http://precisionstratigraphy.com/index.html). Where no section is listed a number of factors were the case, they were: just beyond the buffer zone of interest, questionable data was found, or possibly entered for taxonomic dictionary purposes (i.e. synonyms).

Reference Code:	**Associated Reference Section Name:**	**Reference Citation Used in CONOP:**
ABAW0501	Jambur #46	Abawi, T.S., and Mahmood, S.A. (2005). Biostratigraphy of the Kometan and Gulneri Formations (Upper Cretaceous) in Jambur Well No, 46, Northern Iraq. *Iraqui Journal of Earth Science,* v. 5(1), p. 1-8.
ABDA9587		Abdallah, H., Memmi, L., Damotte, R., Rat, P., and Magniez-Jannin, F. (1995). Le Cretace de la chaine nord des Choffs (Tunisie du centre-sud): biostratigraphie et comparaison avec les regions voisines. *Cretaceous Research,* v. 16, p. 487-538.
ABDA9797	Wadi Berda, Wadi Bou Jarra	Abdallah, H., and Meister, C. (1997) The Cenomanian-Turonian boundary in the Gafsa-Choff area (southern part of central Tunisia): biostratigraphy and palaeoenvironments. *Cretaceous Research,* v. 18, p. 197-236.

ABDE0653	Abu Darag Lighthouse	Abdel-Gawad, G.I., El Qot, G.M., and Mekawy, M.S. (2006). Cenomanian-Turonian macrobiostratigraphy of Abu Darag area, northern Galala, eastern desert, Egypt. *Intern. Conf. Geol. Arab World (GAW8)*, p. 553-568.
ABDE0700	Wadi Qena 1, Wadi Qena 2, Wadi Qena 3, Wadi Qena 5, Wadi Qena 6	Abdelhady, A.A. (2007). *Stratigraphical and palaeontological studies on the Upper Cretaceous strata, North Wadi Qena, Eastern Desert, Egypt* (Master's Thesis), Minia University.
ABUZ0803		Abu-Zied, R.H. (2008). Lithostratigraphy and biostratigraphy of some Lower Cretaceous outcrops from northern Sinai, Egypt. *Cretaceous Research*, v. 29, p. 603-624.
AGTE0500		Agterberg, F. (2005). Geomathematics, chapter 8. *In:* Gradstein, F., Ogg, J., and Smith, A.G. (eds.), *A geologic time scale 2004.* Cambridge University Press.
AGUA9709	Cortijo del Hielo	Aguado, R., Campny, M., Sandoval, J., and Tavera, J.M. (1997). Biostratigraphic events at he Barremian/Aptian boundary in the Betic Cordillera, southern Spain. *Cretaceous Research*, v. 18, p. 309-329.
AGUA9963	Cau	Aguado, R., Castro, J.M., Company, M., and de Gea, G. (1999). Aptian bio-events - and integrated biostratigraphic analysis of the Almadich Formation, Inner Prebetic Domain, SE Spain. *Cretaceous Research*, v. 20, p. 663-683.

AGUI0137	Amacuzac, Barranca del Tigre, La Esperanza, Las Tunas	Aguilera-Franco, N., Hernandez-Romano, U., and Allison, P. A. (2001). Biostratigraphy and environmental chabges across the Cenomanian-Turonian boundary, southern Mexico. *Journal of South American Earth Sciences*, v. 14, p. 237-255.
AHMA1323	Ajlun	Ahmad, F., Barragan, R., Szives, O., and Vega-Vera, F. (2013). Cenomanian ammonites of the Shuayb Formation, Jordan. *Jordan Journal of Earth and Environmental Sciences*, v. 5(1), p. 23-30.
ALAB9509	Ajnyn River, Kruglokamennaja River, Niklekujul River	Alabushev, A. (1995). Ammonite faunas and biostratigraphy of the Albian to middle Cenomanian (Cretaceous) in western Korjak-Kamchatka, NE Russia. *Neues Jahrbuch fuer Geologie und Palaeontologie Abhandlungen*, v. 196(1), p. 109-139.
ALYM0107		Aly, M. F. (2001). Pachydiscus (P.) gollevillensis (d'Orbigny) in the Cretaceous of Jebel Fayah, United Arab Emirates. *Neues Jahrbuch fuer Geologie und Palaeontologie Monatsheft*, v. 10, p. 607-616.
AMED0805	Europe Boreal Zones, Tunisia Tethyan Zones	Amedro, F., and Robaszynski, F. (2008). Zonation by ammonites and foraminifers of the Vraconian - Turonian interval: a comparison of the Boreal and Tethyan domains (NW Europe / Central Tunisia). *Carmets de Geologie,* v. 2008/L02, 5 pp.

AMED7803	Boulonnais MIDK12	Amedro et al. (1978). * *Bulletin Inf. Geol. Bassin Paris,* v. 15, p. 3-20.
AMED7805		Amedro et al. (1978). * *Geologie Mediterraneenne,* v. 5, p. 3-20.
AMED8103	Boulonnais MIDK12	Amedro et al. (1981). * *Bulletin Inf. Geol. Baasin Paris,* v. 18, p. 3-19.
AMED8133	Menneville, Nesles	Amedro, F. and Magniez-Jannin, F. (1981). Correlations lithologiques et biostratigraphiques (ammonites, foraminiferes) dans l-Albien du Boulonnais. *Extrait des Annales de la Societe Geologique du Nord,* p. 133-143.
AMED8515	Autoroute Aquitaine, Charentes Trench S7, Saumer NW,	Amedro, F., and Hancock, J.M. (1985). Les ammonites de L-Autproute L-Aquitaine, France (Turonien et Santonien). *Cretaceous Research,* v. 6, p. 15-32.
AMED9287	Bully-Montreuil, Courcelles, Folkestone 1	Amedro, F. (1992). LAlbien du bassin anglo-parisien ammonites zonation phyletique sequences. *Bulletin du Centre Recherches Exploration-Production Elf Aquitaine,* v. 16, p.187-233.
ANDE5878		Anderson, F.M. (1958). Upper Cretaceous of the Pacific Coast. *Geological Society of America Memoir,* v. 71, 378 pp.
ANDO0585	Kotanbetsu (Coni-Camp)	Ando, H., and Tomosugi, T. (2005). Unconformity between the upper Maastrictian and upper paleocene in the Hakobuchi Formation, north Hokkaido, Japan: a major time gap

		within the Yezo forearc basin sediments. *Cretaceous Research,* v. 26, pp. 85-95.
ANDR0589	Nassau Quarry (Mala11), Votorantin Quarry (Retiro)	Andrade, E.J. (2005). *Turonian inoceramids and biostratigraphy of the Sergipe Basin, northwest Brazil: an integrated study of the Votorantin and Nassua quarries* (Ph. D. dissertation), University of Heidelberg, 189 pp.
ARDE1221	Padeha	Ardestani, M.S., Vahldinia, M., Sadeghi, A., Arz, J.A., and Dochev, D. (2012). Integrated biostratigraphy of the Upper Cretaceous Abderaz Formation of the East Kopet Dagh Basin (NE Iran). *Geologica Balanica*, v. 41(1-3), p. 21-37.
ASIS1289	Darvel Bay 1, Darvel Bay 2	Asis, J., and Jasin, B. (2012). Aptian to Turonian radiolaria from the Darvel Bay ophiolite complex, Kunak, Sabah. *Bulletin of the Geological Society of Malaysia*, v. 58, p. 89-96.
ASIS1361		Asis, J., and Jasin, B. (2013). Aptian to turonian radiolarians from chert blocks in the Kuamut Range, Sabah, Malaysia. *Sains Malaysiana,* v. 42(5), p. 561-570.
BAAD9369		Baadsgaard, H., Lerbekmo, J.F., Wijbrans, J.R., Swisher, C.C., and Fanning, M. (1993). Multimethod radiometric age for a bentonite near the top of the Baculites reesidei zone of southwestern Saskatchewan (Campanian-Maastrichtian stage boundary?). *Canadian Journal of Earth Science*, v. 30, p. 769-775.

BAKK0635	Zasan	Bak, K. (2006). Sedimentological, geochemical and microfaunal responses to environmental changes around the Cenomanian-Turonian boundary in the Outer Carpathian Basin; a record from the Subsilesian Nappe, Poland. *Palaeogeography, Palaeoclimatology, Palaeoecology*, v. 237, p. 335-358.
BAKK0721	Splawa	Bak, K. (2007). Organic-rich and manganese sedimentation during the Cenomanian-Turonian boundary event in the Outer Carpathian basins: a new record from the Skole Nappe, Poland. *Palaeogeography, Paleoclimatology, Palaeoecology*, v. 256, p. 21-46.
BAKK0771	Otsra Gora, Splawa, Trzemesnia	Bak, K. (2007). Environmental changes during the Cenomanian-Turonian boundary event in the outer Carpathian Basins: a synthesis of data from various tectonic facies units. *Annales Societatis Geologorum Poloniae*, v. 77, p. 171-191.
BAKM0009	Barnasiowka-Jasienica, Czarny Potok, Lanckorona, Trzemesnia	Bak, M. (2000). Radiolaria from the upper Cenomanian - Lower Turonian deposits of the Silesian Unit (Polish Flysch Carpathians). *Geologica Carpathica*, v. 51(5), p. 309-324.
BAKM0439	Zasan	Bak, M. (2004). Radiolarian biostratigraphy of the Upper Cenomanian - Lower Turonian deposits in the Subsilesian Nappe (Outer Western Carpathians). *Geologiva Carpathica*, v. 55(3), p. 239-250.

BAKM0575	Barnasiowka-Jasienica, Otsra Gora	Bak, M., Bak, K., and Ciurej, A. (2005). Mid-Cretaceous spicule-rich turbidites in the Silesian Nappe of the Polish Outer Carpathians: radiolarian and foraminiferal biostratigraphy. *Geological Quarterly,* v. 49(3), p. 275-290.
BAKM1105	Barnasiowka-Jasienica, Contessa, Czarny Potok, Lanckorona, Otsra Gora, Trzemesnia, Zasan	Bak, M. (2011). Tethyan radiolarians at the Cenomanian - Turonian Anoxic Event from the Apennines (Umbria-Marche) and the Outer Carpathians: palaeoecological and palaeoenvironmental implications. *Studia Geologica Polonica,* v. 134, p. 5-279.
BAKM9501	Kapusnica, Kietowy Stream, Stare Bystre	Bak, M. (1995). Mid Cretaceous radiolaria from the Pieniny Klippen Belt, Carpathians, Poland. *Cretaceous Research,* v. 16, p. 1-23.
BAKM9921	Polish Radiolarian Comp.	Bak, M. (1999). Cretaceous radiolarian zonation in the Polish part ofthe Pieniny Klippen Belt (Western Carpathians). *Geologica Carpathica,* v. 50(1), p. 21-31.
BARA9975	Akusha Village, Caucasus Zone Composite, Heu River, Kuban River, Urukh River	Baraboshkin, E.J. (1999). Albian ammonite biostratigraphy of the northern Caucasus. *Neues Jahrbuch fuer Geologie und Palaeontologie Abhandlungen,* v. 212(1-3), p. 175-210.
BARR0483	Puentedey	Barroso-Barcenilla, F. (2004). Acanthoceratidae y zonacion de ammonies del Cenomaniense superior y del Turoniense inferior en el area de Puentedey, Cuenca Vasco-

		Cantabria, Espana. *Colloquios de Paleontologia,* v. 54, p. 83-114.
BARR0939	Condemios, Fuentetoba, Tamajon	Barroso-Barcenilla, F., Goy, A., and Segura, M. (2009). Ammonite zonation of the upper Cenomanian and lower Turonian in the Iberian Trough, Spain. *Newsletters on Stratigraphy,* v. 43(2), p. 139-164.
BARR1099	Vascoseras in Iberia	Barroso-Barcenilla, F., and Goy, A. (2010). The ammonite genus *Vascoceras* Choffat, 1898 (familiy Vascoceratidae Douville, 1912) in the Iberian Trough, Spain. *Palaeontographica,* v. A290 (4-6), p. 199-235.
BASO7983	DSDP Site 398D I	Basov, V.A., Lopatin, B.G., Gramberg, I.S., Danjushevskaya, A.I., Kabankov, V.Y., Lazurkin, V.M., and Patrunov, D.K. (1979). Lower Cretaceous Lithostratigraphy Near Galicia Bank. *Initial Reports of the Deep Sea Drilling Project,* v. 47, p. 683-717.
BAUE0407	Gebel Abu Zurub MIDK67, Jebel Arief El Naqa MIDK66	Bauer, et al. (2004). * *Courier Forschungs Senckenbergiana,* v. 247, p. 207-231.
BELO8321	DSDP Site 545, DSDP Site 547A, DSDP Site 547B	Below, R. (1983). Aptian to Cenomanian Dinoflagellate cysts from the Mazagan Plateau, Northwest Africa (Sites 545 and 547, DSDP Leg 79). *Initial Reports of the Deep Sea Drilling Project,* v. 79, p. 621-649.
BENF1073	Jebel Srassif	Ben Fadhel, M., Layeb, M., and Ben Youssef, M. (2010). Upper Albian

		planktic foraminifera and radiolarian biostratigraphy (Nebeur - northern Tunisia). *Compte Rendus Palevol*, v. 9, p. 73-81.
BENF1445	Jebel Garci, Ragoubet Lahneche	Ben Fadhel, M., Zouaghi, T., Amri, A., and Ben Youssef, M. (2014). Radiolarian and planktic formaninifera biostratigraphy of the Early Albian organic-rich beds of Fahdene Formation, Northern Tunisia. *Journal of Earth Science*, v. 25(1), p. 45-63.
BERG8685	DSDP Site 585A, DSDP Site 585	Bergen, J.A. (1986). Nannofossil Biostratigraphy at Site 585, East Mariana Basin. *Initial Reports of the Deep Sea Drilling Project*, v. 89, p. 285-296.
BERT0621	Butte de la Martiniere Qu	Bert, D., Peres, V. and Marchand, D. (2006). Nouvelles donnees stratigraphiques sur le Turonien moyen (Cretace superieur) du versant septentrional du seuil du Poitov (Centre-Ouest de la France): desription de Pseudotissotia faustinleybachae sp. nov. et evolution des Pseudotissotinae Hyatt, 1903 (ammonites). *Annales Musee Naturelle Histoire Nice*, v. 21, 21 pp.
BIRK6592		Birkelund, T. (1965). Ammonites from the Upper Cretaceous of West Greenland. *Meddelelser om Gronland*, v. 179, 192 pp.
BIRK8213		Birkelund, T. (1982). Maastrichtian ammonites from Hemmoor, Niederelbe, (N. W. Germany).

		Geologisches Jahrbuch, v. A61, p. 13-33.
BLEC7927	DSDP Site 398D I, DSDP Site 398D II, DSDP Site 398D link	Blechschmidt, G. (1979). Biostratigraphy of Calcareous Nannofossils: Leg 47B, Deep Sea Drilling Project. *Initial Reports of the Deep Sea Drilling Project,* v. 47(2), p. 327-360.
BOER8177	DSDP Site 463, DSDP Site 465A	Boersma, A. (1981). Cretaceous and Early Tertiary Foraminifers from Deep Sea Srilling Priject Leg 62 sites in the Central Pacific. *Initial Reports of the Deep Sea Drilling Project,* v. 62, p. 377-396.
BOGD9945		Bogdanova, T.N., and Prozorovsky, V.A. (1999). Substantiation of the Barremian/Aptian boundary. *Scripta Geologica Special Issue,* v. 3, p. 45-81.
BOMO1366	Gongzha	Bomou, B., Adatta, T., Tantawy, A.A., Mort, H., Fleitmann, D., Huang, Y., and Follmi, KB. (2013). The expression of the Cenomanian-Turonian oceanic anoxic event in Tibet. *Palaeogeography, Palaeoclimatology, Palaeoecology,* v. 369, p. 466-481.
BRAG0149	Cenoman-Turon radiolaria	Bragin, N., Bragina, L., Tunoglu, C., and Tekin, U.K. (2001). The Cenomanian-Turonian (Late Cretaceous) radioloarians from the Tomalar Formation, Central Pontides, Northern Turkey. *Geologica Carpathica,* v. 52(6), p. 349-360.

BRAG0425	Sel-Bukhra, Aksudere, Belaya Mtn, Tomalar, Urket Settlement	Bragina, L.G. (2004). Cenomanian-Turonian radiolarians of northern Turkey and the Crimean Mountains. *Paleontological Journal,* v. 38 (suppl. 4), p. 325-456.
BRAG0710	Mamedova Shchel, Volkonka Station	Bragina, L.G., Agarov, Y.V., and Bragin, N.Y. (2007). Radiolarians of the Upper Cenomanian and Lower Turonian from deposits of the Aranuri Formation, the Western Caucasus (Lazarevskoe Area). *Stratigraphy and Geological Correlation,* v. 15(3), p. 310-320.
BRAG1115	Sel-Bukhra	Bragina, L.G. (2011). Refined age of the anoxic level in the Cenomanian-Turonian transition of the Mt. Sel-Bukhra section (Crimean Mountains, Ukraine): Implications of radiolarian analysis. *Stratigraphy and Geological Correlation,* v. 19(5), pp. 515-525.
BRAG1315	Karai	Bragina, L.G., and Bragin, N.Y. (2013). New data on the Albian-Cenomanian radiolarians from the Karai Formation (south India). *Stratigraphy and Geological Correlation,* v. 21(5), p. 515-530.
BRAG1379	Ak-Kaya Mountain	Bragina, L.G. (2013). Late Cretaceous radiolarians of the genera Cuboctostylus Bragina and Hexacromyum Haekel: their stratigraphic and paleobiogeographical distribution. *Stratigraphy and Geological Correlation,* v. 21(1), p. 79-95.

BRAG1421	Biyuk-Karasu	Bragina, L.G., Bragin, N.Y., and Kopaevich, L.F. (2014). Radiolaria, planktonic foraminifera and stratigraphy of Turonian - Lower Coniacian in the Biyuk-Karasu section, Crimea. *Mocow University Geology Bulletin,* v. 69(3), p. 121-133.
BRAG1545	Kelevudag	Bragina, L.G., and Bragin, N.Y. (2015). New data on Albian-Coniacian radiolarians from the Kelevudag section (northeastern Azerbaijan). *Stratigraphy and Geological Correlation,* v. 23(1), p. 45-56.
BRAL8875	Blue Point, Cismon CC, Danish Central Graben, Dover, DSDP Site 551, Elsham Quarry, Hannover-Misburg Quarry	Bralower, T.J. (1988). Calcareous nannofossil biostratigraphy and assemblages of the Cenomanian-Turonian boundary interval: implications for the origin and timing of oceanic anoxia. *Paleoceanography,* v. 3(3), p. 275-316.
BRAL9229	ODP Site 761B, ODP Site 762C, ODP Site 763B	Bralower, T.J., and Siesser, W.G. (1992). Cretaceous Calcareous Nannofossil Biostratigraphy of Sites 761, 762, and 763, Exmouth and Wombat Plateaus, Northwest Australia. *Proceedings of the Ocean Drilling Program, Scientific Results,* v. 122, p. 529-556.
BRAL9859	Portland Core MIDK132	Bralower, T.J. and Bergen, J.A. (1998). Cenomanian-Santonian calcareous nannofossil biostratigraphy of a transect of cores drilled across the Western Interior Seaway. *In:* Dean, W. E., and Arthur, M. A. (eds.), *Concepts in Sedimentology and*

		Paleontology, SEPM, Stratigraphy and paleoenvironment of the Cretaceous Western Interior Seaway, USA, v. 6, p. 59-77.
BRAU0117	Bow River, Western Interior Z3	Braunberger, W.F., and Hall, R.L. (2001). Ammonoid faunas from the Cardium Formation (Turonian-Coniacian; Upper Creataceous) and contiguous units, Alberta Canada, II: Collignoniceratidae and Placenticeratidae. *Canadian Journal of Earth Science*, v. 38, p. 1117-1128.
BULO0757		Bulot, L.G., Robert, E., Jaillard, E., and Kennedy, W.J. (2007). The Albian ammonite successions of the Sunamdean Zone of Ecuador. *Cuadernos del Museo Geominero Madrid*, v. 8, p. 57-61.
CALL0353	Figueira da Foz	Callapez, P. (2003). The Cenomanian-Turonian transition in West Central Portugal: ammonites and biostratigraphy. *Ciencias da Terra (UNL)*, v. 15, p. 53-70.
CARO0671	Europe Zones, Oued Bahloul 2, Pueblo, Tunisia Zones	Caron, M., Dall Agnolo, S., Accarie, H., Barrera, E., Kauffman, E.G., Amedro, F., and Robaszynski, F. (2006). High-Resolution stratigraphy of the Cenomanian-Turonian boundary interval at Pueblo (USA) and wadi Bahloul (Tunisia): stable isotope and bio-events correlation. *Geobios*, v. 39, p. 171-200.
CAUS9331	Sopeira MIDK32	Caus et al. (1993). * *Cretaceous Research*, v. 14, p. 531-551.

CECC0115	Cassis 1	Cecca, F. (2001). The ammonites of the Cenomanian-Turonian transition of De Larene section (Cassis, SE France). *Geobios*, v. 34(2), p. 215-223.
CECH0532	Horatev, Nymburk, Velke Zbozi	Cech, S., Hradecka, L., Svobodova, M., and Svabenicka, L. (2005). Cenomanian and Cenomanian-Turonian boundary in the southern part of the Bohemian Cretaceous Basin, Czech Republic. *Bulletin of Geosciences,* v. 80(4), p. 321-354.
CEPE8197	DSDP Site 463, DSDP Site 464, DSDP Site 465, DSDP Site 465A, DSDP Site 466	Cepek, P. (1981). Mesozoic calcareous-nannoplankton stratigraphy of the central north Pacific (Mid-Pacific Mountains and Hess Rise), Deep Sea Drilling Project Leg 62. *Initial Reports of the Deep Sea Drilling Project,* v. 62, p. 397-418.
COBB0529	Kevin	Cobban, W.A., Dyman, T.S., and Porter, K.W. (2005). Paleontology and stratigraphy of upper Coniacian - middle Santonian ammonite zones and application to erosion surfaces and marine transgressive strata in Montana and Alberta. *Cretaceous Research,* v. 26, p. 429-449.
COBB0875	Chispa Summit CEN3, Lozier Cyn CEN8, Ojinaga CEN4, Western Interior Z2	Cobban, W.A., Hook, S.C., and McKinney, K.C. (2008). Upper Cretaceous mullusscan record along a transect from Virden, New Mexico, to Del Rio, Texas. *New Mexico Geology,* v. 30(3), p. 75-92.
COBB5142	Belle Fourche, Sweetgrass Arch	Cobban, W.A. (1951). Scaphitid cephalopods of the Colorado Group.

		United States Geological Survey Professional Paper, v. 239, 42 pp.
COBB6137	Seabee Formation	Cobban, W.A., and Gryc, G. (1961). Ammonites from the Deabee Formation (Cretaceous) of northern Alaska. *Journal of Paleontology*, v. 35(1), p. 176-190.
COBB6413		Cobban, W.A., and Scott, G.R. (1964). Multinodose scaphitid cephalopods from the lower part of the Pierre Shale and equivalent rocks in the conterminous United States. *United States Geological Survey Professional Paper*, v. 483-E, 13 pp.
COBB7071		Cobban, W.A. (1970). Occurrence of the Late Cretaceous ammonites *Didymoceras stevensoni* (Whitfield) and *Exiteloceras jennyi* (Whitfield) in Delaware. *United States Geological Survey Professional Papers*, v. 700-D, p. D71-D76.
COBB7162	Kayenta, Laguna, Model, Pool Creek	Cobban, W.A. (1971). New and little-known ammonites from the Upper Cretaceous (Cenomanian and Turonian) of the Western Interior of the United States. United States Geological Survey Professional Papers, v. 699, 62 pp.
COBB7421		Cobban, W.A. (1974). Ammonites from the Navesink Formation, Atlantic Highlands, New Jersey. *United States Geological Survey Professional Papers*, v. 845, p. 1-21.
COBB8471	Western Interior Z2	Cobban, W.A. (1984). Mid Cretaceous ammonite zones, Western Interior,

		United States. Bull. Geol. S. Denmark, v. 33, pp. 71-89.
COBB8715		Cobban, W.A. (1987). The Upper Cretaceous ammonite Rhaeboceras Meek in the Western Interior of the United States. *United States Geological Survey*, v. 1477, 15 pp.
COBB8830	Western Interior Z1	Cobban, W.A. (1988). Tarrantoceras Stephenson and related ammonoid genera from Cenomanian (Upper Cretaceous) rocks in Texas and the western Interior of the United States. *United States Geological Survey Professional Papers,* v. 1473, 30 pp.
COBB9105		Cobban, W.A., and Kennedy, W.J. (1991). Some Upper Cretaceous ammonites from thte Nacatoch Sand of Hempstead County, Arkansas. United States Geological Survey Bulletin, v. 1985-C, 5 pp.
COBB9106		Cobban, W.A., and Kennedy, W.J. (1991). Upper Cretaceous (Masstrichtian) ammonites from the Nostoceras alternatum Zone in southwestern Arkansas. *United States Geological Survey Bulletin,* 1985-E, 6 pp.
COBB9282		Cobban, W.A., and Kennedy, W.J. (1992). The last Western Interior Baculites from the Fox Hills Formation of South Dakota. *Journal of Paleontology*, v. 66(4), p. 682-684.
COBB9314		Cobban, W.A., and Kennedy, W.J. (1993). The Upper Cretaceous dimorphic pachydiscoid ammonite Menuites in the Western Interior of the United

		States. *United States Geological Survey Professional Paper*, v. 1533, 14 pp.
COBB9371		Cobban, W.A., and Kennedy, W.J. (1993). Middle Campanian ammonites and inoceramids from the Wolfe City Sand in northeast Texas. Journal of Paleontology, v. 67(1), p. 71-82.
COBB9409		Cobban, W.A., and Kennedy, W.J. (1994). Middle Campanian (U. Cretaceous) ammonites from the Pecan Gap Chalk of central and northeastern Texas. *United States Geological Survey Bulletin,* v. 2073-D, B689 pp.
COBB9412		Cobban, W.A., and Kennedy, W.J. (1994). Upper Cretaceous ammonites from the Coon Creek Tongue of the Ripley Formation at its type locality in McNairy County, Tennessee. United States Geological Survey Bulletin, v. 2073-B, 12 pp.
COBB9540		Cobban, W.A., and Kennedy, W.J. (1995). Maastrichtian ammonites chiefly from the Prairie Bluff Chalk in Alabama and Mississippi. *Paleontological Society Memoir,* v. 44, p. 1-40.
COUR9887	Benue Trough Zonal Compos	Courville, P., Lang, J., and Thierry, J. (1998). Ammonite faunal exchanges between south tethyan platforms and south atlantic during the uppermost Cenomanian-lower most/middle Turonian in the Benue Trough (Nigeria). *Geobios,* v. 31(2), pp. 187-214.

CREM8221	Los Tajos, Moralet, Sabinar	Cremades, J., and Linares, A. (1982). Contribucional conocimiento del Albense Superior - Cenomenense dell Prebetico de Alicante. *Cuadernos Geologia Iberica,* v. 8, p. 721-738.
CRES9929	Chimana Grande Is. MIDK88	Crespo de Cabrera, S., Sliter, W.V., and Jarvis, I. (1999). Integrated foraminiferal biostratigraphy and chemostratigraphy of the Querecual Formation (Cretaceous), Eastern Venezuela. *Journal of Foraminiferal Research,* v. 29, p. 487-499.
DAMG9838		Dam, G., Norhr-Hansen, H., and Kennedy, W.J. (1998). The northernmost marine Cretaceous-Tertiary boundary section: Nuuseq, West Greenland. *Geological Survey of Greenland Bulletin,* v. 18, p. 138-144.
DAMO9221	ODP Site 761B, ODP Site 762C, ODP Site 763B	Damotte, R. (1992). Data Report: Cretaceous Ostracodes from Holes 761B and 764A (Wombat Plateau) and Holes 762C, 763B, and 763C (Exmouth Plateau). *Proceedings of the Ocean Drilling Program, Scientific Results,* v. 122, p. 819-834.
DAVE9283	Dugi Otok MIDK81	Davey et al. (1992). * *Neues Jahrbuch fuer Geologie und Palaeontologie Abhandlungen,* v. 186, p. 283-299.
DELA9565		Delanoye, G. (1995). About some significant ammonites from the Lower Aptian (Bedoulian) of the Angles-Barreme area (south-east France). *Memoire Descrittive della*

		Carta Geologica d-Italia, v. 51, p. 65-101.
DUBI1299	Dubivtsi 1	Dubicka, Z., and Peryt, D. (2012). Foraminifers and stable isotope record of the Dubivitsi Chalk (upper Turonian, wetern Ukrain): palaoenvironmental implications. *Geological Quarterly*, v. 56(1), p. 199-214.
DUBI1451	Dubivtsi 2	Dubicka, Z., and Peryt, D. (2014). Classification and evolutionary interpretation of Late Turonian - Early Campanian Gavelinella and Stensioeina (Gavelinellidae, benthic foraminifera) from western Ukraine. *Journal of Foraminiferal Research*, v. 44(2), p. 151-176.
DUTO0503		Dutour, Y. (2005). *Biostratigraphie, evolution et renouvellements des ammonites de l-Aptien superior (Gargasien) du bassin vocontien (Sud-Est de la France)* (PhD dissertation), Universite Claude Bernard, Lyon, 303 pp.
EICH7069	Bunker Hill 2 MIDK133B	Eicher, and Worstell. (1970). * *Micropaleontology*, v. 16, p.269-324.
ELAM1411	Jebel Chemsi, Jebel Ennahli, Jebel Ettout, Shahneshin, Tarfaya 2	Elam, Z., Farouk, S., and Zaghbib-Turki, D. (2014). Santonian planktonic foraminiferal biostratigraphy of the northern Tunisia. *Geologica Croatica*, v. 67(2), p. 111-126.
ELLI9475		Elliot, D.H., Askin, R.A., Kyte, F.T., and Zinsmeister, W.J. (1994). Iridium and dinocysts at the Cretaceous-

		Tertiray boundary on Seymour Island, Antarctica: implications for the K-T event. *Geology*, v. 22(8), p. 675-678.
ELSA1101	Wadi Dakhl, Wadi Feiran	El Sabbagh, A., Tantawy, A.A., Keller, G., Khozyem, H., Spangenberg, J., Adatte, T., and Gertsch, B. (2011). Stratigraphy of the Cenomanian-Turonian Oceanic Anoxic Event OAE2 in shallow shelf sequences of NE Egypt. *Cretaceous Research,* v. 30, p. 1-18.
ENSO0956		Enson, K.V. (2009). Correlation of Aptian-Albian sediments in the central part of North Caucasus and Ciscaucasia. Paper 2: Stratigraphy. *Moscow University Geology Bulletin*, v. 64(4), p. 256-261.
ERBA0457	ODP Site 1257	Erbacher, J., Mosher, D.C., Malone, M.J., et al. (2004). Proceedings of the Ocean Drilling Program (ODP) Initial Reports, 207, CD-ROM. Initial Reports of the Ocean Drilling Program, v. 207, 554 pp.
ERBA0509		Erbacher, J., Friedrich, O., Wilson, P.A., Birch, H., and Mutterlose, J. (2005). Stable organic carbon isotope stratigraphy across Oceanic Anoxic Event 2 of Demerara, western tropical Atlantic. *Geochemistry Geiphysics Geosystems*, v. 6(6), 9 pp.
FATM9941		Fatmi, A.N., and Kennedy, W.J. (1999). Maastrichtian ammonites from Balochistan, Pakistan. *Journal of Paleontology*, v. 73(4), p. 641-662.

FOLL8905	Follmi Apt-Albian Comp	Follmi, K. B. (1989). Beschreibung neugefundener Ammonoidea aus der Vorarlberger Garschella-Formation (Aptian-Albian). *Jarbuch der Geologische Bundes-Amt,* v. 132(1), p. 105-189.
FORE7786		Forester, R.W., Caldwell, W.G.E., and Oro, F.H. (1977). Oxygen and carbon isotopic study of ammonites from the late Cretaceous Bearpaw Formation in southwestern Saskatchewan. *Canadian Journal of Earth Science,* v. 14, p. 2086-2100.
FORS0856	DSDP Site 530A	Forster, A., Kuypers, M.M.M., Turgeon, S.C., Brumsack, H.J., Petrizzo, M.R., and Damste J.S.S. (2008). The Cenomanian-Turonian oceanic anoxic event in the South Atlantic: New insights from a geochemical study of DSDP Site 530A. *Palaeogeography, Palaeoclimatology, Palaeoecology,* v. 267, p. 256-283.
FRIE0621	ODP Site 1258 I, ODP Site 1259, ODP Site 1260, ODP Site 1261	Friedrich, O., Erbacher, J., and Mutterlose, J. (2006). Paleoenvironmental changes across the Cenomanian Turonian Boundary Event (Oceanic Anoxic Event 2) as indicated by benthic foraminifera from the Demerara Rise (ODP Leg 207). *Revue de Micropaleontologie,* v. 49, p. 121-139.
FRIJ1510	Mt Coccovello, Mt Varchera, Trentinara	Frijia, G., Parente, M., DiLucia, M., and Mutti, M. (2015). Carbon and strontium isotope stratigraphy of the Upper Cretaceous (Cenomanian - Campanian) shallow water

		carbonates of southern Italy: Chronostratigraphic calibration of larger foraminifera biostratigraphy. *Cretaceous Research,* v. 53, p. 110-139.
FRUS6900	Ojinaga CEN4	Frush and Eicher. (1969). * *Special Publications of the Canadian Geological Association.*
GALE0045	Eastbourne	Gale, A.S., Smith, A.B., Monks, N.E.A., Young, J.A., Howard, A., Wray, D.S., and Huggett, J.M. (2000). Marine biodiversity through the Late Cenomanian - Early Turonian: palaeoceanographic controls and sequence stratigraphic biases. *Journal of the Geological Society, London,* v. 157, p. 745-757.
GALE0560	Eastbourne	Gale, A.S., Kennedy, W.J., Voigt, S., and Walaszczyk, I. (2005). Stratigraphy of the Upper Cenomanian - Lower Turonian Chalk succession at Eastbourne, Sussex, UK: ammonites, inoceramid bivalves, and stable carbon isotopes. *Cretaceous Research,* v. 26, p. 460-487.
GALE1159	Col de Palluel MIDK143	Gale, A.S., Brown, P., Caron, M., Crampton, J., Crowhurst, S.J., Kennedy, W.J., Petrizzo, M.R., and Wray, D.S. (2011). The uppermost Middle and Upper Albian succession at the Col de Palluel, Hautes-Alpes, France: An integrated study (ammonites, inoceramid bivalves, planktonic foraminifera, nannofossils, geochemistry, stable oxygen and carbon isotopes,

		cyclostratigraphy). *Cretaceous Research*, v. 32, p. 59-130.
GALE8973	Abbots Cliff, Folkestone	Gale, A.S. (1989). Field meeting at Folkestone Warren, 29th November 1987. *Proceedings of the Geologists Association*, v. 100(1), p. 73-82.
GALE9615	Mont Risous 2 MIDK 142X, Mont Risous MIDK 142	Gale, A.S., Kennedy, W.J., Burnett, J.A., Caron, M., and Kidd, B.E. (1996). The Late Albian to Early Cenomanian succession at Mont Risous near Rosans (Drome, SE France): an integrated study (ammonites, inoceramods, planktonic foraminifera, nannofossils, oxygen and carbon isotopes). *Cretaceous Research*, v. 17, p. 515-606.
GALL0793	Villamartin	Gallemi, J., Lopez, G., Martinez, R., and Pons, J.M. (2007). Macrofauna of the Villamartin Section: Coniacian - Santonian boundary, North Castilan Platform, Burgos, Spain. *Cretaceous Research*, v. 28, p. 93-107.
GALL8301	Tremp	Gallemi, J., Martinez, R., and Pons, J.M. (1983). Coniacian-Maastrichtian of the Tremp area (South Central Pyrenees). Newsletters on Stratigraphy, v. 12(1), p. 1-17.
GALL9755		Gallemmi, J., Lopez, G., Maratinez, R., Munoz, J., and Pons, J.M. (1997). Albian-Cenomanian and Campanian-Maastrichtian biostratigraphy of southeast Spain. *Cretaceous Research*, v. 18, p. 355-372.

GAON1343		Gaona-Narvaez, T., Maurrasse, F.J.M., R., and Moreno-Bedmar, J.A. (2013). Stable isotope stratigraphy and ammonite biochronology at Madotz, Navarra, northern Spaoin: Implications for the timing and duration of oxygen depletion during OAE-1a. *Cretaceous Research,* v. 40, p. 143-157.
GARC0934		Garcia-Mondejar, J., Owen, H.G., Raissossadat, N., Millan, M.I., and Fernandez-Mendiola, P.A. (2009). The early Aptian of Aralar (northern Spain): stratigraphy, sedimentology, ammonite biozonation, and OAE1. *Cretaceous Research,* v. 30, p. 434-464.
GARG8315	Djebel Bireno MIDK7, Djebel Mrhila MIDK8	Gargouri-Razgallah, S. (1983). * *Doc et Trav IGAL,* v. 6, 215 pp.
GART8015	DSDP Site 417D, DSDP Site 418A, DSDP Site 418B	Gartner, S. (1980). Calcareous Nannofossils, Deep Sea Drilling Project Holes 417D, 418A, and 418B. *Initial Reports of the Deep Sea Drilling Project,* v. 51-53(2), p. 815-821.
GEOR1203	DSDP Site 463, ODP Site 1050C, ODP Site 762C	Georgescu, M.D. (2012). Origin, evolutionary classification, and biostratigraphic of the Late Cretaceous planktic foraminiferal directional lineage Bollitruncana O.A. Korchagin, 2001. *Studia UBB Geologia,* v. 57(2), p. 3-16.
GERT0818	Wadi El Ghaib	Gertsch, B., Keller, G., Adatte, T., Berner, Z., Kassab, A.S., Tantawy, A.A.A., El-Sabbagh, A.M., and Stueben, D.

		(2008). Cenomanian-Turonian transition in shallow water sequence for the Sinai, Egypt. *Geologische Rundschau*, v. 99(1), p. 165-182.
GERT1030	Azazoul Beach, Azazoul Link, Azazoul Road	Gertsch, B., Adatte, T., Keller, G., Tantawy, A.A.A.M, Berner, Z., Mort, H.P., and Fleitmann, D. (2010). Middle and late Cenomanian oceanic anoxic events in shallow and deeper shelf environments of western Morocco. *Sedimentology*, v. 57, p. 1430-1462.
GHAN1255	South Palmyrides	Ghanem, H., Mouty, M., and Kuss, J. (2012). Biostratigraphy and carbon-isotope stratigraphy of the uppermost Aptian to Upper Cenomania strata of the South Palmyrides, Syria. *GeoArabia*, v. 17(2), p.155-184.
GILL6620		Gill, J.R., and Cobban, W.A. (1966). Regional unconformity in Late Cretaceous Wyoming. *United States Geological Survey Professional Papers*, v. 550-B, p. 20-27.
GILL6669		Gill, J.R., and Cobban, W.A. (1966). The Red Bird section of the Upper Cretaceous Pierre Shale in Wyoming. *United States Geological Survey Professional Paper*, v. 393-A, p. 1-69.
GOOL0413		Goolaerts, S., Kennedy, W.J., Dupuis, C., and Steurbant, E. (2004). Terminal Maastrichtian ammonites from the Cretaceous-Paleogene Global Stratotype Section and Point, El Kef,

		Tunisia. *Cretaceous Research,* v. 25, p. 313-328.
GORK9541	Wladyslawowo	Gorka, H. (1995). Lower Turonian radiolarians (Polysystina) from Borehole Wladyslawowo IG 1 (Baltic Region). *Geological Quarterly*, v. 39(3), p. 341-372.
GRAE0329	Caffiers, Galarreta, Gordoa, Sobron, Urbasa #2 Core, Villasana	Graefe, K.U., and Wendler, J. (2003). Foramonifers and calcareous dinoflagellate cysts as proxies for deciphering sequence stratigraphy, sea-level change, and paleoceanography of Cenomanian-Turonian hemipelagic sediments in western Europe. *SEPM (Society for Sedimentary Geology) Special Publications*, v. 75, p. 229-262.
GRIE9221		Grier, J.C., and Grier, J.W. (1992). Occurrence of the Upper Cretaceous ammonite Rhaeboceras in the Baculites eliasi zone of the Pierre Shale. *Journal of Paleontology*, v. 66(3), p. 521-523.
GRIE9873		Grier, J.C., and Grier, J.W. (1998). New findings of the ammonite Rhaeboceras, including a new species, from the Pierre Shale of Eastern Montana. *Journal of Paleontology*, v. 72(3), p. 473-476.
HABL9770	Ouzon CORB26	Hable, R. (1997). * (Unpublished PhD dissertation), University of Freiburg, v. 1166, p. 70-91.
HANC9159	Madagascar Albian, UK Alb-Tur Zones	Hancock, J.M. (1991). Ammonite scales for the Cretaceous. *Cretaceous Research,* v. 12, p. 259-291.

HANN1110	East Themed, Gebel Arief El-Naqa, Wadi Quseib	Hannaa, W.S.A. (2011). *Taxonomy and palaeoecology of the Cenomanian-Turonian macro-invertebrates from eastern Sinai, Egypt.* (Ph.D. Dissertation), Wurzburg, 410 pp.
HARD0665	ODP Site 1258 I, ODP Site 1259, ODP Site 1260, ODP Site 1261	Hardas, P., and Mutterlose, J. (2006). Calcareous nannofossil biostratigraphy of the Cenomanian/Turonian boundary interval of ODP Leg 207 at the Demerara Rise. *Revue de Microplaeontologie,*v. 49, p. 165-179.
HARD9151		Hardenbol, J., Caron, M., Amedro, F., Dupuis, C., and Robaszynsky, F. (1991). The Cenomanian-Turonian boundary in Central Tunisia in the context of a sequence-stratigraphic interpretation. *Geologie Alpine Memoires*, v. 17, p. 51-52.
HART0511	Rio Mondego	Hart, M.B., Callapez, P.M., Fisher, J.K., Hannant, K., Monteiro, J.F., Price, G.D., and Watkinson, M.P. (2005). Micropalaeontology and Stratigraphy of the Cenomanian/Turonian boundary in the Lusitanian Basin, Portugal. *Journal of Iberian Geology*, v. 31(2), p. 311-326.
HASE9381	Obirashibe-Kanajiri R., Shirakin River	Hasegawa, T., and Saito, T. (1993). Global synchroneity of a positive carbon isotope excursion at the Cenomanian/Turonian boundary: Validation by calcareous microfossil biostratigraphy. *The Island Arc*, v. 3, p. 181-191.

HASE9751	Shirakin River 3	Hasegawa, T. (1997). Cenomanian-Turonian carbon isotope events recorded in terrestrial organic matter from northern Japan. *Palaeogeography, Palaeoclimatology, Palaeoecology,*v. 130, p. 251-273.
HATT6884	Bunker Hill 1 MIDK133	Hattin, (1968). * *Journal of Paleontology,* v. 42, p. 1084-1090.
HATT7516	Bunker Hill 1 MIDK133	Hattin, (1975). * *Bulleton of the Kansas Geological Survey,* v. 209, p. 116-119.
HAYA1339	Haboro, Obira 2	Hayakawa, T., and Hirano, H. (2013). A revised inoceramid biozonation for the Upper Cretaceous based on high resolution carbon isotope stratigraphy in northwestern Hokkaido. *Acta Geologica Polonica,* v. 63(2), p. 239-263.
HAYN1542	Biserial Tree	Haynes, S.J., Huber, B.T., and MacLeod, K.G. (2015). Evolution and phylogeny of Mid-Cretaceous (Albian-Coniacian) biserial planktic foraminifer. *Journal of Foraminiferal Research,* v. 45(1), p. 42-81.
HEND7371	Coverham	Henderson, R.A. (1973). Clarence and Raukumana series (Albian - ?Santonian) ammonoidea from New Zealand. *Journal of the Royal Society of New Zealand,* v. 3(1), p. 71-123.
HEND8535		Henderson, R.A., amd McNamara, K.A. (1985). Maastrichtian non-heteromorph ammonites from the

		Miria Formation, Western Australia. *Paleontology*, v. 28, p. 35-88.
HEND9233		Henderson, R.A., Kennedy, W.J., and McNamara, K.A. (1992). Maastrichtian heteromorph ammonites from the Carnarvon Basin, Western Australia. *Alcheringa*, v. 16, p. 133-170.
HERN9761	Axaxcoalco, Barranca del Tigre 2, Zotoltitlan	Hernandez-Romano, U., Aguilera-Franco, N., Martinez-Medrano, M., and Barcelo-Duarte, J. (1997). Guerrero-Morales platform drowning at the Cenomanian-Turonian boundary, Huitziltepac area, Guerrero State, southern Mexico. *Cretaceous Research*, v. 18, p. 661-686.
HIRA7701	Hakkinzawa River, Takinosawa River	Hirano, H., Matsumoto, T., and Tanabe, K. (1977). Mid-Cretaceous stratigraphy of the Oyubari area, central Hokkaido. *Special Papers of the Palaeontological Society of Japan*, v. 21, p. 1-10.
HISZ9125	Metelen 1001 Core	Hisz, M., and Lommerzheim, A. (1991). Stratigraphische Interpretation der Makrofauna imSanton/Campan-Profil der Bohrung Metelen 1001 im nordwestlichen Muensterland (NW Deutschland). *Facies*, v. 24, p. 125-128.
HOCH8097	DSDP Site 417D, DSDP Site 418A, DSDP Site 418B	Hochuli, P. & Kelts, K. (1980). Palynology of Middle Cretaceous Black Clay Facies from Deep Sea Drilling Project Sites 417 and 418 of the Western North Atlantic. *Initial Reports of the Deep Sea Drilling Project*, v. 51-53(2), p. 897-935.

HOLL0135	Japanese Radiolaria	Hollis, Christopher J., and Kimura, Katsumi (2001). A unified radiolarian zonation for the Late Cretaceous and Paleocene of Japan. *Micropaleontology,* v. 47(3), p. 235-255.
HOOK1313	Bull Gap Cyn	Hook, S.C., and Cobban, W.A. (2013). Middle Turonian (Late Cretaceous) rudists from the lower tongue of the Mancos Shale, Lincoln County, New Mexico. *New Mexico Geology,* v. 35(1), p. 13-20.
HOOK8348	Gold Hill MIDK134	Hook, (1983). * *New Mexico Bureau of Mines and Mineral Resources Circular,* v. 185, p. 48-54.
HUBE9992	ODP Site 1050C	Huber, B.T., Leckie, R.M., Norris, R.D., Bralower, T.J., & CoBabe, E. (1999). Foraminiferal Assemblage and Stable Isotopic Change Across the Cenomanian-Turonian Boundary in the Subtropical North Atlantic. *Journal of Foraminiferal Research,* v. 29(4), p. 392-417.
HUSI0953	Croatian Foram Comp.	Husinec, A., Velic, I., and Sokac, B. (2009). Diversity patterns of Mid-Cretaceous benthic foraminifers and dasycladalean algae of the Southern part of the Mesozoic Adriatic Platform, Croatia. *SEPM Special Publications,* v. 93, p. 153-170.
IFRI0475		Ifrim, C., Stinnesbeck, W., and Lopez-Oiva, J.G. (2004). Maastrichtian cephalopods from Cerralvo, northeastern Mexico. *Palaeontology,* v. 47(6), p. 1575-1627.

IFRI0742	Vallecito	Ifrim, C., and Stinnesbeck, W. (2007). Early Turonian ammonites from Vallecito, northeast Mexico: taxonomy, biostratigrpahy and paleobiogeographical significance. *Cretaceous Research,* v. 28, p. 642-664.
IFRI0843	Vallecito	Ifrim, C., and Stinnesbeck, W. (2008). Cenomanian-Turonian high resolution biostratigraphy of northeastern Mexico and its correlation with the GSSP and Europe. *Cretaceous Research,* v. 29, p. 943-956.
IONJ0451	Romanian Comp	Ion, J., Antonescu, E., Melinte, M.C., and Szasz, L. (2004). Integrated biostratigraphy if tge Turonian of Romania. *Acta Palaeontologica Romaniae,* v. 4, p. 151-161.
IVAN1347		Ivanov, M., and Idakieva, V. (2013). Lower Aptian ammonite biostratigraphy anf potential for further studies of OAE 1a in Bulgaria. *Cretaceous Research,* v. 39, p. 47-69.
JAGT0303		Jagt, J.W.M., and Kennedy, W.J. (2003). First record of Pachydiscus noetlingi Kennedy, 1999, (Ammonoidea) from the Maastrichtian type area (the Netherlands). *Geologie en Mijnbouw (Netherlands Journal of Geology,* v. 82(3), p. 303-307.
JAGT1115	Sakhalin Zonal Composite	Jagt-Yazykova, E.A. (2011). Palaeobiogeographical and palaeobiological aspects of mid- and Late Cretaceous ammonite evolution

		and bio-events in the Russian Pacific. *Scripta Geologica,* v. 143, pp. 15-121.
JAGT1272	Japan Zones 1, Japan Zones 2, Russia Zones NE, Sakhalin Zones 1, Sakhalin Zones 2	Jagt-Yazykova, E.A., and Zonova, T.D. (2012). Paleogeography of Cretaceous ammonoids of the Pacific Coast of Russia. *Stratigraphy and Geological Correlation,* v. 20(3), p. 295-315.
JAGT9465		Jagt, J.W.M., and Kuypers, M.M.M. (1994). A note on Hoploscaphites pupngens (Binckhorst, 1861) (Cretaceous Ammonoidea). *Cretaceous Research,* v. 15, p. 765-770.
JAGT9653		Jagt, J.W.M. (1996). Late Maastrichtian and early Paleocene index macrofossils in the Maastrichtian type area (S.E. Netherlands, N.E. Belgium). *Geologie en Mijnbouw,* v. 75, p. 153-162.
JAIL9003	Peru N Zones	Jaillard, E. (1990). Evolucion de la margen Andina en el norte del Peru desde el Aptiano hasta el Senoniano. *Boll. Soc. Geologicas del Peru,* v. 81, p. 3-13.
JAIL9385	Cajamarca, Rentema, Tembladera	Jaillard, E., and Arnaud-Vanneau, A. (1993). The Cenomanian-Turonian transition on the Peruvian margin. *Cretaceous Research,* v. 14, p. 585-605.
JARV0215		Jarvis, I., Mabrouk, A., Moody, R.T.J., and de Cabrera, S. (2002). Late Cretaceous (Campanian) carbon isotope events, sea level change, and

		correlation of the Tethyan and Borreal realms *Paleogeography Paleoclimatology and Paleoecology*, v. 188, p. 215-248.
JARV8803	Danish Central Graben, Horatev, Nymburk, Velke Zbozi, Dover, DSDP Site 551, Eastbourne, Eastbourne2	Jarvis, I.,Carson, G.A., Cooper, M.K.E., Hart, M.B., Leary, P.N., Tocher, B.A., Horne, D., and Rosen (1988). Microfossil Assemblages and the Cenomanian-Turonian (late Cretaceous) Oceanic Anoxic Event. *Cretaceous Research,* v. 9, p. 3-103.
JARV8847	Hooken Cliffs	Jarvis, I., Carson, G., Hart, M., Leary, P., and Tocher, B. (1988). The Cenomanioan-Turonian (late Cretaceous) anoxic event in SW England: evidence from Hooken Cliffs near Beer, SE Devon. *Newsletters on Stratigraphy,* v. 18(3), p. 147-164.
JOLE0125	La Bedoule	Jolet, P., Philip, J., Cecca, F., Thomel, G., Lopez, G., Tronchetti, G., and Babinot, J.F. (2001). Integrated platform/basin biostratigraphy of the Upper Cenomanian - Lower Tyronian in provence (SE France). *Geobios,* v. 34(2), p. 225-238.
JOLE9703	Cassis 2, Cassis 3 MIDK42	Jolet, P., Philip, J., Thomel, G., Lopez, G., and Tronchetti, G. (1977). Nouvelles donnees biostratigraphiques sur la limite Cenomanien-Turonien. La coupe de Cassis Sud-Est de la France): proposition d-un hypostratotype europeen. *Comptes Rendu Academie Sciece Paris,* v. 325, p. 703-709.

JOLY0860	Vocontien Composite	Joly, B., and Delamette, M. (2008). Les Phylloceratoidea (Ammonoidea) aptiens et albiens du bassin vocontien (Sud-Est de la France). *Carnets de Geologie Memoire,* v. 2008(4), 60 pp.
JUIG8030		Juignet, P. (1980). * *BRGM,* v. 109, p. 130-138.
KAIH9313	Penkemoyuparogawa R.	Kaiho, K., Fujiwara, O., and Motoyama, I. (1993). Mid-Cretaceous faunal turnover of intermediate-water benthic foraminifera in the northwestern Pacific Ocean margin. *Marine Micropaleontology,* v. 23, p. 13-49.
KAIH9429	Oyubari 2, Shirakin River 2	Kaiho, K., and Hasegawa, T. (1994). End-Cenomanian benthic foraminiferal extinctions and oceanic dysoxic events in the northwestern Pacific Ocean. *Palaeogeography Palaeoclimatology Palaeoecology,* v. 111(1-2), p. 29-43.
KAPL8609	Germany NW Zones	Kaplan, J. (1986). Ammonite stratigraphy of the Turonian of NW-Germany. *Mewsletters on Stratigraphy,* v. 17(1), p. 9-20.
KASS0105		Kassab, A. S., and Obaidalla, N. A. (2001). Integrated stratigraohy and inter-regional correlation of the Cenomanian-Turonian deposits of Wadi Feirian. *Cretaceous Research,* v. 22, p. 105-114.
KAWA0381	Oyubari MIDK94	Kawabe, F., Takashima, R., Wan, R., Nishi, H., and Moriya, K. (2003). *

		Acta Geologica Polonica, v. 53, p. 81-91.
KELL0191	Eastbourne2	Keller, G., Han, Q., Adatte, T., and Burns, S.J. (2001). Palaeoenvironments of the Cenomanian-Turonian transition at Eastbourne, England. *Cretaceous Research,* v. 22, p. 391-422.
KELL0876	Tazra	Keller, G., Adatte, T., Chellai, E.H., & Stueben, D. (2008). Oceanic events and biotic effects of the Cenomanian-Turonian anoxic event, Tarfaya Basin, Morocco. *Cretaceous Research,* v. 29, p. 976-994.
KELL9983		Kelly, S.R.A., and Witham, A.G. (1999). Deshayesitid ammonites from the lower Aptian (Lower Greensand) of Northeast Greenland. *Scripta Geologica Special Issue,* v. 3, p. 83-95.
KENN0030		Kennedy, W.J., Landman, N.H., Cobban, W.A., and Johnson, R.O. (2000). Additions to the ammonite fauna of the Upper Cretaceous Navesink Formation of New Jersey. *American Museum Novitates,* v. 3306, p. 1-30.
KENN0053		Kennedy, W.J., Jagt, J.W.M., HAnna, S.S., adn Schlup, A.S. (2000). Late Campanian ammonites from the Saiwan area (Huqf Desert, Sultanate of Oman). *Cretaceous Research,* v. 21, p. 553-562.
KENN0064		Kennedy, W. J., and Lunn, G. (2000). Upper Campanian (Cretaceous) ammonites from the Shinarish Formation, Djebel Sinjar, northwest

		Iraq. *Journal of Paleontology,* v. 74, p. 464-473.
KENN0091	Col de Pre-Guittard, Hyeges, Tartonne	Kennedy, W.J., Gale, A.S., Bown, P.R., Caron, M., Davey, R.J., Groecke, D., and Wray, D.S. (2000). Integrated stratigraphy across the Aptian-Albian boundary in the Marnes Bleues at the Col de Pre-Guittard, Arnayon (Drome), and at Tartomme (Alpes-d-Haute-Provence, France: a candidate Global Boundary Stratotype Section and Point for the base of the Albian. *Cretaceous Research,* v. 21, p. 591-720.
KENN0101	Collignoniceratid Tree	Kennedy, W.J., Cobban, W.A., and Landman, N. (2001), A revision if the Turonian of the ammonite subfamily Collignoniceratinae from the United States Western Interior and Gulf Coast. *Bulletin of the American Museum of Natural History,* v. 267, p. 1-148.
KENN0159		Kennedy, W.J., Bilotte, M., and Morala, A. (2001). Pseudokossmaticeras brandti Redtenbacher, 1873, an Upper Campanian marker fossil in northern Aquitaine, France. *Cretaceous Research,* v. 22, p. 259-262.
KENN0163		Kennedy, W.J., Gale, A.S., and Hansen, T.A. (2001). The last Maastrichtian ammonites from the Brazos River sections in Falls County, Texas. *Cretaceous Research,* v. 22, p. 163-177.
KENN0259		Kennedy, W.J., and Bilotte, M. (2002). Baculites ovatus Say, 1820, a north

		American ammonite from the Maastrichtian of Roquefort, Landes, France. *Neues Jahrbuch fuer Geologie und Palaeontologie Monatsheft*, v. 3, p. 159-170.
KENN0301		Kennedy, W.J., Juignet, P., and Girard, J. (2003). Uppermost ammonites from Eure, Haute Normandie, northwest France. *Acta Geologica Polonica*, v. 53(1), p. 1-18.
KENN0349		Kennedy, W.J., and Kulbrook, F. (2003). An upper Maastrichtian ammonite from the Eastern Desert, Egypt *Neues Jahrbuch fur Geologie und Palaenotologie Monatsheft*, v. 8, p. 449-462.
KENN0465	Pawpaw Ck.	Kennedy, W.J. (2004). Ammonites from the Pawpaw Shale (Upper Albian) in northeast Texas. *Cretaceous Research*, v. 25, p. 865-905.
KENN0593	Pueblo, Pueblo Reservoir	Kennedy, W.J., Walaszczyk, I., and Cobban, W.A. (2005). The Global Boundary Stratotype Section and Point for the base of the Turonian Stage of the Cretaceous: Pueblo, Colorado, U.S.A. *Episodes*, v. 28(2), p. 93-104.
KENN0753	Montlaux	Kennedy, W.J., and Latil, J.L. (2007). The Upper Albian ammonite succession in the Montlaux section, Hautes-Alpes, France. *Acta Geologica Polonica*, v. 57(4), p. 453-478.
KENN0817	Kolbay	Kennedy, W.J., King, C., and Ward, D.J. (2008). The Upper Albian and Lower Cenomanian succession at

	Kolbay, eastern Mangyshlak (southwest Kazakhstan). *Buttelin de lInstitute Royal des Sciences Naturelle de Belgique*, v. 78, p. 117-147.
KENN0835	Kennedy, W.J., Jagt, J.W.M., Amedro, F., and Robaszynski, F. (2008). The late Late Albian (Mortoniceras fallax Zone) cephalopod fauna from the Bracquegnies Formation at Strepy-Thieu (Hainaut, southern Belgium). *Geologica Belgica*, v. 11, p. 35-69.
KENN8601	Kennedy, W.J., Bilotte, M., Lepicard, B., and Segura, F. (1986). Upper Campanian and Maastrichtian ammonites from the Petits-Pyrenees, southern France. *Eclogae Geologicae Helvetiae,* v. 79, p. 1001-1037.
KENN8645	Kennedy, W.J. (1986). Campanian and Maastrichtian ammonites from northern Aquitaine, France. *Palaeontological Association Special Papers in Palaeontology,* v. 36, 145 p.
KENN8649	Kennedy, W.J. (1986). The Campanian-Maastrichtian ammonite sequence in the environs of Maastricht (Limburg, the Netherlands). *Newsletters on Stratigraphy,* v. 16, p. 149-168.
KENN8681	Kennedy, W.J., and Summesberger, H. (1986). Lower Maastrichtian ammonites from Neuberg, Stiermark, Austria. *Beitraege zur Palaeontologie von Osterreich,* v. 12, p. 181-242.

KENN9281	Kennedy, W.J. and Henderson, R.A. (1992). Non-heteromorph ammonites from the upper Maastrichtian of Pondicherry, South India. *Palaeontology,* v. 35, p. 381-442.
KENN9293	Kennedy, W.J., and Henderson, R.A. (1992). Heteromorph ammonites from the Upper Maastrichtian of Pondicherry, South India. *Paleontology,* v. 35, p. 693-371.
KENN9297	Kennedy, W.J., Cobban, W.A., and Scott, G.R. (1992). Ammonite correlation of the uppermost Campanian of Western Europe, U.S. Gulf Coast, Atlantic Seaboard and Western Interior, and the numerical age of the base of the Maastrichtian. *Geological Magazine,* v. 129(4), p. 497-500.
KENN9304	Kennedy, W.J., and Cobban, W.A. (1993). Ammonites from the Saratoga Chalk (U. Cretaceous), Arkansas. *Journal of Paleontology,* v. 67(3), p. 404-434.
KENN9357	Kennedy, W.J., and Cobban, W.A. (1993). Maastrichtian ammonites from the Corsicana Formation in northeast Texas. *Geological Magazine,* v. 130(1), p. 57-67.
KENN9383	Kennedy, W.J., and Cobban, W.A. (1993). Campanian ammonites from the Annona Chalk near Yancy Arkansas. *Journal of Paleontology,* v. 67(1), p. 83.

KENN9463	Rochers de Fiz	Kennedy, W.J. and Delamette, M. (1994). Lyelliceratidae and Flickiidae (Ammonoidea) from the Upper Aplbian of the Helvetic Shelf (Western Alps, France and Switzerland). *Journal of Palaeontology,* v. 68(6), p. 1263-1284.
KENN9485		Kennedy, W.J., and Cobban, W.A. (1994). Upper Campanian ammonites from the Mount Laurel Sand at Biggs Farm, Delaware. *Journal of Paleontology,* v. 68(6), p. 1285-1305.
KENN9495		Kennedy, W.J., and Cobban, W.A. (1994). Ammonite fauna from the Wenonah Formation (Upper Cretaceous) of New Jersey. *Journal of Paleontology,* v. 68(1), p. 95-110.
KENN9607	Rabot Hill, Sezenac	Kennedy, W.J., Bilotte, M., and Hansotte, M. (1996). Cenomanian ammonites from Pech de Foix (Arriege, France). *Geobios,* v. 29(3), p. 307-318.
KENN9618	Bell Fourche Reservoir	Kennedy, W.J., Cobban, W.A., and Landman, N.H. (1996). New records of Acanthoceratid ammonoids from the Upper Cenomanian of South Dakota. *American Museum Noviates,* v. 3161, 18 pp.
KENN9698		Kennedy, W.J., and Cobban, W.A. (1996). Maastrichtian ammonites from the Hornerstown Formation in New Jersey. *Journal of Paleontology,* v. 70(5), p. 798-804.

KENN9730		Kennedy, W.J., Cobban, W.A., and Landman, N.H. (1997). Maastrichtian ammonites from te Severn Formation in Maryland. *American Museum Novitates,* v. 3210, 30 p.
KENN9762		Kennedy, W.J., and Cobban, W.A. (1997). Campanian (Upper Cretaceous) ammonites from the Marshaltown Formation - Mt Laurel Boundary beds in Delaware. *Journal of Paleontology*, v. 71(1), p. 62-73.
KENN9775		Kennedy, W.J., and Christensen, W.K. (1997). Santonian to Maastrichtian ammonites from Scania, southern Sweden. *Fossils and Strata,* v. 44, p. 75-128.
KENN9845		Kennedy, W.J., Landman, N.H., Christenson, W.K., Cobban, W.A., and Hancock, J.M. (1998). Marine connections in North America during the late Maastrichtian: paleogeographic and paleobiogeographic significance of Jeletzkytes nebrascense Zone cephalopod fauna from the Elk Butte Member of the Pierre Shale, S.E. South Dakota and N.E. Nebraska. *Cretaceous Research,* v. 19, p. 745-775.
KIRK9112	Black Mesa CEN10	Kirkland, J.I. (1991). Lithostratigraphic and biostratigraphic framework for the Mancos Shale (Late Cenomanian to Middle Turonian) at Black Mesa, northeastern Arizona. *Geological Society of America Special Paper,* v. 260, p. 85-112.

KODA0069		Kodama, K., Maeda, H., Shigata, Y., Kase, T., and Takeuchi, T. (2000). Magnetostratigraphy of the Upper Cretaceous strata in South Sakhalin, Russian Far East. *Cretaceous Research*, v. 21, p. 469-478.
KOPA0229	Selbukhra 2 MIDK30B	Kopaevich and Kuzmicheva (2002). in Wagreich (ed.) Aspects of Cretaceous stratigraphy and palaeobiogeography. *Oesterreichische Akademie der Wissenschaften*, v. 15, p. 129-147.
KOPA1433	Baksan, Kheu	Kopaevich, L.F., and Khotylev, A.O. (2014). The stratigraphic setting of Cretaceous volcanic rocks in Crimea ans in the North Caucasus. *Moscow University Geology Bulletin*, v. 69(6), p. 433-444.
KORA0235	Wadi Sudr	Kora, M., Hamama, H., and Sallam, H. (2002). Senonian macrofauna from west-central Sinai: Biostratigraphy and palaeobiogeography. *Egyptian Journal of Palaeontology,* v. 2, p. 235-258.
KORC0455	Koikitau, Rovik	Korchagin, O.A. (2004). On events of the terminal Cenomanian in the easterb Central Asia. *Russian Journal of Earth Sciences*, v. 6(4), p. 355-377.
KORC1273	Ak-Kaya Mountain	Korchangin, O.A., Bragona, L.G., and Bragin, N.Yu. (2012). Planktonic foraminifers and radiolarians from the Coniacian-Santonian deposits of the Mt. Ak-Kaya, Crimean Mountains, Ukraine. *Stratigraphy and Geological Correlation,* v. 20(1), p. 73-96.

KUCH0123		Kuchler, T., Kutz, A., and Wagereich, M. (2001). The Campanian-Maastrichtian boundary in northern Spain (Navarra Province): the Imiscoz and Erro sections. in Odin, G. S. (ed.) The Campanian-Maastrichtian Stage Boundary. *Elsevier,* p. 723-744.
KUMO9700	Kii Peninsula	Kumon, F., Matsuyama, H., and Musashino, M. (1997). An oceanic fragment in the Upper Cretaceous Miyama Formation of the Shimanto Belt, Kii Peninsula, Japan. *Memoirs of the Geological Society of Japan,* v. 48, p. 100-109.
KURI0600	Ikushumbetsu 2	Kurimara, K. (2006). Cenomanian-Turonian stage boundary in the north-west Pacific: Marine biodiversity and palaeogeographic background. (Unpublished PhD dissertation), Waseda University.
LAMO8945	Estella 2 MIDK28	Lamolda, Lopez and Martinez (1989). Turonian integrated biostratigraphy in the Estella Basin. *in Wiedmann, Proceedings of the 3rd international Cretaceous Symposium,* p. 145-159.
LAMO9731	Ganuza	Lamolda, M.A., Gorostidi, A., Martinez, R., Lopez, G., and Peryt, D. (1997). Fossil occirrences in the Upper Cenomanian - Lower Turonian at Ganuza, northern Spain: an approach to Cenomanian/Turonian boundary chronostratigraphy. *Cretaceous Research,* v. 18, p. 331-353.
LAND0345		Landman, H.H., and (2003). Ammonites from the upper part of the Pierre

		Shale and Fox Hills Formation of Colorado. *American Museum Novitates,* v. 3388, 45 pp.
LAND0345		Landman, N.H., and Cobban, W.A. (2003). Ammonites from the upper part of the Pierre Shale and Fox Hills Formation of Colorado. *American Museum of Natural History Novitates,* v. 3388, 45 pp.
LAND0407		Landman, N.H., Johnson, R.O., and Edwards, L.E. (2004). Cephalopods from the Cretaceous/Tertiary boundary interval on the Atlantic Coastal Plain, with a description of the highest ammonite zones in North America, Part 2, Northeastern Monmouth County, New Jersey. *American Museum of Natural History Bulletin,* v. 287, 107 pp.
LAND0464		Landman, N.H., Johnson, R.O., and Edwards, L.E. (2004). Cephalopods from the Cretaceous/Tertiary boundary interval on the Atlantic Coastal Plain, with a description of the highest ammonite zones in North America, Part 1, Maryland and North Carolina. *American Museum Novitates,* v. 3454, 64 pp.
LEBE0604	Berezovskaya Core 23K, Leningradskaya Core	Lebedev, N.K. (2006). Dinocyst biostratigraphy of the Upper Cretaceous of Northern Siberia. *Paleontological Journal,* v. 40 (Suppl. 5), p. S604-S621.
LEBE1379	Goulmima, Tazzouguert, Ziz	Lebedel, V., Lezin, C., Andreu, B., Wallez, M.-J., Ettachfini, E. M., and Riquier, L. (2013). Geochemical and

		plaeoecological record of the Cenomanian-Turonian anoxic event in the carbonate platform of the Preafrican Trough, Morocco. *Palaeogeography Palaeoclimatology Palaeoecology,* v. 569, p. 79-98.
LECK8479	DSDP Site 545, DSDP Site 547A, DSDP Site 547B	Leckie, R.M. (1984). Mid-Cretaceous Planktonic Foraminiferal Biostratigraphy off Central Morocco, Deep Sea Drilling Project Leg 79, Sites 545 and 547. *Initial Reports of the Deep Sea Drilling Project,* v. 79, p. 579-620.
LECK9763	Mesa Verde, Mesa Verde MIDK130	Leckie, M., Kirkland, J.I., and Elder, W.P. (1997). Stratigraphic framework and correlation of a principal reference section of the Mancos Shale (Upper Cretaceous), Mesa Verde, Colorado. *New Mexico Geological Society Guidebook,* v. 48, p. 163-216.
LEES0840	Salzgitter-Salder Quarry, Slupia Nadbrzezna	Lees, J.A. (2008). The calcareous nannofossil record across the Late Cretaceous Turonian/Coniacian boundary, including new data from Germany, Poland, the Czech Republic and England. *Cretaceous Research,* v. 29, p. 40-64.
LEHM0041	ODP 1052E	Lehmann, J. (2000). Upper Albian ammonites from ODP Leg 171B of northern Florida. *Palaeontology,* v. 43(1), p. 41-61
LEHM0945	Assaka-n Aouam, Atlas Composite	Lehmann, J,M and Herbig, H.-G. (2009). Late Cretaceous ammonites from Bou Angeur synclines (Middle Atlas, Morocco) - stratigraphic and

		palaeobiogeographic implications. *Palaeontographica Abteilung A,* v. 289(1), p. 45-87.
LEHM0995		Lehmann, J., Heldt, M., Bachmann, M., and Negra, M.E.H. (2009). Aptian (Lower Cretaceous) biostratigraphy and cephalopods from north central Tunisia. *Cretaceous Research,* v. 30, p. 895-910.
LEHM1123	Lahe Core	Lehmann, J. (2011). Ammonite biostratigraphy and correlation of Middle/Late Albian drilling cores in the Hannover are (northern Germany). *Newletters on Stratigraphy,* v. 44(2), p. 123-135.
LEHM9858	Munsterland Composite	Lehmann, J. (1998). Systematic oalaeontology of the ammonite of the Cenomanian-Lower Turonian (Upper Cretaceous) of northern Westphalia, North Germany. *Tuebinger Geowissenschaftlicher Arbeiten,* v. A37, 58 pp.
LENN1499	May Point	Linniger, M., Nohr-Hansen, H., Hills, L.V., and Bjerrum, C.J. (2014). Arctic black shale formation during Cretaceous Oceanic Anoxic Event 2. *Geology,* v. 42(9), p.799-802.
LIGU0905	Zanda	Li, G., Jiang, G., Hu, X., and Wan, X. (2009). New biostratigraphic data from the Cretaceous Bolinxiala FOrmation in Zanda, southwest Tibet of China and their paleogeographic and palaeoceanographic implications. *Cretaceous Research,* v. 30, p. 1005-1018.

LOPE0985	Armintza	Lopez-Horgue, M.A., Owen, M.A., Aranburu, A., Fernandez-Mendoza, P.A., and Garcia-Modejar, J. (2009). Early late Albian (Cretaceous) of the central region of the Basque-Cantabrian Basin, northern Spain: biostratigraphy based on ammonites and orbitilinids. *Cretaceous Research*, v. 30, p. 385-400.
LOPE9969	Estella-Lizarra MIDK60	Lopez-Horgue, M.A., Owen, H.G., Rodriguez-Lazaro, J., Orue-Etxebarria, X., Fernandez-Mendiola, P.A., (1999). Late Albian-Early Cenomanian stratigraphic succession near Estella-Lizarra (Navarra, central northern Spain) and its regional and interregional correlation. *Cretaceous Research*, v. 20, p. 369-402.
LUDV9445	Big Sioux R. MIDK136	Ludvigson et al. (1984). * *Geological Society of America Special Paper*, v. 287, p. 145-173.
MACE8499		MAcellari, C.E. (1984). Late Cretaceous stratigraphy, sedimentology, and macropaleontology of Seymour Island, Antarctic Peninsula. *unpublished PhD dissertation The Ohio State University*, 599 pp.
MACH0447		Machalsky, M., Kennedy, W.J., and Kin, A. (2004). Early Late Campanian ammonite fauna from Busko Zdroj (Nida Trough, southern Poland). *Acta Geologica Polonica*, v. 54(4), p. 447-471.
MAED0525	Acacia River	Maeda, H., Shigeta, Y., Fernando, A.G.S., and Okada, H. (2005). Stratigraphy

		and fossil assemblages of the Upper Cretaceous system in the Makarov area, southern Sakhalin, Russian Far East. *Monographs of the National Science Museum,* v. 31, p. 25-120.
MANC7913	Waco Lk Spillway MIDK115	Mancini, E.A. (1979). Late Albian and Early Cenomanian Grayson ammonite biostratigraphy in north-central Texas. *Journal of Paleontology*, v. 53(4), p. 1013-1022.
Mar-01		Marcinowski, R., Walaszczyk, I., and Olszewska-Nejbert, D. (1996). Stratigraphy and regional development of the mid-Cretaceous (Upper Albian through Coniacian) of the Mangyshlak Mountains, Western Kazakhstan. *Acta Geologica Polonica,* v. 46(1-2), p. 1-60.
MART9773		Martinez, R. (1977). Campanian and Maastrichtian ammonites from southeast Spain. *Cretaceous Research,* v. 18, p. 373-384.
MAST8300	La Boca Cyn CEN9	Masters, Kidson, Lewy, and Scott. (1983). * *Research Department Report, Amoco Production Company,* v. M83-G-2.
MATS8471	Ikushumbetsu 3, Pombets, Pombets-Gonosawa	Marsumoto, T. (1984). The so-called Turonian-Coniacian boundary in Japan. *Bulletin of the Geological Society of Denmark,* v. 33, p. 171-181.

MCAR9495	Strontium Composite	MaArther, J.M., Kennedy, W.J., Chen, M., Thirlwall, M.F., and Gale, A.S. (1994). Strontium isotope stratigraphy for Late Cretaceous time: direct numerical calibration of the Sr isotope curve based on the wUS Western Interior. *Palaeogeography, Paleoclimatology, Palaeoecology*, v. 108, p. 95-119.
MEIS0341	Libreville PK8	Meister, C., Mbina-Mounguengui, M., and Lang, J. (2003). Les ammonites du Cenoman0-Turonien du bassin cotier nord gabonnaise: systematique et interet paleogeographique pour la liasson Tethys-Atlantique Sud. *Revue de Paleobiologie Geneve*, v. 22(1), p. 341-355.
MEIS0511	Jabal Askar, Jebel Zitouna, Khanguet Halfaya Kbira, Oued Beida, Oued el Hessi, Oued Essalite	Meister, C., and Abdallah, H. (2005). Precision sur les successions d-ammonites du Cenomanien-Turonien dans la region du Gafsa, Tunisie du centre-sud. *Revue de Paleobiologie Geneve*, v. 24(1), p. 111-199.
MEIS1185	Sumbe North	Meister, C., Buta, A., David, B., and Tavares, T (2011). Les ammonites de la limite Albien-Cenomanien dans la region Sumbe (Bassin de la Kwanza, Angola). *Revue de Paleobiologie Geneve*, v. 30(2), p. 685-781.
MEIS1383	Tethys South Composite	Meister, C., and Piuz, A. (2013). Late Cenomanian - Early Turonian ammonites of the nothern Tethys margin from Morocco to Oman:

		Biostratigraphy, paleobiogeography and morphology. *Cretaceous Research,* v. 44, p. 83-103.
MEIS9255	Abalak, Berere, Birgimari, Monts Iguelela, Niger Zonation, Niger-Nigeria Zonation, Tanout	Meister, C., Alzouma, K., Lang, J., and Mathey, B. (1992). Les ammonites du Niger (Afrique occidentale) et la transgression transsaharienne au cours du Cenomanien-Turonien. *Geobios,* v. 25(1), p. 55-100.
MEIS9489	Cheffadene	Meister, C., Alzouma, K., Lang, J., Mathey, B., and Pascal, A. (1994). Nouvelles donnees sur les ammonites du Niger oriental (Tenere, Afrique Occidentale) dans le cadre de la transgression du Cenomanien-Turonien. *Geobios,* v. 27(2), p. 189-219.
MELI0824	Ohaba-Ponor	Melinte-Drobinescu, M.C., and Bojar, A.V. (2008). Biostratigraphic and isotopic record of the Cenomanian-Turonian deposits in the Ohaba-Puor section (S.W. Hateg, Romania). *Cretaceous Research,* v. 29, p. 1024-1034.
MELI1095	Fizesti	Melinte-Dobrinescu, M.C., and Bojar, A.V. (2010). Late Cretaceous carbon and oxygen isotope stratigraphy. nannofossil events and paleoclimate fluctuations in the Hateg area (SW Romania). *Palaeogeography Palaeoclimatology Palaeoecology,* v. 293, p. 295-305.
MELI1322	Arobe	Melinte-Dobrinescu, M.C., Bernardez, E., Kaiho, K., and Lamolda, M.A. (2013). Cretaceous Oceanic Anoxia Event 2 in the Arobes section,

		northern Spain: nannofossil fluctuations and isotope events' 'in Bojar, A. V., Melinte-Dobrinescu, M. C., and Smit, J. *Isotopic Studies in Cretaceous Research, Geological Society of London Special Publications,* v. 382, 22 pp.
MERE1113	Black Hills, Buckeye, Colfax Co., Kassler-Littleton, Lykins, Pueblo 3, Red Bird 2, Rock River, Springer, Thornton Dome, Rock River 2	Merewether, E.A., Cobban, W.A., and Obradovich, J.D. (2013). Biostratigraphic data from Upper Cretaceous formations -- Eatern Wyoming, Central Colorado, and Northeastern New Mexico. *United States Geological Survey Scientific Investigations Map,* v. 3175, 13 pp.
MILE8091	DSDP Site 417D, DSDP Site 418A, DSDP Site 418B	Miles, G.A. & Orr, W. (1980). Planktonic Foraminifers from the Bermuda Rise, Deep Sea Drilling Project Legs 51, 52, and 53. *Initial Reports of the Deep Sea Drilling Project*, v. 51-53(2), p. 791-813.
MILL0992		Millan, M.I., Weissert, M.J., Fernandez-Mendiola, P.A., and Garcia-Mondejar, J. (2009). Impact of Early Apltian carbon cycle perturbations on evolution of a marine shelf system in the Basque-Cantabrian basin (Aralar, N. Spain). *Earth and Planetary Science Letters,* v. 287, p. 392-401.
MILL1167		Millan, M.I., Weissert, H.J., Owen, H., Fernandez-Mendoza, P.A., and Garcia-Mondejar, J. (2011). The Madotz Urgonian platform (Aralar, northern Spain): Paleoecological changes in response to Early Aptian

		global environmental events. *Palaeogeography, Palaeoclimatology, Palaeoecology,* v. 312, p. 167-180.
MITC9803	Folkestone	Mitchell, S.F., & Carr, I.T. (1998). Foraminiferal response to mid-Cenomanian (Upper Cretaceous) palaeoceanographic events in the Anglo-Paris Basin (Northewest Europe). *Palaeogeography, Palaeoclimatology, Palaeoecology,* v. 137, p. 103-125.
MOLE0201	Coyote Creek, Kenton, Quemado	Molenaar, C.M., Cobban, W.A., Merewether, B.A., Pillmore, C.L., Wolfe, D.G., and Holbrook, J.M. (2002). Regional stratigraphic corss-section of Cretaceous rockks from east central Arizona to the Oklahoma Panhandle. *United States Geological Survey Miscellaneous Field Studies Map,* MF 2382, 3 sheets.
MONN0717	Europe NW Uas, Tunisia Central Uas, Western Interior Uas	Monnet, C., and Bucher, H. (2007). Ammonite-based correlations in the Cenomanian-lower Turonian of north-west Europe, central Tunisia and the Western Interior (North America). *Cretaceous Research,* v. 28, p. 1017-1032.
MONO0077		Monod, O., Busnardo, R., and Guerrero-Suastegui, M. (2000). Late Albian ammonites from the carbonate cover of the Telocoapan arc volcanic rocks (Guerrero State, Mexico). *Journal of South American Earth Sciences,* v. 13, p. 377-388.

MORE0964		Moreno-Bedmar, J.A., Company, M., Bover-Arnal, T., Salas, R., Delanoy, G., Matrinez, R., and Grauge (2009). Biostratigraphic characterization by means of ammonoids of the lower Aptian Oceanic Anoxic Event (OAE1a) in the eastern Iberian Chain (Maestrat Basin, eastern Spain). *Cretaceous Research,* v. 30, p. 864-872.
MORE1031	Alcoria, Cau 2, Raco Ample	Moreno-Bedmar, J.A. (2010). Ammonits de l-Aptia Inferior de la peninsula iberica; biostratigrafia i aportacions a l-etudi del Oceanic Anoxic Event 1a. *PhD dissertation, University of Barcelona,* 331 pp.
MORE1233	Alcoria, Cau 2, Font Calent, Font Calent 1, Raco Ample	Moreno-Bedmar, J.A., Company, M., Sandoval, J., Tavera, J.M., Bover-Arnal, T., Salas, R., Delanoy, (2012). Lower Aptian ammonite and carbon isotope stratigraphy in the eastern Prebetic domain (Betic Cordillera, southeastern Spain). *Geologica Acta,* v. 10(4), p. 333-350.
MORT0797	Gola del Furlo, Monte Petrano, Valle del Burano	Mort, H., Jacquat, O., Adatte, T., Steinmann, P., Follmi, K., Matera, V., Berner, Z., and Stueben, D. (2007). The Cenomanian/Turonian anoxic event at the Bonarelli Level in Italy and Spain: enhanced productivity and/or better preservation? *Cretaceous Research,* v. 28, p. 597-612.
MORT8743	North Sea Coccoliths	Mortimer, C.P. (1987). Upper Cretaceous nannofossil biostratigraphy of the Southern Norwegian and Danish

		North Sea areas. *Abhandlungen Geologische Bundesanstalt Wien,* v. 39, p. 143-175.
MOSA1175	Ghareshu, Gorghoreh, Taherabad	Mosavinia, A., and Wilmsen, M. (2011). Cenomanian Acanthoceratoidea (Cretaceous Ammonoidea) fro the Koppeh Dagh, N.E. Iran: taxonomy amd stratigraphic implications. *Acta Geologica Polonica,* v. 61(2), p. 175-192.
MUSA0641	ODP Site 1258 I, ODP Site 1261	Musavu-Moussavou, B., and Danelian, T. (2006). The radiolarian biotic response to Oceanic Anoxic Event 2 in the southern part of the Northern proto-Atlantic (Demerara Rise, ODP Leg 207). *Revue de Microplaeontologie,* v. 49, p. 141-163.
MUSA0753	Bottaccione Gorge, Umbria Basin Composite	Musavu-Moussavou, B., Danelian, T., Baudin, F., Coccioni, R., and Froehlich, F. (2007). The radiolarian biotic response during OAE2: A high-resolution study across the Bonarelli level at B. *Revue de Microplaeontologie,* v. 50, p. 253-287.
MWEN1419	Kisarawe 1A, Kisarawe 1A-B, Kisarawe 1B, Songo Songo 4	Mweneinda, A.K. (2014). Mid-Cretaceous stratigraphy and micropalaeontology of the coastal basins of Tanzania. *PhD dissertation, University of Cardiff,* 419pp.
NAGM0913	Wadi Askhar, Wadi Ghonima, Wadi Ghonima E	Nagm, E.H.M. (2009). Integrated stratigraphy, palaeontology and facies analysis of the Cenomanian-Turonian (Upper Cretaceous) Galala and Naghra El Hadida formations of

		the western Wadi Araba, Eastern Desert, Egypt. *PhD dissertation, Wurzburg University*, 213 pp.
NAGM1263	Wadi el Burga, Wadi Qena N	Nagm, E., and Wilmsen, M. (2012). Late Cenomanian - Turonian (Cretaceous) ammonites from Wadi Qena, central Eastern Desert, Egypt: taxonomy, biostratigraphy and palaeobiogeographic implications. *Acta Geologica Polonica*, v. 62(1), p. 63-89.
NAGM1509	Wadi El Dakhl 1, Wadi Hawashiya	Nagm, E. (2015). Stratigraphic significance of rapid faunal change across the Cenomanian-Turonian boundary in the Eastern Desert, Egypt. *Cretaceous Research*, v. 52, p. 09-24.
NIEB0357		Niebuhr, B., and Esser, K. (2003). Late Campanian and early Maastrichtian ammonites from the White Chalk of Kronsmoor (northern Germany) - taxonomy and stratigraphy. *Acta Geologica Polonica*, v. 53(4), p. 257-281.
NIEB0473		Niebuhr, B. (2004). Late Campanian nostoceratid ammonites from the Lehrte West Syncline near Hannover, northern Germany. *Acta Geologica Polonica*, v. 54(4), p. 473-487.
OBRA0249	Hotei-zawa, Kyoei-Sakin-zawa	Obradovich, J.D., Matsumoto, T., Nishida, T., and Inoue, Y. (2002). Integrated biostratigraphic and radiometric study on the Lower Cenomanian (Cretaceous) of Hokkaido, Japan. *Proceedings of the Japanese*

		Academy, Series B, v. 78(6), p. 149-153.
OBRA7531		Obradovich, J.D., and Cobban, W.A. (1975). A time scale for the Late Cretaceous of the Western Interior of North America' 'in Caldwell, W. G. E. (ed.). *The Cretaceous system in the Western Interior of North America, Geological Association of Canada Special Paper*, v. 13, p. 31-54.
OBRA9379	Sheep Mtn MIDK37	Obradovich, J.G. (1993). Evolution of the Western Interior Basin' 'in Cardwell, W.G.E. and Kauffman, E.G. (eds.). *A Cretaceous Time Scale, Geological Association of Canada, Special Paper*, v. 39, pp. 379-396.
ODIN0150		Odin, G. S., Courville, P., Machalski, M., and Cobban, W. A. (2001). The Campanian-Maastrichtian ammonite fauna from Tercis (Landes, France); a synthetic view' 'in Odin, G. S. (ed.) The Campanian-Maastirchtian Stage boundary, characterization at Tercis les Bains (France) and correl. *Elsevier, Amsterdam*, p. 550-567.
OGGJ0444		Ogg, J.G., Agterberg, F.P., and Gradstein, F.M. (2004). The Cretaceous Period. Gradstein, F. M., Ogg, J. G., and Smith, A. G. (eds.), *In: A Geologic Time Scale*, Cambridge University Press, p. 344-383.
OHME1137	Schellenbach	Ohmert, W. (2011). Radiolarien-Faunen und Stratigraphie der Pattenau-Formation (Campanium bis

		Maastrichtium) in Helvetikum von Bad Toelz (Oberbayern). *Zitteliana,* v. 51, p. 37-98.
OLDE1501	Bechary #1 Core	Olde, K., Jarvis, I., Pearce, M., Ulicny, D., Tocher, B., Trabucho-Alexandre, J., and Groecke, D. (2015). A revised northern European Turonian (Upper Cretaceous) dinoflagellate cyst biostratigraphy: integrated palynology and carbon isotope events. *Review of Palaeobotany and Palynology,* v. 213, p. 1-16.
OLFE0501	Chernetovo, Sobolevskoe	Oferiev, A.G., Kopaevich, L.F., Valashchik, I., Vishnevskaya, V.S., and Gabdullin, R.R. (2005). New data on the structure of the Cenomanian-Coniacin deposits on the western slope of the Voronezh anteclise (Bryansk Region). *Moscow University Geology Bulletin,* v. 60(4), p. 1-17.
OLFE0710	Vishnevoe	Olferiev, A.G., Beniamovski, V.N., Vishnevskaya, V.S., Ivanov, A.V., Kopaevich, I.F., Pervushov (2007). Upper Cretaceous deposits in the northwest of Saratov Oblast, Part 1: Litho- and biostratigraphic analysis of the Vishnevoe section. *Stratigraphy and Geological Correlation,* v. 15(6), p. 610-655.
OLIV8926		Olivero, E.B., and Zinsmeister, W.J. (1989). Large heteromorph ammonites from the Upper Cretaceous of Seymour Island, Antarctica. *Journal of Paleontology,* v. 63(5), p. 626-636.

OMAN1257	Sierra de Alvarez	Omana, L., Doncel, R.L., Torres, J.R., and Alencaster, G. (2012). Biostratigraphy and paleoenvironment of the Canomanian/Turonian boundary interval based on foraminifera from W Valles - San luis Potosi platform, Mexico. *Micropaleontology,* v. 58(6), p. 457-485.
PALE1063	Jebel Garci, Kamchatskii Mys Penin.	Palechek, T.N., Savelev, D.P., and Saveleva, O.L. (2010). Albian-Cenomanian radiolarian assemblage from the Smaginsk Formation, the Kamchatskii Mys peninsula of eastern Kamchatka. *Stratigraphy and Geological Correlation,* v. 18(1), p. 63-82.
PASS9121	Gola del Furlo, Monte Petrano, Valle del Burano	Passerini, M.M., Bettinin, P., Dainelli, J., and Sirugo, A. (1991). The Bonarelli Horizon in the central Apennines (Italy): radiolarian biostratigraphy. *Cretaceous Research,* v. 12, p. 321-331.
PAUL9401	Menoyo	Paul. C. R.C., Mitchell, S., Lamolda, M., and Gorostidi, A. (1994). The Cenomanian-Turonian boundary event in northern Spain. *Geological Magazine,* v. 131(6), p. 801-817.
PAUL9983	Eastbourne	Paul, C.R.C., Lamolda, M.A., Mitchell, S.F., Vaziri, M.R., Gorostidi, A., and Marshall, J.D. (1999). The Cenomanian-Turonian boundary at Eastbourne (Sussex, UK): a proposed European reference section. *Palaeogeography, Palaeoclimatology, Palaeoecology,* v. 150, p. 83-121.

PEAR0907	Eastbourne	Pearce, M.A., Jarvis, I., and Tocher, B.A. (2009). The Cenomanian-Turonian boundary event, OAE2 and palaeoenvironmental change in epicontinental seas: New insights from the dinocyst and geochemical records. *Palaeogeography, Palaeoclimatology, Palaeoecology,* v. 280, p. 207-234.
PERY9645	Menoyo	Peryt, D., and Lamolda, M. (1996). Benthonic foraminiferal mass extinction and survival assemblages from the Cenomanian-Turonian boundary event in the Menoyo section, northern Spain.' 'in Hart, M. B. (ed.). *Biotic Recovery from Mass Extinction Events, Geological Society of London Special Publications,* v. 102, p. 245-258.
PEYB1349		Peybernes, C., Giraud, F., Jaillard, E., Robert, E., Masrour, M., Aoutem, M., and Icame, N. (2013). Stratigraphic framework and calcareous nannofossil productivity of the Essaouir-Agadir Basin (Morocco) during the Aptian - Early Albian: Comparison witrh the north-Tethyan margin. *Cretaceous Research,* v. 39, p. 149-169.
PEYR1104	Puentedey	Peyrot, D., Barroso-Barcenilla, F., Barron, E., and Comas-Rengifo, M.J. (2011). Palaeoenvironmental analysis of Cenomanian-Turonian dinocycst assmblages from the Castilian Platform (North Central Spain). *Cretaceous Research,* v. 32, p. 504-526.

PEZA9417	Arrez, Krejlure, Pushtrik Mtns, Shengjin	Peza, L.H., and Pirdeni, A. (1994). Cenomanian-Turonian boundary in the Mirdita zone, Albania. *Cretaceous Research*, v.15, p. 217-225.
PHIL9887	Cassis MIDK100, Font Blance MIDK101	Philip. J. (1998). Sequences and systems tracts of mixed carbonate-siliciclastic platform-basin settings: The Cenomanian-Turonian stages in Provence (Southeastern France): Mesozoic and Cenozoic Sequence Stratigraphy of European Basins, *SEPM Special Publications,* v. 60, p. 387-395.
PORT7600	La Farette	Porthault, B., and Mennessier, G. (1976). Le Cretace superior de la Fosse Vocontienne et des regions voisines: Excursion du groupe francais du. *
PRAU1519	Tarfaya 2	Prauss, M.L. (2015). Marine palynology of the Oceanic Anoxia Event 3 (OA3, Coniacian-Santonian) at Tarfaya, Morocco, NW Africa - transition from preservation to production controlled accumulation of marine organic carbon. *Cretaceous Research,* v. 53, p. 19-37.
PREM8139	DSDP Site 462	Silva, I.P. & Brusa, Chiara. (1981). Shallow-Water Skeletal Bebris and Large Foraminifers from Deep Sea Drilling Project Site 462, Nauru Basin, Western Equatorial Pacific. *Initial Reports of the Deep Sea Drilling Project,* v. 61, p. 439-473.
PREM9489	Bottaccione Gorge	Premoli-Silva, I., and Sliter, W.V. (1994). * *Paleontographia Italia,* v. 82, 89 pp.

PUGH1401	Ellef Ringnes Island	Pugh, A.T., Schroeder-Adams, C.J., Carter, E.S., Herrle, J.O., Galloway, J., Haggart, J.W., And (2014). Cenomanian to Santonian radiolarian biostratigraphy, carbon isotope stratigraphy and paleoenvironments of the Sverdrup Basin, Ellef Ringnes Island, Canada. *Palaeogeography Palaeoclimatology Palaeoecology*, v. 413, pp. 101-122.
QUID1172	Tengu	Quidelceur, X., Paquette, J.L., Fiet, N., Takashima, R., Tiepolo, M., Desmares, D., Nishi, H., and (2011). New U-Pb (ID-TIMS) and LA-ICPMS and 40Ar/39Ar geochronological constraints of the Cretaceous geologic time scale calibration from Hokkaido, Japan. *Chemical Geology*, v. 286, p. 72-83.
RAZM1483	Shahneshin	Razmjooei, M.J., Thibault, N., Kani, A., Mahanipour, A., Boussaha, M., and Korte, C. (2014). Coniacian-Maastrichtian calcareous nannofossil biostratigraphy and carbon-isotope stratigraphy in the Zagros Basin (Iran): consequences for the correlation of Late Cretaceous stage boundaries between Tethyan and Boreal realms. *Newsletters on Stratigraphy*, v. 47(2), p. 183-209.
REBO1370	Blieux	Reboulet, S., Giraud, F., Colombie, C., and Carpentier, A. (2013). Integrated stratigraphy of the Lower and Middle Cenomanian in a Tethyan section (Blieux, southeast France) and correlations with Boreal basin.

		Cretaceous Research, v. 40, p. 170-189.
REMI1054	Lipnik-Kije	Remin, Z. (2010). Upper Coniacian, Santonian and lowermost Campaniam ammonites of the Lipnik-Kije, central Poland - taxonomy, stratigraphy, and palaeogeographic significance. *Cretaceous Research,* v. 31, p. 154-180.
REOL1591	Oued Bahloul 2	Reolid, M., Sanchez-Quinonez, C.A., Alegret, L., and Molina, E. (2015). Palaeoenvironmental turnover across the Cenomanian-Turonian transition in Oued Bahloul, Tunisia: foraminifera and geochemical proxies. *Palaeogeography Palaeoclimatology Palaeoecology,* v. 417, p. 491-510.
ROBA0703	Oued Smara	Robaszynski, F., Amedro, F., Gonzales-Donoso, J.M., and Linares, D. (2007). Les bioevenements de la limite ALbien (Vraconien) - Cenomanien aux marges nord et sud de la Tethys (S.E. de la France et Tunisie Centrale). Bulot, L.G., Ferry, S., and Grosheny, D. (eds.), *In: Relations entre les marges septentrionale et meridionale de la Tethys au Cretace*. Carnets de Geologie, v. 2007/02, p. 3-15.
ROBA1001	Bou Ghanem	Pobaszynski, F., Zagrarni, M. F., Caron, M., and Amedro, F. (2010). The global bio-events at the Cenomanien-Turonian transition in the reduced Bahloul Formation of

		Bou Ghanem (Central Tunisia). *Cretaceous Research,* v. 31, p. 1-15.
ROBA8671	Cap Blanc Nez, Wissant	Robaszynski, F., and Amedro, F. (1986). The Cretaceous of the Boulonnais (France) and a comparison with the Cretaceous of Kent (United Kingdom). *Proceedings of the Geologists Association*, v. 97(2), p. 171-208.
ROBA9113		Robaszynsky, F., Amedro, F., and Caron, M. (1991). A limite Cenomano-Turonien et la formation Bahloul dans quelques localites de la Tunisie Centrale. *Geologie Alpine Memoires,* v. 17, p. 113-114.
ROBE0359	Banos del Inca, Pongo de Rentema, Puente Zonanga, Tamberia West	Robert, E., Bulot, L.G., Jaillard, E., and Peybernes, B. (2003). Revision bioestratigrafia del Albiano inferior a superior basal em la cuenca Andina Peruana (Peri central y norte). *Bolletin de la Sociedad Geologica del Peru,* v. 95, p. 59-74.
ROBE0411	Banos del Inca, Pongo de Rentema, Puente Zonanga, Tamberia West	Robert, E., and Bulot, L.G. (2004). Origin, phylogeny, faunal composition, and stratigraphical significance of the Albian engonoceratidae (puchelliaceae, ammonitina) of Peru. *Journal of South American Earth Sciences*, v. 17, p. 11-23.
ROPO9959		Ropolo, P., Gommet, R., and Conte, G. (1999). The Pseudocrioceras interval and adjacent beds at LA BEdoule (SE France): implications to highest Barremian/lowest Aptian biostratigraphy. *Scripta Geologica Special Issue,* v. 3, p. 159-213.

SABE1200	Abu Darag 2, Wadi el Dakhl 2	Saber, S.G. (2012). Depositional framework and sequence stratigraphy of the Cenomanian-Turonian rocks on the western side of the Gulf of Suez, Egypt. *Cretaceous Research,* v. 37, p. 300-318.
SAGE9786	Portland Core MIDK132	Sageman, B.B., Rich, J., Arthur, M.A., Birchfield, G.E., and Dean, W.E. (1997). Evidence for Milankovitch periodicities in Cenomanian-Turonian lithologic and geochemical cycles, Wesdtern Interior U.S.A. *Journal of Sedimentary Research,* v. 67(2), p. 286-302
SAIN7437	Dlebt-Chenin Aair MIDK23, Nahr Ibrahim MIDK22	Saint-Marc (1974). * *Notes et Memoires sur le Moyen Orient Musee Nationale d-Histoire Naturelle,* v. 13, p. 37-48.
SALM1433	Jebel Chemsi	Salmouna, D.J., Chaabani, F., Dhahri, F., Mzough, M., Salmouna, A., and Zilstra, H.B. (2014). Lithostratigraphic analysis of the Turonian-Coniacian Bireno and Douleb carbonate members in Jebels Berda and Chemsi, Gafsa BAsin, central-southern Altlas of Tunisia. *Journal of African Earth Sciences,* v. 100, p. 733-754.
SALV9877	Albacini, Bosso, Carcoselle, Castel Toblino, Cismon RA, Piobbico, Segusino	Salvini, G., and Passerini, M.M. (1998). The radiolarian assemblages of the Bonarelli Horizon in the Umbria-Marche apennines and Southern Alps. *Cretaceous Research,* v. 19, p. 777-804.

SANT9271	Ganuza 1, Ganuza 2, Ganuza 4	Santamaria-Zabala, R. (1992). Los ammonoides del Cenomaniense superior al Santoniense de laplataforma nord-castellana y la cuenca navarro-cantabrica: Parte 1 Bioestratigrafia y sistematica: Phyllorceratina, Ammonitina (Desmocerataceae y Hoplitaceae) y Ancyloceratina. *Treb Museo Geologia Barcelona*, v. 2, p. 171-268.
SANT9341	Losa Valley	Santamaria, R., and Ricardo, M. (1993). Preliminary report on Middle Coniacian - Lower Santonian ammonite distribution from the Basque Cantabrian Basin (Northern Spain). *Geobios,* v. 15, p. 341-345.
SCHA8119	DSDP Site 463, DSDP Site 464, DSDP Site 465, DSDP Site 465A, DSDP Site 466	Schaaf, Andre. (1981). Late Early Cretaceous Radiolaria from Deep Sea Drilling Prject Leg 62. *Initial Reports of the Deep Sea Drilling Project,* v. 62, p. 419-470.
SCHA8621	DSDP Site 585, DSDP Site 585A	Schaaf, Andre. (1986). Radiolaria From Deep Sea Drilling Project Leg 89. *Initial Reports of the Deep Sea Drilling Project,* v. 89, p. 321-326.
SCHI9813	Ben More, Kekerengu	Schioler, P., and Wilson, G.J. (1998). Dinoflagellate biostratigraphy of the middle Coniacian - lower Campanian (Upper Cretaceous) in south Marlborough, New Zealand. *Micropaleontology,* v. 44, p. 313-349.
SCHM1245		Schmitz, M. (2012). Appendix. in Gradstein et al. GTS 2012. * 45 pp.

SCHR9611	Anderson Roros MIDK36	Schroeder-Adams, C.J., Leckie, D.A., Bloch. J., Craig, J., McIntyre, D.J., and Adams, P.J. (1996). Paleoenvironmental changes in the Cretaceous (Albian-Turonian) Colorado Group of western Canada: microfossil, sedimentological and geochemical evidence. *Cretaceous Research,* v. 17, p. 311-365.
SCHU0341	Rumaymin 2, Rumaymin 4, Silla 1-2, Wadi Abu Kusheiba 3	Schulze, F., Lewy, Z., Kuss, J., and Gharaibeh. A. (2003). Cenomanian-Turonian carbonate platform deposits in west central Jordan. *Geologische Rundschau,* v. 92, p. 641-660.
SCHU0409	Jordan Zonal Composite	Schulze, F., Marzouk, A.M., Bassiouni, M.A.A., and Kuss, J. (2004). The late Albian - Turonian carbonate platform succession of west-central Jordan: stratigraphy and crises. *Cretaceous Research,* v. 25, p. 709-737.
SCOP0859	Novara di Sicilia	Scopelliti, G., Bellanca, A., Erba, E., Jenkyns, H.C., Neri, R., Tamagnini, P., Luciani, V., & Maset (2008). Cenomanian-Turonian carbonate and organic-carbon isotope records, biostratigraphy and provenance of a key section in NE sicily, Italy: Palaeoceangraphic and palaeogeographic implications. *Palaeogeography, Palaeoclimatology, Palaeoecology,* v. 265, p. 59-77.

SCOT1323	Amoco Bounds Core MIDK9, Anderson Roros MIDK36, Austin Comp 1 MIDK21, Austin Comp 1B MIDK21B, Austin Comp2 UPK1, Big Sioux R. MIDK136, Black Mesa CEN10, Blanco River MIDK85, Blue Point MIDK107, Boulonnais MIDK12, Buchberg CORB27, Bunker Hill 1 MIDK133, Bunker Hill 2 MIDK133B, Bystry Creek CORB, Canteloup Quarry MIDK83, Cassis 3 MIDK42, Cassis MIDK100, Chimana Grande Is. MIDK88, Chispa Summit CEN3, Col de Palluel MIDK143, Covasna Valley CORB, Djebel Bireno MIDK7, Djebel Mrhila MIDK8, Dlebt-Chenin Aair MIDK23, Dugi Otok MIDK81,	Scott, R.W. (compiler). (2013). Appendix 7. Section catalog files for Cretaceous Chronostratigraphic Database: Projects MIDK3, MIDK4, MIDK41, MIDK42, MIDK45, LOK, CRET1 and CRET2. *precisionstratigraphy.com,* 323 pp.

Escalante Core #1 MIDK131, Estella 2 MIDK28, Estella-Lizarra MIDK60, Font Blance MIDK101, Gebel Abu Zurub MIDK67, Gebel Guna MIDK68, Gold Hill MIDK134, Grayson Bluff MIDK51, Hameau-Fredet Quarry MIDK82, Hot Springs MIDK65, Jebel Arief El Naqa MIDK66, Kalaat Senan MIDK1, Kalaat Senan MIDK10, Kalagork CORB, Kef el Azreg MIDK31, La Boca Cyn CEN9, Leon R. Comp. MIDK86, Lozier Cyn CEN8, Mansfield Core16 MIDK45, Mansfield Rd MIDK45B, Mesa Verde MIDK130, Mont Risous 2 MIDK 142X, Mont Risous MIDK 142, Nahr Ibrahim MIDK22, Oberaschau CORB 28,

	Ojinaga CEN4, Ouzon CORB26, Oyubari MIDK94, Portland Core MIDK132, Rehkogel CORB33, Rosans, Sarth MIDK6, Selbukhra 2 MIDK30B, Selbukhra Composite MIDK30, Sheep Mtn MIDK37, Sopeira MIDK32, Tingri 2, Tingri 3, Waco Lk Spillway MIDK115, Zasadne CORB14, Zongshan	
SCOT6504		Scott, G.R., and Cobban, W.A. (1965). Geologic and biostratigraphic map of the Pierre Shale between Jarre Creek and Loveland, Colorado. *United States Geological Survey Miscellaneous Geologic Investigations,* Map I-439, 4 pp.
SCOT7501		Scott, G.R., and Cobban, W.A. (1975). Geologic and biostratigraphic map of the Pierre Shale in the Canon City - Florence Basin and the Twelvemile Park area, south central Colorado. *United States Geological Survey Miscellaneous Investigations Series,* v. I-937, 1 pp.

SCOT8601		Scott, G.R., and Cobban, W.A. (1986). Geologic and biostratigraphic map of the Pierre Shale in the Colorado Springs - Pueblo area, Colorado. *Uinted States Geological Survey Miscellaneous Investigations Map,* v. I-1627.
SCOT8602		Scott, G.R., and Cobban, W.A. (1986). Geologic, biostratigraphic and structure map of the Pierre Shale between Loveland and Round Butte, Colorado. *United States Geological Survey Miscellaneous Investigations Map*, I-1700.
SCOT9489	Amoco Bounds Core MIDK9	Scott, R.W., et al. (1994). Dolson et al. (eds.) Unconformity-related hydrocarbons in sedimentary sequences. *Rocky Mountain Association of Geologists,* p. 89-98.
SCOT9611	Amoco Bounds Core MIDK9	Scott, R.W. et al. (1996). * *SEPM Concepts in Stratigraphy and Paleontology*, v. 6, p. 11-34.
SHAM0983	Evolution of Eiffellithus	Shamrock, J.L., and Watkins, D.K. (2009). Evolution of the Cretaceous Calcareous Nanofossil Genus Eiffellithus and Its Biostratigraphic Significance. *Cretaceous Research,* v. 30, p. 1083-1102.
SHIG9901	Gorbusha River, Kura River	Shigeta, Y., Maeda, H., Uemura, K., and Solovyov, A. (1999). Stratigraphy of the Upper Cretaceous System in the Krilon Peninsula, South Sakhalin, Russia. *Bulletin of the Natural Science Museum of Tokyo, Series C.,* v. 25(1-2), p. 1-27.

SIES8023	DSDP Site 417D, DSDP Site 418A	Siesser, W.G. (1980). Calcareous Nannofossils: Legs 51 and 52 of the Deep Sea Drilling Project. *Initial Reports of the Deep Sea Drilling Project,* v. 51-53(2), p. 823-845.
SILV8123	DSDP Site 462, DSDP Site 462A	Silva, I.P. and Sliter, W.V. (1981). Cretaceous Planktonic Foraminifers From the Nauru Basin, Leg 61, Site 462, Western Equatorial Pacific. *Initial Reports of the Deep Sea Drilling Project,* v. 61, p. 423-437.
SILV8697	DSDP Site 585, DSDP Site 585A	Silva, Premoli & Sliter, William V. (1986). Late Aptian and Cenomanian-Turonian Planktonic Foraminifers from Deep Sea Drilling Project Site 585, Leg 89, East Mariana Basin. *Initial Reports of the Deep Sea Drilling Project,* v. 89, p. 297-309.
SKUP0365	Bystry Creek CORB	Skupien and Vasicek. (2003). * *Transactions of the VSB Tech. Univ. Ostrava, Mining and Geology Series,* v. 8, p. 65-93.
SLIT7757	DSDP Site 355, DSDP Site 356, DSDP Site 357	Sliter, W.V. (1977). Cretaceous Benthic Foraminifers from the Western South Atlantic Leg 39, Deep Sea Drilling Project. *Initial Reports of the Deep Sea Drilling Project,* v. 39, p. 657-697.
SLIT8627	DSDP Site 585, DSDP Site 585A	Sliter, W.V. (1986). Cretaceous Redeposited Benthic Foraminifers from Deep Sea Drilling Project Site 585 in the East Mariana Basin, Western Equatorial Pacific, and Implications for the Geologic History of the Region. *Initial*

		Reports of the Deep Sea Drilling Project, v. 89, p. 327-361.
SMRE1131	Cervena Skala	Smreckova, M. (2011). Lower Turonian radiolarians from the Cervena Skala section (Pieniny Klippen Belt, Western Carpathians). *Mineralia Slovaca*, v. 43, p. 31-38.
SOUA1337	Oued Kharroub	Soua, M. (2013). Siliceous and organic-rich sedimentation during the Cenomanian-Turonian Oceanic Anoxic Event (OAE2) on the northern margin of Africa: an evidence from the Bargou area, Tunisia. *Arabian Journal of Geoscience*, v. 6(5), p. 1537-1557.
STEP5597		Stephenson, L.W. (1955). Owl Creek (Upper Cretaceous) fossils from Crowleys Ridge, southeastern Missouri. *US Government Printing Office*, v. 274E, p. 97-140.
STIN0501	El Rosario	Stinnesbeck, W., Ifrim, C., Scmidt, H., Rindflaisch, A., Buchy, M.-C., Frey, E., Gonzales-Gonzales. (2005). A new lithographic limestone deposit in the Upper Cretaceous Austin Group, county of Muzquiz, Coahuila, northeastern Mexico. *Revista Mexicana de Ciencias Geologicas*, v. 22(3), p. 401-418.
STIN8699		Stinnesbeck, W. (1986). Zu den faunistischen und paleokologischen Verhaeltnisse in der Quiriquina Formation (Maastrichtium) Zentral Chile. *Palaeontographica*, v. A194, p. 99-237.

STOF0149		Stoffer, P. W., Messina, P., Chamberlain, J. A., and Terry, D. O. (2001). The Cretaceous-Tertiary boundary inteval in Badlands National Park, South Dakota. *United States Geological Survey Open File Report,* v. 01-56, 49 pp.
SUMM8545	Austrian Zones	Summesberger, H. (1985). Ammonite zonation of the Gosau Group (Upper Cretaceous, Austria). *Annaler der Naturhistorisches Museum Wien,* v. 87A, p. 146-166.
SYKO9743	Krety Creek	Sykora, M., Ozvoldova, L., and Boorova, D. (1997). Turonian silicified sediments in the Czorsztyn succession of the Pienny Klippen Belt (Western Carpathians, Slovakia). *Geologica Carpathica,* v. 48(4), p. 243-261.
SZIV0782	Boly 1 Core, Jasd 1 Quarry, , Jasd 36 Core, Jasd 42 Core, Oroszlany 1881 Core,Tatabanya 1462 Core, Tilos Forest, Zsido Hill	Szives, O. (2007). Aptian-Campanian ammonites of Hungary. *Geologica Hungarica Series Palaeontologica,* v. 57, 182 pp.
TANA7611	Ikushumbetsu, Obira	Tanabe, K. (1976). Mid-Cretaceous scaphitid ammonites from Hokkaido. *Palaeontological Society of Japan Special Papers,* v. 21, p. 11-22.
THIE8175	DSDP Site 462, DSDP Site 462A	Thierstein, H.R. & Manivit, Helene. (1981). Calcareous-Nannofossil Biostratigraphy, Nauru Basin, Deep Sea Drilling Project Site 462, and

		Upper Cretaceous Nannofacies. *Initial Reports of the Deep Sea Drilling Project,* v. 61, p. 475-494.
THUR8879	N Atlantic Radiolaria, DSDP Site 603B	Thurow, J. (1988). Cretaceous Radiolarians of the North Atlantic Ocean: ODP Leg 103 (Sites 638, 640, and 641) and DSDP Legs 93 (Site 603) and 47B (Site 398). *Preceedings of the Ocean Drilling Program, Scientific Results,* v. 103, p. 379-418.
TOSH0728	Japan Con-Santon comp	Toshimitsu, S., Hasegawa, T., and Tsuchiya, K. (2007). Coniacian-Stantonian stratigraphy in Japan: a review. *Cretaceous Research,* v. 28, p. 128-131.
TRAB1100	Moria	Trabucho-Alexandre, J., Negri, A., and de Boer, P.L. (2011). Early Turonian pelagic sedimentation at Moria (Umbria-Marche, Italy): Primary and diagenetic controls on lithologic oscillations. *Palaeogeography Palaeoclimatology Palaeoecology*, v. 311, p. 200-214.
TREM0241	Bottaccione Gorge	Tremolda, F. (2002). Aptian to Campanian clacareous nannofossil biostratigraphy from the Bottaccione section, Gubbio, Central Italy. *Rivista Italiana di Paleontologia e Stratigrafia,* v. 108(3), p. 441-456.
TURN9659	Bass	Tur, N.A. (1996). Plankonic foraminifera recovery from the Cenomanian-Turonian mass extinction event, northeastern Caucasus. Hart, M. B. (ed.), *In: Biotic recovery from mass extinction events,* Geological

		Society of London Special Publication, v. 102, p. 259-264.
VINC1039	Kabir Kuh, Kuh-E-Bangestan	Vincent, B., van Buchem, F. S. P., Bulot, L. G., Immenhauser, A., Caron, M., Baghbani, D., and Huc. (2010). Carbon isotope stratigraphy, biostratigraphy, and organic matter distribution in the Aptian - Lower Albian successions of southeast Iran (Daryan and Kazhdumi formations). *Special Publications of Geoarabia,* v. 4(1), p. 139-197.
VISH9835	Moscow Basin Composite	Vishnevskaya, V.S., and de Wever, P. (1998). Upper Cretaceous radiolaria from the Russian Platform (Moscow Basin). *Revue de Micropaleontologie,* v. 41(3), p. 235-265.
WAGR0383		Wagreich, M., Kuchler, T., and Summesberger, H. (2003). Correlation of calcareous nannofossil zones to the first occurrence of Pachydiscus neubergicus (von Hauer, 1858) (Ammonoidea) in European Upper Cretaceous sections. *Geologie en Mijnbouw (Netherlands Journal of Geology),* v. 82(3), p. 283-288.
WAGR0643	Oberaschau CORB 28	Wagreich, M., Pavilshina, P., and Malata, E. (2006). Biostratigraphy of the lower red shale interval in the Rhenodanubian flysch zone of Austria. *Cretaceous Research,* v. 27, p. 743-753.

WAGR9205	Gosau Valley, Strobl-Weissenbach	Wagreich, M. (1992). Correlation of Late Cretaceous calcareous nannofossils with ammonite and planktonic foraminifer: the Austrian Gosau sections. *Cretaceous Research,* v. 13, p. 505-516.
WALA0443	Manassa	Walaszczyk, I., Marcinowski, R., Praskier, T., Dembicz, K., and Bienkowska, M. (2004). Biogeographical and stratigraphical significance of latest Turonian and early Coniacian inocerammid/ammonite succession of the Manassa section on the Onilahy River, southwest Madagascar. *Cretaceous Research,* v. 25, p. 543-576.
WALA1045	Salzgitter-Salder Quarry, Slupia Nadbrzezna	Walaszczyk, I., Wood, C.J., Lees, J.A., Peryt, D., Voigt, S., and Wiese, F. (2010). The Salzgitter-Salder Quarry (Lower Saxony, Germany) and Slupia Nadbrzezna river cliff section (Central Poland): a proposed candidate composite Global Boundary Stratotype Section and Point for the base of the Coniacian Stage (Upper Cretaceous). *Acta Geologica Polonica,* v. 60(4), p. 445-477.
WALA1479	Antsirasira-Ampolipoly, Vohipaly-Mahaboboka	Walaszczyk, I., Kennedy, W.J., Dembicz, K., Gale, A.S., Praszkier, T., Rasoamiaramana, A.H., (2014). Ammonite and inoceramid biostratigraphy and biogeography of the Cenomanian through basal Middle Campanian (Upper Cretaceous) of the Morondava Basin, western Madagascar. *Journal of African Earth Sciences,* v. 89, p. 79-132.

WANG0181	Zongshan	Wang, C.S., Hu, X.M., Jansa, L., Wan, X.Q., and Tao, R. (2001). The Cenomanian-Turonian anoxic event in southern Tibet. *Cretaceous Research,* v. 22, p. 481-490.
WANI0371	Kotanbetsu (Coni-Camp), Kotanbetsu (Turo-Camp)	Wani, R. (2003). Taphofacies models for Upper Cretaceous ammonoids from the Kotanbetsu area, northwestern Hokkaido, Japan. *Palaeogeography, Palaeoclimatology, Palaeoecology,* v. 199, p. 71-82.
WANX0383	Gamba, Tingri 3B	Wan, X., Wignall, P.B., and Zhao, W. (2003). The Cenomanian-Turonian extinction and oceanic anoxic event: evidence from southern Tibet. *Palaeogeography Palaeoclimatology Palaeoecology,* v.199, p. 183-298.
WARD9358		Ward. P.D., and Kennedy, W.J. (1993). Maastrichtian ammonites from the Bsicay region (France, Spain). *Journal of Paleontology Memoir*, v. 34, 58 pp.
WARD9707		Ward, P.D., and Orr, W. (1997). Campanian-Maastrichtian ammonite and planktonic foraminiferal biostratigraphy from Tercis, France: implications for defining stage boundary. *Journal of Paleontology*, v. 71(3), p. 407-418.
WIED0161	Kirchrode I Core	Wiedmann, J., and Owen, H.G. (2001). Late Albian ammonite biostratigraphy of the Kirchrode I borehole, Hannover, Germany. *Palaeogeography,*

		Palaeoclimatology, Palaeoecology, v. 174, p. 161-181.
WIED7927	Pedrosa, Puentadei 14A, Puentadei 14B	Wiedmann, J (1979). Itineraire geologique a traverse le Cretace Moyen des chaines vascogotiques et celtoberiques (Espagne du Nord). *Cuadernos Geologia Iberica,* v. 5, p. 127-214.
WIED9377		Wiedmann, J., and Schmidt, W. (1993). Upper Cretaceous ammonites from Jamaica and their stratigrpahic and paleogeographic implications. *Geological Society of America Memoir,* v. 182, p. 77-91.
WIED9695		Wiedmann, J., and Kullmann, J. (1996). Chapter 19, Crises in ammonoid evolution. Landman, N. H., Tanabe, K., and Davis, R. A. (eds.), *In: Ammonoid Paleobiology*. Topics in Geobiology, v. 13, p. 795-813.
WIEG8463	DSDP Site 545, DSDP Site 547A, DSDP Site 547B	Wiegand, George E. (1984). Cretaceous Nannofossils from the Northwest African Margin, Deep Sea Drilling Project Leg 79. *Initial Reports of the Deep Sea Drilling Project,* v. 79, p. 563-578.
WIES0429	Upohlavy Quarry	Wiese, F., Cech, S., Ekrt, B., Kost ak, M., Mazuch, M., and Voigt, S. (2004). The Upper Turonian of the Bohemian Cretaceous Basin (Czech Republic) exemplified by the Upohlavy working quarry: integrated stratigraphy and palaeoceanography of a gateway to the Tethys. *Cretaceous Research,* v. 25, p. 329-352.

WILK0478	Ventnor	Wilkinson, I.P. (2004). The Biostratigraphy of the Albian and Cenomanian succession in the Ventnor No. 2 Borehole, Isle of Wight. *British Geological Survey Internal Report, IR/04/078,* 20 pp.
WILM0728	Wunstorf Quarry AM	Wilmsen, M., Niebuhr, B., Wood, C. J., and Zawischa, D. (2007). Fauna and palaeocology of the Middle Cenomanian Praeactinocamax primus Event at the type locality, Wunstorf Quarry, northern Germany. *Cretaceous Research,* v. 28, p. 428-460.
WILM0911	Regensburg-Kelheim	Wilmsen, M., Wood, C.J., Niebuhr, B., and Kaplan, U. (2009). Cenomanian-Coniacian ammonoids of the Danubian Cretaceous group (Bavaria, Southern Germany). *Sud-Deutscher Geologischer Gesellschaft*, v. 65, p. 111-124.
WOND9287	ODP Site 761B, ODP Site 762C	Wonders, A.A.H. (1992). Cretaceous Planktonic Foraminiferal Biostratigraphy, Leg 122, Exmouth Plateau, Australia. *Proceedings of the Ocean Drilling Program, Scientific Results*, v. 122, p. 587 - 599.
YAZY0251	Yazykova Sakhalin Comp	Yazykova, E. (2002). Ammonite and inoceramid radiations after the Santonian-Campanian bioevent in Sakhalin, Far East Russia. *Lethaia,* v. 35, p. 51-60.
YAZY0491	Naiba River, Sakhalin	Yazykova, E.A., Peryt, D., Zonova, T.D., and Kasintzova, L.I. (2004). The Cenomanian/Turonian boundary in

		Sakhalin, Far East Russia: Ammonites, inoceramids, foraminifera, and radiolarians. *New Zealand Journal of Geology and Geophysics,* v. 47(2), p. 291-320.
YOUN7475	Austin Comp 1 MIDK21, Austin Comp 1B MIDK21B	Young (1974). * *Geoscience and Man,* v. 8, p. 175-228.
YOUN8525		Young and Woodruff (1985). * *Austin Geological Society Guidebook,* v. 7, p. 25-43.
YURT0341	Doryan	Yurtsever, T.S., Tekin, U.K., and Demirel, I.H. (2003). First evidence of the Cenomanian/Turonian boundary event (CTBE) in the Alakircay Nappe of the Antalya Nappes, southwest Turkey. *Cretaceous Research*, v. 24, p. 41-53.
ZABO8671	Calabar 1, Calabar 2	Zaborski, P.M.P. (1986). Lower Cenomanian (Mid Cretaceous). ammonites drom southeast Nigeria. *Journal of African Sciences,* v. 5(4), p. 371-380.
ZABO9359	Ashaka, Pindiga	Zaborski, P.M.P. (1993). Some new and rare Upper Cretaceous ammonites from north-eastern Nigeria. *Journal of African Earth Sciences,* v. 17(3), p. 359-371.
ZAKH1383	Ulyanovsk Composite	Zakharov, Y.D., Baraboshkin, E.Y., Weissert, H., Michailova, I.A., Smyshlyaeva, O.P., and Safron (2013). Late Barremian-early Aptian climate of the northetrn middle latitudes: stable isotope evidence

		from bivalve and cepha;opod molluscs of the Russian Platform. *Cretaceous Research,* v. 44, p. 183-201.
ZINS8931		Zinsmeister, W.J., Feldmann, R.M., Woodburne, M.O., and Elliot, D.H. (1989). Latest Cretaceous - earliestTertiary transition on Seymour Island, Antarctica. *Journal of Paleontology*, v. 63(6), p. 731-738.
ZONO9883	Ochotsk Zones	Zonova, T.D., and Yazykova, E.A. (1998). Biostratigraphy and correlation of the Turonian-Coniacia succession and the Turonian-Coniacian boudary problem in Far East Russia. Acta Geologica Polonica, v. 4A1:C4138(4), p. 483-494.